Alex Rosa Casla

Effects of environmental conditions and seasonality on Barents Sea shrimp dynamics and consequences for stock assessment

Universidade do Algarve

2025

Alex Rosa Casla

Effects of environmental conditions and seasonality on Barents Sea shrimp dynamics and consequences for stock assessment

Mestrado em Aquacultura e Pescas

(Especialidade em Pescas)

Trabalho efetuado sob a orientação de:

Dr. Fabian Zimmermann

Dr. Pedro Miguel Guerreiro Da Costa Guerreiro

Universidade do Algarve

2025

Effects of environmental conditions and seasonality on Barents Sea shrimp dynamics and consequences for stock assessment

Declaração de autoria

Declaro ser o autor deste trabalho, que é original e inédito. Autores e trabalhos consultados estão devidamente citados no texto e constam da listagem de referências incluída

Alex Rosa Casla

Acknowledgments

First of all, I would like to thank Fabian for all the support and trust he has placed in me throughout this year. From the very first email, he made everything easy, and the opportunities I have had thanks to him have allowed me to live incredible experiences that I couldn't even have imagined a few years ago. Of course, none of it would have been possible without the support of the Norwegian Institute of Marine Research, which I also have to thank for welcoming me and providing excellent working conditions during the development of my master thesis.

I would also like to thank Pedro Miguel Guerreiro for his support as a co-supervisor of the work from UAlg, as well as Johanna and John for their valuable input on scientific writing and the overall development of the project.

I also want to thank Ana Gomes for her help in correcting my Portuguese texts and for giving me such a warm welcome to Tromsø, together with Fabian.

On another note, this master's thesis marks the completion of an important phase in my life, which began almost two years ago in Faro. During this time, I met amazing people, made new friends and even fell in love. However, none of it would have been possible if I had not been taken into the program, which is why I want to thank Elsa Cabrita for her work as director of the master's program and for giving me the opportunity to enroll, almost at the last minute.

To my friends, who always supported me, even from far away. Thank you for keeping in touch no matter what.

To Anna, my partner, who I am grateful to have in my life. Late-night calls with you, venting about the pressures of daily life, have kept my spirits up during the most intense and stressful times.

Finally, thanks to my family for their everlasting support. Mum, Dad, everyday I try to remind myself how lucky I am to have you. Thank you for giving me wings to fly across the world following my dreams, and roots to know where I belong. I love you so much.

Abstract

Northern shrimp (*Pandalus borealis*) stock can be found across most of the Barents Sea, sustaining a large and valuable trawl fishery with an estimated sustainable catch of around 150,000 tonnes annually. The stock is monitored by Norway and Russia, and scientific advice is provided annually. However, the shrimp fishery in the Barents Sea has remained largely unregulated without any catch restrictions, with changes in catches mostly driven by economic factors, especially white fish accessibility and global shrimp prices.

The current Northern shrimp stock assessment uses a biomass index from a spatiotemporal distribution model based on a relatively short survey time series. We evaluated whether including available time series of shrimp survey data from winter and environmental data could improve the model's predictive potential and, thus, the quality of the assessment. While environmental variables did not provide a significant improvement in the biomass index model, the winter data aligned well with the summer data, providing valuable information on stock trends throughout the year.

This research led to the implementation of a winter biomass index in the Barents Sea shrimp stock assessment model. The results showed that the inclusion of winter data provided similar estimates of biomass and fishing mortality compared to the former model, but with increased predictive performance and accuracy. However, significant spatial and spatiotemporal random effects indicate that shrimp distribution and dynamics are linked to biotic and abiotic processes that are currently not explicitly accounted for in our modelling framework, which should be subject to further research. This project provides an important contribution to an improved stock assessment for the shrimp stock in the Barents Sea and, thus, sustainable catch advice. This is particularly relevant given the species' important role in a changing arctic marine ecosystem, and the growing fishing pressure Northern shrimp is subjected to.

Keywords: Northern shrimp, Spatiotemporal distribution models, *Pandalus borealis*, Arctic fisheries.

Resumo

A pescaria do camarão boreal no Mar de Barents tem sido caracterizada pela natureza flutuante dos seus "stocks" desde o início da atividade pesqueira, em 1970. Esta variabilidade, aliada a níveis de exploração irregulares, resultou em taxas de captura instáveis ao longo dos anos, incluindo capturas extremamente baixas no início dos anos 2000.

Inicialmente, a pesca concentrava-se em torno de Svalbard, a leste da Ilha do Urso e na Depressão de Hopen. No entanto, nos últimos anos, a atividade nestas zonas tradicionais tem vindo a diminuir, enquanto a pesca tem-se deslocado para áreas mais a leste, em direção ao centro do Mar de Barents e às águas internacionais da chamada "loophole area" uma região no centro do Mar de Barents que está fora das zonas econômicas exclusivas da Noruega e da Rússia, sendo governada apenas pela convenção da Comissão das Pescarias do Atlântico Nordeste. A ausência de regulamentação nestas águas internacionais, combinada com uma gestão pouco rigorosa nas zonas norueguesas e russas, tem levantado preocupações, especialmente perante outros impactos antropogénicos, como as alterações climáticas, que poderão trazer novos desafios, como a deslocação dos stocks e mudanças nas condições ambientais.

Os stocks de camarão são monitorizados pela Noruega e pela Rússia, com aconselhamento científico fornecido aos gestores através do Grupo de Trabalho Conjunto Russo-Norueguês para as Pescas Árticas, ativo desde 2004. Este grupo estabeleceu, em 2022, um modelo de avaliação de referência que combina dados de captura com índices de biomassa. O principal índice de biomassa é calculado com base num modelo de distribuição espácio-temporal que utiliza campos aleatórios espaciais e temporais para estimar efeitos aleatórios. Os dados utilizados neste modelo provêm exclusivamente das campanhas conjuntas entra a Rússia e a Noruega para a avaliação do ecossistema do Mar de Barents, realizadas anualmente no verão desde 2004. Contudo, estes dados apenas ficam, em geral, disponíveis tardiamente e por isso estão frequentemente incompletos no momento da avaliação, que ocorre em novembro. Importa ainda referir que, o modelo de referência baseia as suas previsões principalmente na profundidade do fundo marinho, ignorando outras variáveis ambientais que influenciam a biologia do camarão boreal, como a temperatura, a salinidade ou a velocidade das correntes.

Neste projeto, o objetivo principal foi avaliar o modelo de referência para o camarão boreal no Mar de Barents e analisar se este poderia ser melhorado através da adição de dados ambientais e de campanhas de investigação pesqueira adicionais. Para tal, dados ambientais mensais (temperatura do fundo, velocidade das correntes, salinidade e profundidade da camada mista do oceano) foram extraídos do serviço Copernicus, e dados adicionais foram adquiridos da campanha demersal de inverno, realizada desde 2004 como parte da colaboração entre a Noruega e a Rússia. O potencial preditivo das variáveis ambientais foi analisado utilizando o critério de informação de Akaike, e a relevância dos dados de inverno foi avaliada através da comparação das tendências de biomassa entre o verão e o inverno, de modo a verificar se seguiam padrões semelhantes, de forma que os dados de inverno pudessem servir como sinal antecipado de alterações nos stocks.

Após a revisão e extensão do modelo de indexação, os novos índices de biomassa foram utilizados para atualizar o modelo de avaliação de referência. As implicações desta nova configuração para a avaliação e gestão mais abrangente do stock foram avaliadas através da comparação dos pontos de referência fornecidos por ambos os modelos. Os principais pontos de referência utilizados foram o *Bmsy* e o *Fmsy*, que indicam, respetivamente, a biomassa ótima do stock e a mortalidade por pesca que permitem o rendimento máximo sustentável.

Foi ainda realizada uma análise retrospetiva de ambos os modelos (atualizado e de referência), recuando cinco anos, para simular a situação no final do ano, momento em que a avaliação do camarão é realizada, mas com dados de verão incompletos e dados de inverno disponíveis. As previsões de biomassa e mortalidade por pesca para o ano seguinte foram comparadas com os valores estimados pelo modelo treinado com a série completa de dados. Foram calculados o *Rho de Mohn* (uma métrica para avaliar o viés das estimativas) e os erros totais de estimativa para ambos os modelos, de forma a identificar o modelo com melhor desempenho.

Os modelos de índice de biomassa e de avaliação do stock do camarão do Mar de Barents foram adaptados para incluir, pela primeira vez, dados das campanhas de inverno nas avaliações. As tendências observadas nos dados de inverno alinharam-se bem com os dados de verão, confirmando que a distribuição e densidade dos camarões são relativamente estáveis, possivelmente devido à sua reduzida mobilidade. Esta estabilidade facilitou a integração dos dois conjuntos de dados num único modelo de índice, embora alargado, tendo em conta também os desafios colocados por *outliers*, inconsistências e problemas de manutenção a longo prazo nos dados de inverno.

As previsões de biomassa ao longo do tempo revelaram a evolução da abundância e distribuição dos camarões. As zonas

com biomassa consistentemente elevada, como a Depressão de Hopen e a “loophole area”, coincidem com as áreas de maior esforço de pesca. Em contraste, regiões com biomassa média ou baixa permanecem praticamente inexploradas, podendo funcionar como refúgios que sustentam a produtividade do stock a longo prazo.

Por outro lado, as variáveis ambientais não melhoraram o desempenho do modelo e, portanto, foram excluídas. Uma possível explicação é o limitado contraste nos dados, que abrangem apenas partes relativamente homogéneas do Mar de Barents, representando, maioritariamente, habitats potenciais de camarão. A análise, por esta razão, não incluiu muitas observações nas extremidades ou fora do intervalo ambiental habitada pelo camarão. Além disso, a utilização de médias mensais para os dados ambientais representa uma limitação adicional, pois pode atenuar variações de curto prazo que afetam significativamente as comunidades marinhas.

Ao comparar o modelo de avaliação alargado com o modelo de referência, observou-se que ambos produziram estimativas semelhantes para o *Bmsy* e *Fmsy*. No entanto, ambos os modelos apresentaram níveis elevados de incerteza, o que é comum na estimativa de valores absolutos em avaliações de stocks. Estes modelos tendem a ter um desempenho melhor na avaliação de tendências relativas, especialmente porque os índices em que se baseiam são normalizados.

Os resultados da análise retrospetiva com dados parciais demonstraram que o modelo de avaliação alargado teve um melhor desempenho do que o modelo de referência, apresentando erros de previsão mais baixos para a biomassa e a mortalidade por pesca. Isto sublinha o valor da integração de dados de inverno para melhorar a precisão das previsões, especialmente quando os dados de verão estão incompletos ou indisponíveis.

Por fim, embora a pesca do camarão no Mar de Barents seja atualmente considerada sustentável, a crescente pressão de impactos antropogénicos, como as alterações climáticas, representa riscos sérios para os ecossistemas marinhos árticos. Este cenário deve incentivar os gestores e responsáveis políticos a adotarem uma gestão mais ativa e preventiva deste recurso valioso, com ênfase na sustentabilidade ecológica, social e económica a longo prazo.

Palavras-chave: Camarão boreal, Modelos de distribuição espaço-temporal, *Pandalus borealis*, Pescarias do Ártico.

Index

Acknowledgments i

Abstract ii

Resumo iii

Index v

List of Figures vii

List of Tables xi

List of abbreviations xii

1 Introduction 1

1.1 Northern shrimp biology . . . 1

1.2 Barents Sea shrimp fishery . . . 4

2 Methodology 9

2.1 Survey data . . . 9

2.2 Spatiotemporal distribution model . . . 11

2.3 Environmental data . . . 12

2.4 Winter data relevance . . . 14

2.5 Extended index model structure selection . . . 14

2.6 Extended index model diagnostics . . . 14

2.7 Extended index model predictions . . . 14

2.8 Implications for assessment . . . 15

3 Results 15

3.1 Spatiotemporal distribution model . . . 15

3.2 Environmental effects . . . 16

3.3 Winter data relevance . . . 22

3.4 Extended index model structure selection . . . 25

3.5 Extended index model diagnostics . . . 26

3.6 Extended index model predictions . . . 26

3.7 Implications for assessment . . . 30

4 Discussion **36**

4.1 Spatiotemporal distribution model 36

4.2 Environmental effects 36

4.3 Winter data relevance 37

4.4 Implications for assessment 38

5 Conclusions **39**

6 Bibliography **40**

7 Annex **44**

List of Figures

1.1 Northern shrimp geographical distribution. Modified from Bergström, 2000. 2
1.2 Main features of circulation and bathymetry in the Barents Sea. Extracted from Stiansen et al., 2009. . 2
1.3 Sediment map for the study area. Blue dots represent shrimp catches during the 2023 Winter and Summer Surveys. Dot size is proportional to catch size. Sediment data from the Geological Survey of Norway. 3
1.4 Total reported catches by country and year. Data for 2024 is based on preliminary results. Extracted from Zimmermann et al., 2024. 5
1.5 Indices of stock biomass from the (1) joint Russian-Norwegian Barents Sea ecosystem survey (BESS, since 2004), (2) Norwegian logbook data from the fishery (CPUE), and (3) a historic index based on the annual sum of Norwegian shrimp survey and the Russian survey (1984–2002). Lines show the mean estimates, the shaded area the 95% confidence interval. All indices were standardized to their respective mean. Extracted from Zimmermann et al., 2024. 6
2.1 Summer survey data coverage of the study area. 10
2.2 Winter Survey data coverage of the study area. 10
2.3 Strata division of the study area. 1- West Svalbard, 2- Southwestern Barents Sea, 3- Northern Barents Sea, 4- Northeastern Barents Sea, 5- Southeastern Barents Sea 11
2.4 Stochastic partial differential equation mesh (A), and alternative mesh with dispersion barrier in Svalbard (B). Black dots in A represent sampling locations and white dots in B represent mesh vertices. Red crosses represent mesh nodes where spatial correlation is constrained. 12
2.5 Data treatments applied to environmental data. Blue squares represent the 12 months before a sampling event, in this case during August. Brackets represent the mean of environmental values that is associated with each treatment (T). T1 uses the environmental value for the same month when the survey was conducted; T2 takes the month before sampling; T3 the 6 months before, averaged; T4 the 12 months before, averaged; and T5 uses the standard deviation (SD) of the last 12 months. 13
3.1 Mean monthly salinity in sampling month (data treatment 1) against shrimp density. Dots show each observed pair of current velocity and shrimp density. Blue columns represent the mean shrimp density at each interval of the environmental variable. Percentages display the amount of data concentrated at a given interval. 17
3.2 Mean monthly mixed ocean layer depth in sampling month (data treatment 1) against shrimp density. Blue columns represent the mean shrimp density at each interval of the environmental variable. Percentages display the amount of data concentrated at a given interval. 18

3.3 Mean monthly bottom temperature in sampling month (data treatment 1) against shrimp density. Blue columns represent the mean shrimp density at each interval of the environmental variable. Percentages display the amount of data concentrated at a given interval. 19
3.4 AIC score difference between baseline model and models including environmental variables. 20
3.5 Bottom temperature conditional effects for data treatments 1-4 (A-D). Gray dots represent the observed data, and the blue lines indicate the predicted shrimp density, which the model calculates keeping all other variables constant. 21
3.6 Conditional effect of depth standardized, for baseline model. 22
3.7 Winter and Summer Surveys shrimp density boxplots. Outliers over 1.5 interquartile ranges from the third quartile are colored. Density values over 200000 Kg/NM² are colored red. 23
3.8 Percentage of zero catch events per year in the Winter Survey data. 24
3.9 Summer and Winter Survey indices for Stratum 2, with plus/minus one standard deviation (shaded regions). 25
3.10 Northern shrimp biomass predictions obtained using the extended index model, showing the combined outcome of fixed and random effects predicted over the study area for years 2004, 2010, 2016, 2018, 2021 and 2023. HD refers to Hopen Deep and LA to Loophole Area. 27
3.11 Predicted fixed effects for the extended index model for 2024. Estimates are on the log-scale, and correspond to density when back-transformed. 28
3.12 Predicted spatially varying coefficient (zeta s), modelling the season effect in the extended index model. Estimates are on the log-scale, and correspond to density when back-transformed. 28
3.13 Predicted spatial random effects (omega s) for the extended index model. Estimates are on the log-scale, and correspond to density when back-transformed. 29
3.14 Predicted spatiotemporal random effects (epsilon st) for the extended index model, for years 2004, 2010, 2016, 2018, 2021 and 2023. The complete time series can be accessed in the Annex. Estimates are on the log-scale, and correspond to density when back-transformed. 30
3.15 Indices of stock biomass from the benchmark index model (Summer index) and extended index model (Summer and Winter indices). Lines show the mean estimates. All indices were standardized to their respective mean. 31
3.16 Reference points Bmsy (A) and Fmsy (B) for the benchmark and extended assessment models, with confidence intervals. 31
3.17 Relative biomass estimated by the extended assessment model, with 95% uncertainty ribbons and index data. Circles represent the CPUE index, diamonds are for the Historic Surveys index, Triangles refer to the winter index, and squares to the summer index. Colors refer to the month when the data was collected (see legend). 32

3.18 Retrospective analysis for biomass, using the benchmark assessment model, with Mohn's Rho and total prediction error for each retrospective run compared to the baseline. The baseline model represents the complete benchmark assessment model, trained with all data available until summer 2024. Each retrospective model is trained with one year less of data, and the last yearly data segment of each line is a forecast. 33
3.19 Retrospective analysis for biomass, using the extended assessment model, with Mohn's Rho and total prediction error for each retrospective run compared to the baseline. The baseline model represents the complete extended assessment model, trained with all data available until summer 2024. Each retrospective model is trained with one year less of data, and the last yearly data segment of each line is a forecast. 34
3.20 Retrospective analysis for fishing mortality, using the benchmark assessment model. 35
3.21 Retrospective analysis for fishing mortality, using the extended assessment model. 35
7.1 Mean monthly current velocity in sampling month (data treatment 1) against shrimp density. Dots show each observed pair of current velocity and shrimp density. Blue columns represent the mean shrimp density at each interval of the environmental variable. Percentages display the amount of data concentrated at a given interval. 44
7.2 Current velocity against shrimp density for data treatments 2 through 5 (A-D): A (1-month lagged mean), B (6-month lagged mean), C (12-month lagged mean) and D (12-month lagged standard deviation). Dots show each observed pair of current velocity and shrimp density, blue columns represent the mean shrimp density at each interval of the environmental variable, and percentages display the amount of data concentrated at a given interval. 45
7.3 Salinity against shrimp density for data treatments 2 through 5 (A-D): A (1-month lagged mean), B (6-month lagged mean), C (12-month lagged mean) and D (12-month lagged standard deviation). Dots show each observed pair of current velocity and shrimp density, blue columns represent the mean shrimp density at each interval of the environmental variable, and percentages display the amount of data concentrated at a given interval. 46
7.4 Mixed ocean layer depth against shrimp density for data treatments 2 through 5 (A-D): A (1-month lagged mean), B (6-month lagged mean), C (12-month lagged mean) and D (12-month lagged standard deviation). 47
7.5 Bottom temperature against shrimp density for data treatments 2 through 5 (A-D): A (1-month lagged mean), B (6-month lagged mean), C (12-month lagged mean) and D (12-month lagged standard deviation). 48
7.6 Q-Q plot showing mle-mvn calculated residuals from the extended index model. 49
7.7 Q-Q plot showing mcmc calculated residuals from the extended index model. 49
7.8 Model residuals distribution from the extended index model in the study area between 2004 and 2024. 51
7.9 Northern shrimp biomass predictions obtained using the extended index model, showing the combined outcome of fixed and random effects predicted over the study area between 2004 and 2024. 53

7.10 Predicted fixed effects from the extended index model over the study area between 2004 and 2024. Estimates are on the log-scale, and correspond to density when back-transformed.. 55
7.11 Predicted spatiotemporal random effects (omega s) from the extended index model over the study area between 2004 and 2024. Estimates are on the log-scale, and correspond to density when back-transformed. 57
7.12 Extended assessment model OSA residuals. 58
7.13 Extended assessment model process residuals. 59
7.14 Benchmark assessment model OSA residuals. 60
7.15 Benchmark assessment model process residuals. 61

List of Tables

1 Model parameters including phi (tweedie dispersion), range (matérn range distance), rho (spatiotemporal correlation), sigma E (spatiotemporal field standard deviation), sigma O (spatial field standard deviation) and tweedie p (tweedie power parameter). Estimates and confidence intervals (CI), are shown for a regular mesh model (model 1), and a barrier mesh model (model 2). 16

2 Different model configurations used to test the relevance of sun altitude as a predictor, compared to hour. Coef.est.3, coef.se.3 and std.dev.3 refer to the estimated intercept, standard error and standard deviation explained by the third main effect (either hour or sun altitude). Std. dev. depth refers to the amount of standard deviation explained by the depth smoother, and the last column shows the Akaike Information Criterion (AIC) score. 16

3 Cross validation results between baseline model and alternative model with 12-month lagged mean temperature. 22

4 Model configurations to model the effect of seasonality. SVC(Season) refers to the addition of a spatially varying coefficient for the Season factor variable. Models are sorted by descending AIC. *Spatial random effect overdispersion parameter unusually large. 26

List of abbreviations

AIC - Akaike Information Criterion

BESS - Barents Sea Ecosystem Survey in Summer

Bmsy - Biomass at maximum sustainable yield

CI - Confidence interval

CL - Carapace length

CPUE - Catch Per Unit of Effort

CMEMS - Copernicus Marine Environment Monitoring Service

EEZ - Exclusive Economic Zone

EU - European Union

Fmsy - Fishing mortality at maximum sustainable yield

FPZ - Fisheries Protection Zone

GAM - Generalized Additive Models

HD - Hopen Deep

ICES - International Council for the Exploration of the Sea

INLA - Integrated Nested Laplace Approximations

LA - Loophole Area

MCMC - Markov Chain Monte Carlo

MGCV - Mixed GAM Computation Vehicle

MLD - Mixed ocean Layer Depth

NGU - Geological Survey of Norway (Norges Geologiske Undersøkelse)

NM - Nautical Miles

OSA - One Step Ahead (residuals)

PPT - Parts Per Thousand (‰)

QQ - Quantile-Quantile (plot)

SD - Standard Deviation

SDM - Spatiotemporal Distribution Model

SF - Simple Features

SPDE - Stochastic Partial Differential Equations

SPiCT - Stochastic surplus Production model in Continuous Time

SVC - Spatially Varying Coefficient

T - Treatment

TAC - Total Allowable Catch

TMB - Template Model Builder

US - United States

UTM - Universal Transverse Mercator (coordinate system)

WS - Winter Survey

1 Introduction

Fisheries sustain countless communities around the world and provide a valuable protein source for people across the globe (Johnson et al., 2019). However, fisheries are also highly vulnerable to environmental variations, which have been exacerbated in the last decades by climate change and other anthropogenic impacts (Brander, 2010), including overfishing (Hilborn et al., 2020), pollution (Turner et al., 2023), and introduced species (Brander, 2013). Climate-driven shifts in marine species distributions pose a challenge to the ecological, economic and social sustainability of the affected fisheries (Galappaththi et al., 2022; Perry et al., 2005). Distribution shifts of fish stocks can reduce their productivity and overall fitness due to environmental degradation and the increased energy expenditure during the exploration of new areas (Pörtner & Peck, 2010). Additionally, fishers' operational costs can increase due to longer travelling times to reach the stocks, and conflicts can arise if stocks move between different territorial waters and become available to different communities (Mendenhall et al., 2020; Palacios-Abrantes et al., 2022; Pinsky et al., 2018). The rapidly changing Arctic ecosystems in the Barents Sea and the cost- and energy-intensive trawling fleets from the European Union, Norway and Russia operating there are a prime example of the compound effects of environmental change as well as geopolitical and economic challenges.

Science-based management, international cooperation and enforcement of regulations are key components in maintaining the health and productivity of marine ecosystems. Science-based management of fish stocks builds on stock assessment to monitor the state of fish stocks, including their distribution, a key step in ensuring sustainable fishing practices (Hilborn et al., 2020). The spatial component of fisheries and stock distributions have been progressively introduced in the stock assessment modelling framework to account for a changing climate (Goethel et al., 2023). Spatial models allow for the integration of species distribution data together with spatial environmental data, which can improve the predictability of stock assessment models, particularly for species where the relationship between spawning biomass and recruitment is heavily influenced by environmental variability (Isaac et al., 2020). While the first models including spatial components were developed in the 1950's, they only started to be adopted during the 1990's, and their implementation is still surging (Punt, 2019).

1.1 Northern shrimp biology

Pandalus borealis (hereafter Northern shrimp) is a pandalid shrimp that inhabits cold deep waters in and adjacent to the Northern Atlantic Ocean, from Canada and the US east coasts to the Kara Sea in Russia (Figure 1.1).They have been recorded as far south as 35°N, but they are more commonly found further north to 82°N (Bergström, 2000; Garcia, 2007; Shumway et al., 1985).

The vertical distribution of Northern shrimp spans between 20 and 900 m bottom depth, and their presence is associated with muddy or sandy silt sea floors (Shumway et al., 1985; Zimmermann et al., 2019). Despite the wide range of bottom depths where they can be found, Northern shrimp is usually more abundant between 150 and 600 m bottom depth (Garcia, 2007). The Barents Sea as a relatively shallow shelf sea (mean bottom depth 230m) with abundant sandy and muddy substrates (NGU, 2013) represents therefore an ideal ecosystem for Northern shrimp (Figures 1.2 and 1.3).

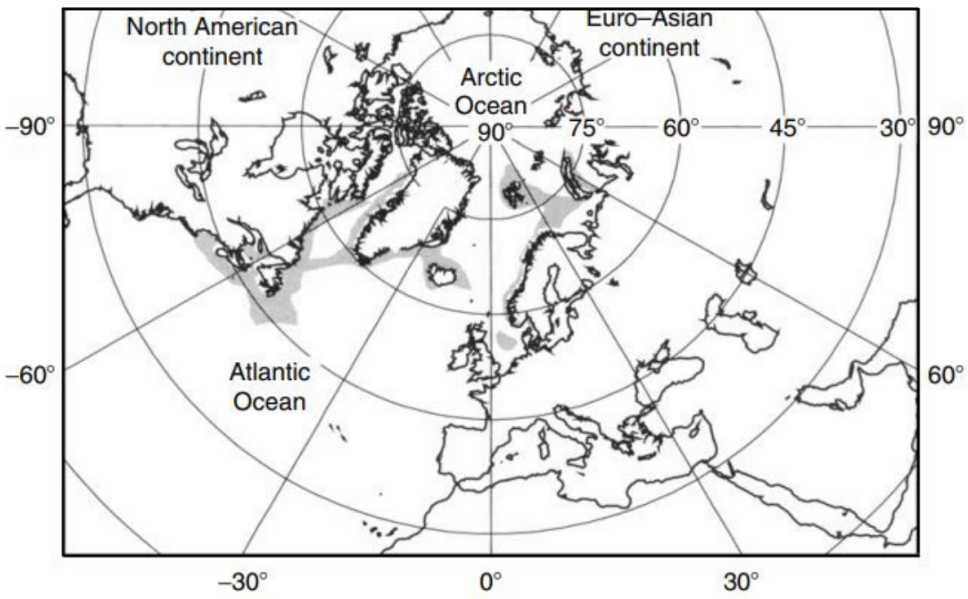

Figure 1.1: Northern shrimp geographical distribution. Modified from Bergström, 2000.

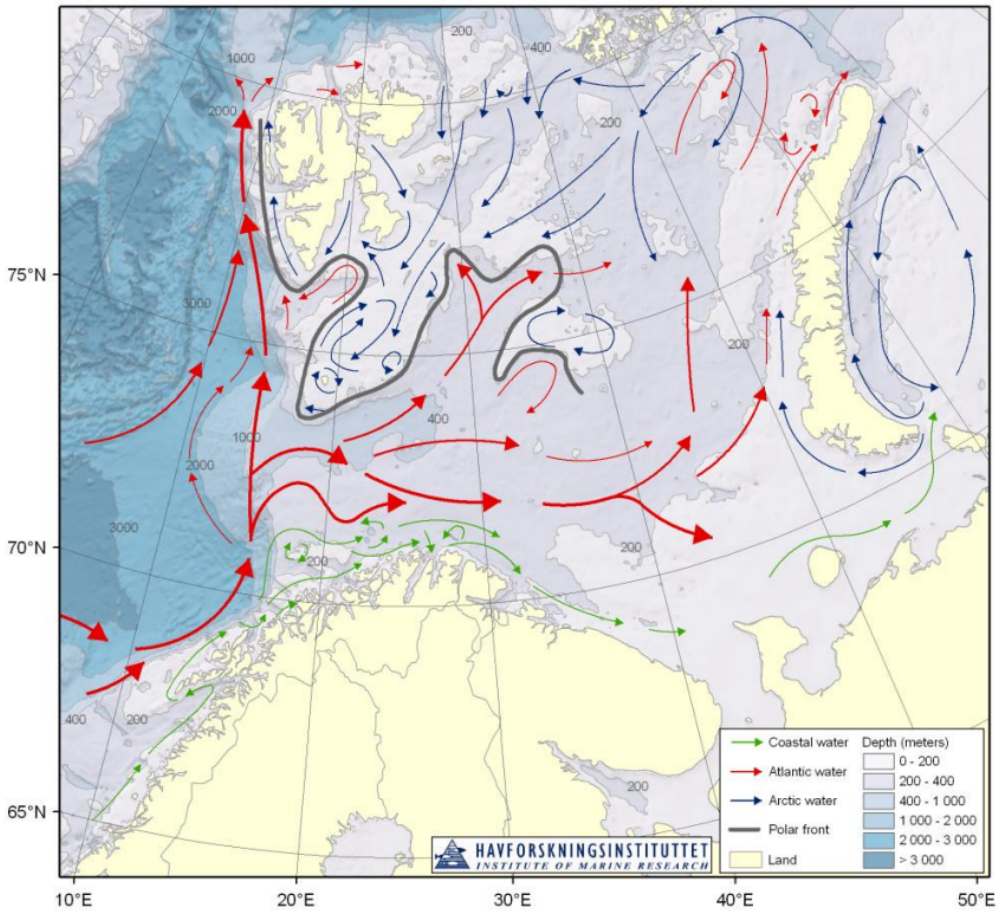

Figure 1.2: Main features of circulation and bathymetry in the Barents Sea. Extracted from Stiansen et al., 2009.

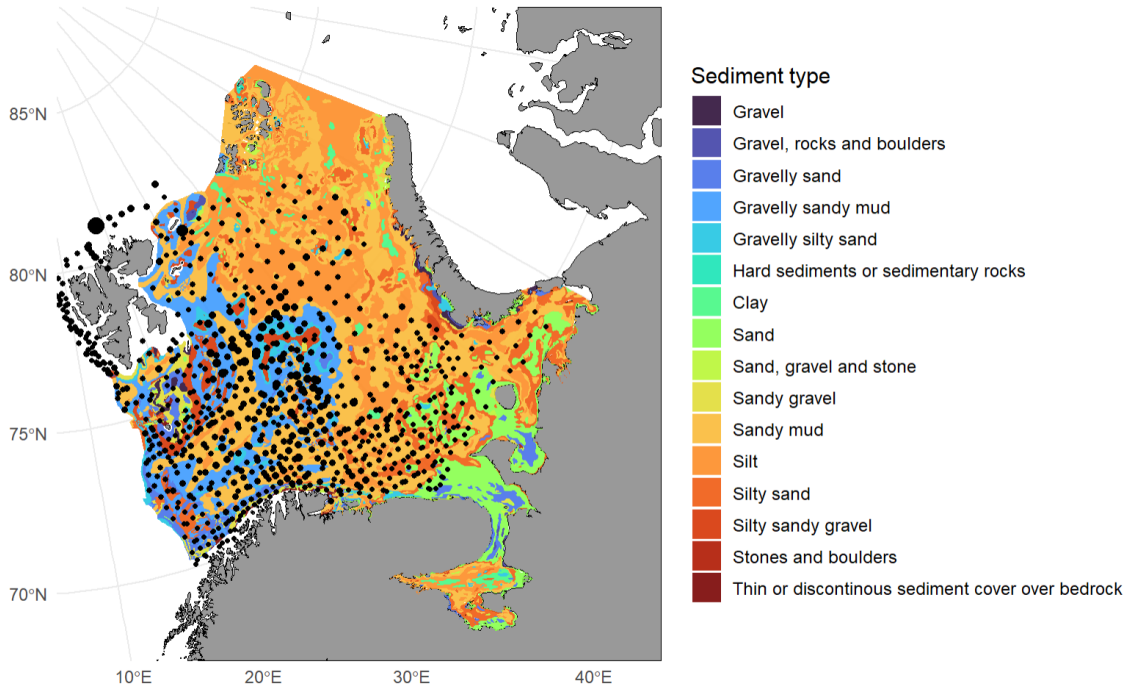

Figure 1.3: Sediment map for the study area. Blue dots represent shrimp catches during the 2023 Winter and Summer Surveys. Dot size is proportional to catch size. Sediment data from the Geological Survey of Norway.

Northern shrimp carry out daily vertical migrations, ascending in the water column during the night to feed and descending back to the sea floor during the day (Barr, 1970; Bergström, 2000; Hudon et al., 1992). They feed mainly on zooplankton, such as copepods or tintinnids, as well as on polychaetes, foraminifera, and remains of Porifera and Holothuroidea (Garcia, 2007; Horsted, 1956; Shumway et al., 1985). Diet composition changes during life history (Ariza & Ouellet, 2009), together with diel migration patterns. These aspects should be taken into account when modelling shrimp biomass densities, as shrimp presence will be linked to areas with zooplankton, and the percentage caught through bottom trawling will vary depending on the vertical migration stage (Hudon et al., 1992), obtaining larger catches during the day when shrimp are not feeding higher in the water column.

Northern shrimp reproduction is highly related to environmental factors such as temperature, but also to phytoplankton blooms, which need to match in time with larval hatching, to maximize larval survival (Cushing, 1990; Ouellet et al., 2007). Even though research has found that larger female sizes can lead to higher larval production, (Wieland & Siegstad, 2012), it remains difficult to link shrimp stock biomass with recruitment into the fishery (Jónsdóttir et al., 2013). Aside from the already mentioned impact of temperature, which also favors larval survival when there is a slight but progressive increment of temperature over time (T. Rasmussen & Tande, 1995), another important variable that is thought to affect larval survival is cod (*Gadus morhua*) and greenland halibut (*Reinhardtius hippoglossoides*) predation, which can be especially prevalent among young individuals around 1 year old (Aschan & Ingvaldsen, 2009; Björnsson et al., 2011). However, this effect depends on high predator densities and strong spatial overlap with shrimp populations (Björnsson et al., 2011; Wieland et al., 2007).

Northern shrimp is a protandric hermaphroditic species, which means that all individuals are born as male, and they later transition to female. Sex change is thought to be affected by environmental factors, as shrimp in relatively warm waters transition at earlier ages and smaller sizes compared to those in colder waters (Bergström, 1992; Shumway et al., 1985). In the Barents Sea, this and other related attributes such as growth are highly variable (Aschan, 2000; Bergström, 1992; B. Rasmussen, 1953), due to the large area where the species is found and the shifting nature of the abiotic environment (Stiansen et al., 2009), largely driven by the back-and-forth dynamic of Atlantic and Polar water masses (Bodur et al., 2023; Lundesgaard et al., 2022), represented in Figure 1.2). Due to the key role temperature plays modulating shrimp biology, it has been suggested several times as a potentially good predictor of shrimp density (Hall, 2017; ICES, 2022; Krawczyk et al., 2024).

Other environmental factors such as current velocity and direction are known to affect shrimp biology, not only by modulating population connectivity during the planktonic larval stages, but also during the adult stages, since the limited swimming ability of shrimp makes their movements and orientation dependent on current velocity, affected in turn by tidal cycles and deep water circulation patterns (Ivanov & Stolyarenko, 1995). However, previous studies attempting to directly link environmental variables such as temperature, current velocity or salinity to shrimp density have been unsuccessful (ICES, 2022; Krawczyk et al., 2024).

The wide range of ecosystems that are part of the large study area of the Barents Sea includes fjords, continental shelf and open ocean, and ranges from continental Norway up to the Arctic waters around Svalbard (Figure 1.1). Consequently, it has been hypothesized that different ecosystems could have led to different adaptations in shrimps across the study area, that in turn could be considered as different subpopulations and hence treated as different stocks. As a matter of fact, studies have found genetic differences between shrimp populations in the central Barents Sea and southern populations in fjords along the Norwegian coast (Hansen et al., 2021), as well as genetically differentiated shrimp communities around the Barents Sea, based on a temperature gradient (Jorde et al., 2015). Despite the available evidence, Northern shrimp is managed as a single stock comprising the entire Barents Sea and adjacent inshore areas.

1.2 Barents Sea shrimp fishery

The Northern shrimp commercial fishery in the Barents Sea started in the 1970's, initially concentrated around Svalbard, east of Bjørnøya and Hopen islands (Garcia, 2007). However, in recent years, activity around these traditional fishing grounds has diminished, moving further east into the central Barents Sea and international waters of the so-called "Loophole Area" (Hvingel & Zimmermann, 2023). Traditionally, the main nations taking part in the fishery were Norway and Russia, but also vessels from Iceland, Faroes, Greenland, Great Britain and the EU have participated in the fishery. Fleet dynamics have been driven by shifting shrimp market prices and the availability of other fishing grounds and species. International interest in the shrimp fishery followed often external triggers, such as the imposition of a quota system by Greenland in 1977, which limited the exploitation of their shrimp fishing grounds; or in recent years the decline of demersal fish stocks such as Atlantic cod (Garcia, 2007; Hvingel & Zimmermann, 2023).

Shrimp catches since the start of the fishery in the 1970's have been unstable (Melaa et al., 2022), ranging from a few

thousand tons in the early days of the fishery to over 100,000 tons in 1984 (Figure 1.4). However, this instability has not been related to unstable shrimp stocks, but rather to external factors such as market prices (Aschan et al., 2004) and availability of alternative stocks like cod (Zimmermann et al., 2024).

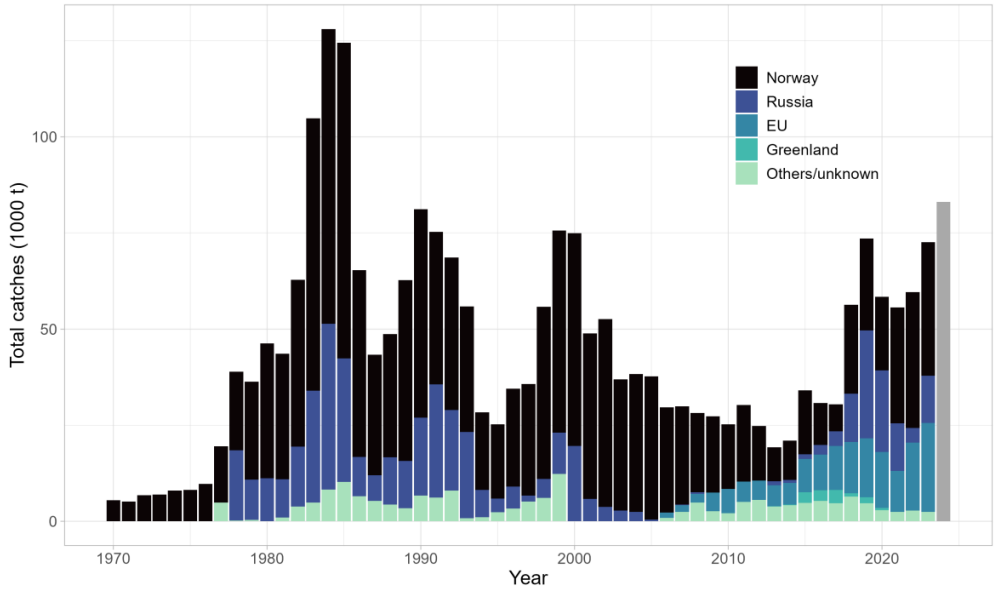

Figure 1.4: Total reported catches by country and year. Data for 2024 is based on preliminary results. Extracted from Zimmermann et al., 2024.

The management of this fishery is based on a minimum landing size of >15 mm carapace length (CL) and a minimum stretched mesh size of 35 mm, together with mandatory sorting grids and other bycatch regulations which lead to the closure of the fishery in areas with large abundance of undersize shrimp, cod, haddock, redfish or Greenland halibut. Aside from this, the fishery is open throughout the year, but most of the fishing effort is concentrated in summer (May to August) due to weather and sea ice restrictions.

Licenses are required to operate in the Norwegian Exclusive Economic Zone (EEZ) and Svalbard temporary Fisheries Protection Zone (FPZ), with stricter restrictions for foreign vessels, which are allowed a set number of effective fishing days and a limited number of licenses by country (Zimmermann et al., 2024). In the Russian EEZ, a Total Allowable Catch (TAC) is also in place to further control fishing effort (Aschan et al., 2004). However, the increasing proportion of the fishery taking place in international waters of the central Barents Sea is subject to a legal vacuum, which practically means that shrimp fishing in this area is unrestricted (Oanta, 2018; Stokke, 2010).

Currently, there is no common management plan for the Northern shrimp fishery in the Barents Sea, posing a substantial risk for overfishing due to the lack of restrictions, especially in international waters of the “Loophole Area” (Zimmermann et al., 2024). While the adoption of a common TAC for the entire fishery has been recurrently proposed by scientists, arguing it would be a good measure to help stabilize the stock and guarantee the long-term sustainability of the fishery (Garcia, 2007), it has not been introduced to this date.

Every year, the Joint Russian-Norwegian Arctic Fisheries working group releases a report presenting shrimp stock assessment results, together with summarized commercial and survey data, and research recommendations. The assessment model being used is a Stochastic surplus Production model in Continuous Time (SPiCT), which can account for catch uncertainty and separate it from natural stock variations, and provide biomass and fishing mortality estimates at any point in time, with their associated uncertainties (Pedersen & Berg, 2017). These models provide a flexible and statistically strong framework that adapts to data sources with different measurement errors and time frames, while providing all the relevant metrics and reference points used in stock assessment to inform management decisions, such as Fishing mortality at maximum sustainable yield (*Fmsy*) or total biomass.

The data used to fit the SPiCT model which is currently in use (hereafter benchmark assessment model) consists of a Catch per Unit of Effort (CPUE) index, obtained from logbook data provided by Norwegian vessels; a biomass index from the joint Norwegian-Russian Barents Sea Ecosystem Survey in Summer (BESS), and a historic biomass index, based on the annual sum of Norwegian and Russian surveys before the start of joint surveys in 2004 (Figure 1.5) (Zimmermann et al., 2024).

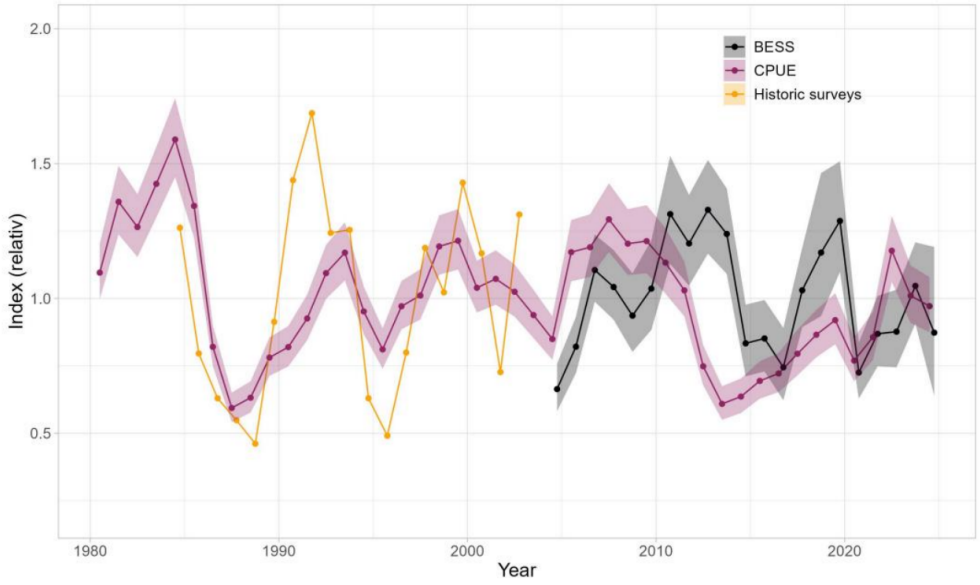

Figure 1.5: Indices of stock biomass from the (1) joint Russian-Norwegian Barents Sea ecosystem survey (BESS, since 2004), (2) Norwegian logbook data from the fishery (CPUE), and (3) a historic index based on the annual sum of Norwegian shrimp survey and the Russian survey (1984–2002). Lines show the mean estimates, the shaded area the 95% confidence interval. All indices were standardized to their respective mean. Extracted from Zimmermann et al., 2024.

The biomass index used for the benchmark assessment model is produced using a spatiotemporal distribution model (SDM), which uses the BESS survey data to predict Northern shrimp density in the Barents Sea, while accounting for spatial and spatiotemporal variations in the data. This model was ratified during the benchmark workshop of *Pandalus* stocks in 2022 (ICES, 2022), after outperforming other non-spal models, such as design-based approaches or a simpler generalised linear mixed model.

The spatiotemporal distribution model currently in use to obtain the biomass index (hereafter benchmark index model) consolidated during the benchmark uses generalised additive mixed-effect models that include Gaussian Markov random fields, used for spatial and spatiotemporal random effects modelling, estimated through stochastic partial differential equations (SPDE) (ICES, 2022). This workflow is implemented in R through the "R-INLA" (Beguin et al., 2012) and "sdmTMB" (Anderson et al., 2025) packages. The general SDM formula from "sdmTMB" is the following:

$$E[y_{s,t}] = \mu_{s,t},$$

$$\mu_{s,t} = f^{-1}(X^{\text{main}}_{s,t}\beta + \omega_s + \epsilon_{s,t})$$

where:

- $E[y_{s,t}]$ represents the mean expected value of the response data $y_{s,t}$ at point s and time t;
- mu represents the mean;
- f represents a link function (log), and f^{-1} its inverse;
- X^{main} represents the main effects matrix;
- β is the vector of fixed-effect coefficients;
- ω_s is the spatial component (a random field);
- $\epsilon_{s,t}$ is the spatiotemporal component (a random field).

In the current model, the main effects included to model shrimp density are year, depth and hour:

$$\text{Shrimp density} \sim \text{Year} + s(\text{Depth}, k = 3) + s(\text{Hour}, k = 3)$$

Year is included as a categorical variable to prevent bias and control for unobserved variations over time, with 21 levels, one per surveyed year. Depth is the average bottom depth measured during trawling, in meters, and is included in the model as a smooth term using a thin plate regression spline, with k =3 basis functions. Hour is the hour of the day when trawling started, also introduced in the model as a smooth term with a cubic spline (k=3). Hour is included to control for variations in shrimp catches due to vertical migration, which can bias data collection since sampling is carried out during day and night. Splines are built from the "mgcv" package (Wood, 2011) and are implemented into "sdmTMB".

Aside from the main effects, an isotropic spatial random field and a spatiotemporal random field with an autoregressive correlation of order 1, are used to account for spatial and spatiotemporal variations in the data. Isotropy implies that there is no preferred direction for shrimp mobility around the study area, and the autoregressive correlation acknowledges that data points from one year to the next will likely be correlated, due to their proximity in time (Anderson et al., 2025).

This approach excludes the influence of environmental variables, which we hypothesize can significantly improve

Northern shrimp biomass index estimates, based on previous studies linking environmental variability to shrimp abundance (Aschan, 2000; Ouellet et al., 2007). Additionally, BESS data becomes available late in the year (October–November) and is often incomplete by the time the assessment is due in November. We hypothesize that winter survey data will correspond well with summer data, offering an early indication of stock status and supporting more informed decision-making. Moreover, a Winter Survey index could help model the seasonal dynamics of the fishery, which is particularly relevant given that most commercial shrimp fishing occurs between surveys, from May to August (Zimmermann et al., 2024).

2 Methodology

The project aimed at evaluating the current spatiotemporal distribution model for Northern shrimp in the Barents Sea, used for stock assessment, and explore whether it could be improved by adding environmental data and incorporating additional survey data. It was evaluated based on whether the additions to the spatiotemporal model enhanced its predictive potential or not. In addition, we determined the consequences and implications of this research for the Barents Sea shrimp stock assessment.

2.1 Survey data

Fisheries independent data were obtained from the Barents Sea Ecosystem Survey in Summer and from the Winter Survey (WS). Standardized bottom trawling stations were evenly distributed all over the Barents Sea, with the objective of obtaining a representative picture of the species that inhabit it and their abundance. There is a special interest in commercial species, as the survey data obtained for several of the species sampled is used to guide stock assessments and fisheries management decisions.

Sampling took place 24 hours a day, and 15-minute bottom trawls with a cod end mesh size of 20 mm were conducted at each station, at approximately 3 knots trawling speed. While trawl width showed some stochastic variation between trawling events, it was assumed to be constant at 11.7 meters for shrimp modelling purposes.

At each station, the catch was sorted to the lowest taxonomic level possible, before weighting. For Northern shrimp, maturation stages were registered, and carapace lengths were measured in some catches, but not consistently over the years. In cases where it was not possible to sort the entire catch, representative subsamples were taken, and raising factors were applied to calculate original sample composition. All data was systematically registered on board with the FishData and Biotic editor softwares, which flag inconsistencies in the data to help minimize human error during data collection. For each survey station the sampled shrimp density in kg per NM^2 was calculated, by dividing the shrimp catch weight by the trawled distance and the trawl width in nautical miles.

After completing the survey data collection and compilation, over 15600 trawls from 10 different vessels were present in the data, spanning 21 years, from 2004 until 2024. Most of the sampling effort was concentrated in the months of February (34%), September (27%), August (18%) and March (13%), resulting in a balanced combination of Winter Survey data (53.5%) and Summer Survey data (46.5%).

The study area covers most of the Barents Sea, from the Norwegian and Russian continental coasts to Novaya Zemlya and Svalbard (Figures 2.1 and 2.2). This area was divided into several coarse strata, defined on a geographic and political basis (Figure 2.3). Even if these were not very relevant biologically, it was a way of creating smaller divisions within the large area covered by the Barents Sea, and it was used in the past when shrimp modelling was based on a design-based stratified approach. The Svalbard area was divided into two strata, which cannot be surveyed during the winter due to ice formation. The southwestern Barents Sea, up to the Norwegian coastline makes the biggest stratum. Two more strata are found in the Russian side of the study area.

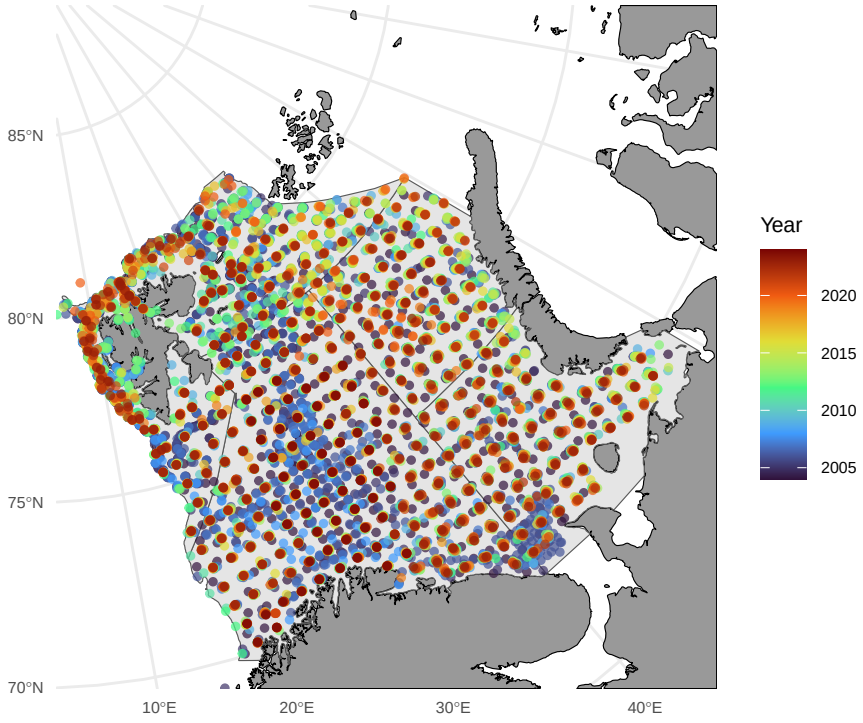

Figure 2.1: Summer survey data coverage of the study area.

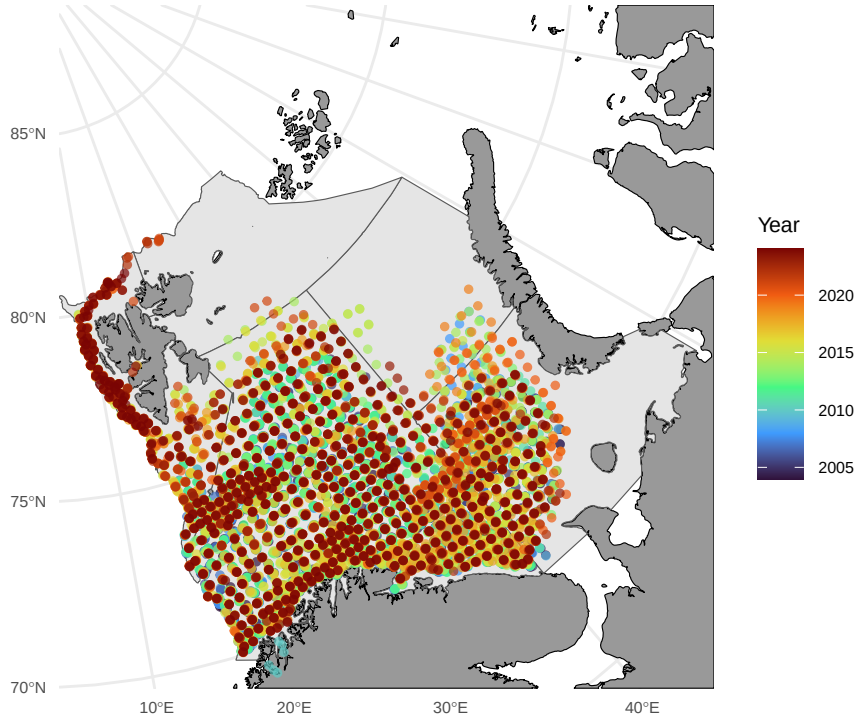

Figure 2.2: Winter Survey data coverage of the study area.

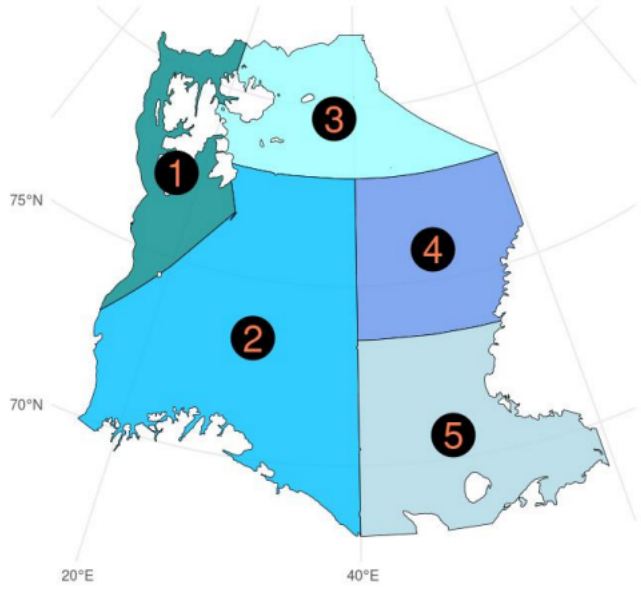

Figure 2.3: Strata division of the study area. 1- West Svalbard, 2- Southwestern Barents Sea, 3- Northern Barents Sea, 4- Northeastern Barents Sea, 5- Southeastern Barents Sea

The Barents Sea template was merged with the survey data, so that every data point received a stratum number based on its coordinates. All spatial operations were performed using the R "sf" package (Pebesma, 2018). Latitude and longitude coordinates were transformed into the UTM coordinate reference system (zone 37), to standardize distances across the study area and make them comparable. This step was especially relevant given the large latitudinal range of the study area and the distortion of distances in the lat-long projection near the poles.

2.2 Spatiotemporal distribution model

To define the spatial structure of the SDM, a network of interconnected points covering the study area, or mesh, was created. Each of these locations are used by the model to evaluate the surrounding data points and fit the model formula, accounting for spatial variation. The mesh was calculated using the Stochastic Partial Differential Equation (SPDE) approach for Gaussian random fields, implemented in the "make_mesh" function through the "sdmTMB" package in R. Minimum distance between knots (points) was set to 60 km, based on the average distance between sampling stations, and maximum triangle length was set to 200 km for the inner mesh and 1000 km for the outer mesh.

While this mesh structure accounted for the amount of data by placing knots closer together in data-rich areas, and spacing them in data-poor areas, the mesh did not account for land masses, which limit population connectivity. For example, the Svalbard archipelago was modeled with a coarser mesh due to limited data, but the mesh failed to reflect how Svalbard might act as a barrier to shrimp movement. Given the historically high shrimp density in Northern Svalbard and trying to stop the model from predicting shrimp mobility across Svalbard, the option was explored to

use a barrier mesh, implemented through the "add_barrier_mesh" function in the "sdmTMBextra" package (Anderson, 2024), using 0.1 as range fraction, which determines the fraction of the spatial range that barrier triangles have (Figure 2.4).

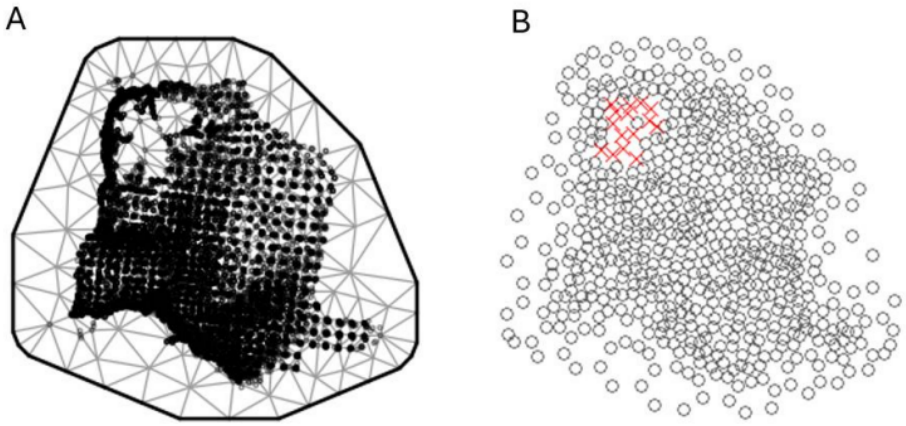

Figure 2.4: Stochastic partial differential equation mesh (A), and alternative mesh with dispersion barrier in Svalbard (B). Black dots in A represent sampling locations and white dots in B represent mesh vertices. Red crosses represent mesh nodes where spatial correlation is constrained.

The second model feature which was explored was the smoother effect of hour. While shrimp are known to perform daily vertical migrations, these are more likely driven by light intensity (Brierley, 2014), which can be detected by shrimp, instead of hour, which is only a rough estimator of light intensity especially in circumpolar areas, where daylight times vary significantly over the year. Therefore, sun altitude over the horizon was computed, by supplying hour, date, latitude and longitude to the "getSunlightPosition" function in the "suncalc" package (Thieurmel & Elmarhraoui, 2022).

The last model feature to be explored was the distribution family, and the Tweedie distribution was initially applied. Newer options implemented in the "sdmTMB" package, such as delta-gamma and delta-generalised gamma models were also tested, as they have been proven successful in similar studies (Rubec et al., 2016; Smith & Johnson, 2024). However, these new models exhibited unstable parameter estimates, and higher computational burden compared to the initial choice. Therefore, Tweedie was kept as the preferred distribution for modelling our data.

2.3 Environmental data

Statistical models allow for integration of environmental data, which can help explain spatial and temporal patterns in the stock distribution. To evaluate whether environmental variables could improve the spatiotemporal distribution models for the Northern shrimp stocks in the Barents Sea, we extracted relevant variables from the real-time global forecasting Copernicus Marine Environment Monitoring Service (CMEMS). The specific product used was the GLORYS12V1 (CMEMS, 2024).

Monthly means for bottom temperature, salinity, mixed ocean layer depth, and current velocity were compiled for the

study area with a grid resolution of 1/12° (approximately 8 km), for the years 2003-2023. Grid resolution was predefined in the data, and its fine scale allowed for accurate merging with survey data. Environmental data was merged with survey data using the "sf" R package, by assigning environmental data values corresponding to the nearest sampled locations.

Five different data treatments were explored, to extract as much information as possible from the environmental data available (Figure 2.5). Data treatments refer to different ways of calculating means of environmental data that could help display environmental variation over time. The different treatments were based on assumptions of how environment possibly affects stock distribution or density on the temporal scale. The first and second treatment used the value for the same month and the month before the survey was conducted, respectively, assuming immediate or slightly lagged effects of current environment. The third and the fourth treatment utilized the averages of the last 6 and 12 months prior to sampling, respectively, assuming lagged effects of the past environment over a longer period. The fifth treatment used the standard deviation of the last 12 months, assuming environmental variation over the last year before the survey as a driver of shrimp density. We explored the relationship between shrimp densities and changes in the 20 combinations of treatments and environmental variables, without assumptions regarding normality or homoscedasticity.

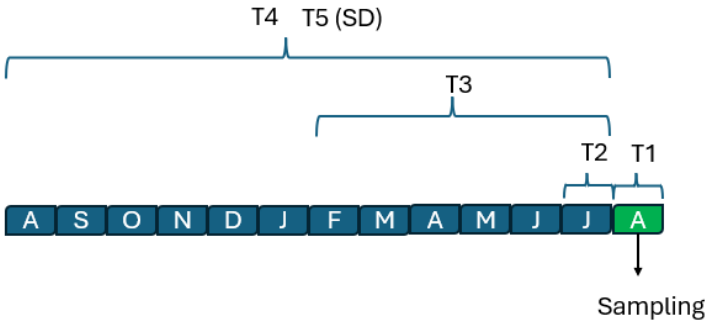

Figure 2.5: Data treatments applied to environmental data. Blue squares represent the 12 months before a sampling event, in this case during August. Brackets represent the mean of environmental values that is associated with each treatment (T). T1 uses the environmental value for the same month when the survey was conducted; T2 takes the month before sampling; T3 the 6 months before, averaged; T4 the 12 months before, averaged; and T5 uses the standard deviation (SD) of the last 12 months.

Every environmental variable was added to a separate "sdmTMB" baseline model with year, time and depth as other covariates. The environmental variable was added to the model by means of a thin plate spline (restricted to 3 knots). To determine whether the addition of a new variable was informative enough compared to the added complexity, the new models were compared to the baseline model without environmental effects by means of the Akaike information criterion (AIC). In addition, variable relevance was assessed by plotting their conditional effects, using the "visreg" R package (Breheny & Burchett, 2017). In cases where the relevance of the new variables remained unclear, due to very minor improvements in AIC, a random sampling cross validation with 10 folds was run. Then, the sum of predictive log-likelihoods from all the folds tested was calculated for each model, and were later compared to determine which model had a better predictive performance, keeping in mind that a lower score of log-likelihood indicates higher predictive power.

2.4 Winter data relevance

Winter data was first explored using descriptive statistics, and results were compared to summer data metrics to assess coherence. The occurrence of zero catches was also plotted to detect patterns or inconsistencies in the data.

Secondly, summer and winter data were used independently to build spatiotemporal models and estimate stock indices. After this, biomass trends over time were compared to elucidate whether they followed similar patterns, in a way that winter data could be used as an early sign of what the stock could look like the following season.

2.5 Extended index model structure selection

To incorporate the winter and summer data into a single extended biomass index model (hereafter extended index model), there were several options available and compatible with the "sdmTMB" modelling framework. One option was to change the time steps that the model uses to operate, from yearly steps, jumping from one summer to the next, in the absence of more data, to half year (season) time steps that use winter data.

Another option was to keep whole year time steps, while adding a fixed effect to account for the season when the data was collected, integrated in the model as a categorical variable with two levels, indicating whether the data was from the "Winter" or "Summer" data series. Also, since seasonal effects on shrimp density can be related to year effects, an interaction factor between the "Season" and "Year" effects was also tested, to account for their hypothetical interaction.

Due to the large size of the study area, we considered that the seasonal effect on shrimp density could also vary spatially. Consequently, the "Season" factor was also included as a spatially varying coefficient (SVC), which the model can adapt across the study area. All these configurations were tested by adding them to a baseline model without season effects. Model performance was evaluated using sanity checks and AIC comparisons.

2.6 Extended index model diagnostics

The best model according to the AIC criterion was analyzed to verify that it did not violate any assumptions. First, residuals were extracted using two complementary methods provided in the "sdmTMB" package; one which calculates multivariate normal residuals, based on maximum likelihood estimations, and a second method which employs a Markov Chain Monte Carlo (MCMC) algorithm, implemented in the "sdmTMBextra" package (Anderson, 2024). This is the recommended method for residual extraction, in spite of its high computational burden, as it usually gives more reliable results.

2.7 Extended index model predictions

Model predictions were then calculated by feeding the model with data from the study area without providing information about shrimp density. A spatial grid of the study area containing depth data was completed with constant values of sun altitude and season, to control for the effect of these variables in the predictions. Sun altitude was set to its mean

value, and season was set to “Summer”. This grid was expanded over the years 2004-2024 and provided to the extended index model, returning predictions on shrimp density.

Several maps were plotted to visualize model predictions and disentangle the impact of different model components. Fixed effects, spatial random effects and spatiotemporal random effects were plotted separately. While fixed effects showed the basic model estimation without accounting for random effects, spatial and spatiotemporal effects maps showed the effect through time and space of abiotic and biotic factors in shrimp biomass density (Anderson et al., 2025) that were not explicitly included in the model.

Finally, biomass indices for summer and winter were extracted from the predictions, summarizing all the spatial data into a single data point per year, which referred to Northern shrimp yearly biomass in the Barents Sea.

2.8 Implications for assessment

The new indices from the extended index model were incorporated into a new SPiCT assessment model (hereafter extended assessment model), while keeping the commercial CPUE and Historic Surveys indices unchanged. SPiCT models assumptions were checked through One-Step-Ahead (OSA) residuals diagnostic plots. Residuals for process errors of biomass and fishing mortality were also analyzed.

Subsequently, reference points provided by the extended assessment model were compared to those provided by the benchmark assessment model, currently used in the assessment. The main reference points utilized in the stock assessment were *Bmsy* and *Fmsy*, which refer to the optimum stock biomass and fishing mortality, that would provide the maximum sustainable yield.

Finally, retrospective analysis of the updated and extended assessment models with 5 peels back in time were conducted, aiming to simulate the situation by the end of the year, when the shrimp assessment is due, with incomplete BESS data for that year, but with Winter Survey data available. Biomass and fishing mortality predictions for the next year after the data peel were compared with the values provided by the model trained with the complete data series. Mohn’s Rho and total estimation errors were computed for both models, and results were compared, in search for the most accurate model.

3 Results

3.1 Spatiotemporal distribution model

The new barrier mesh was first introduced with a baseline model using only summer data, which predicted density based on year, depth and hour. Fixed and smoother effects did not show large differences across models. However, random effects from the barrier mesh model showed large deviations from its regular mesh counterpart (Table 1). The spatial and spatiotemporal fields standard deviations (sigma O and sigma E) indicate instability in the model with a barrier mesh, which makes random effects contributions soar, in contrast to the moderate contributions in the regular

mesh model. Furthermore, an AIC value of 91829 compared to 91818 for the barrier free model, confirms that adding a barrier mesh in this case would be an unnecessary source of complexity.

Table 1: Model parameters including phi (tweedie dispersion), range (matérn range distance), rho (spatiotemporal correlation), sigma E (spatiotemporal field standard deviation), sigma O (spatial field standard deviation) and tweedie p (tweedie power parameter). Estimates and confidence intervals (CI), are shown for a regular mesh model (model 1), and a barrier mesh model (model 2).

Parameter	Estimate 1	C.I. low 1	C.I. high 1	Estimate 2	C.I. low 2	C.I. high 2
phi	11.64	11.14	12.16	11.65	11.15	12.17
range	244.79	201.63	297.20	283.29	237.18	338.37
rho	0.77	0.63	0.86	0.78	0.64	0.87
sigma_E	0.89	0.75	1.06	40.77	29.96	55.47
sigma_O	1.53	1.31	1.79	75.84	55.27	104.07
tweedie_p	1.65	1.64	1.65	1.65	1.64	1.66

To assess the relevance of sun altitude as an alternative covariable instead of hour, three different models were fitted using year and depth as a baseline model, and sequentially adding either hour or sun altitude as a smoother effect (Table 2). Surprisingly, hour outperformed sun altitude as a shrimp density predictor. However, the actual contributions of any to the model are small, more so compared to the amount of standard deviation explained by the depth smoother (23.6). However, there is an improvement in terms of AIC, which supports the addition of one of the main effects. Although sun altitude shows less predictive power than hour, the causal inference supporting its addition is stronger, and it is more biologically accurate, making it more relevant.

Table 2: Different model configurations used to test the relevance of sun altitude as a predictor, compared to hour. Coef.est.3, coef.se.3 and std.dev.3 refer to the estimated intercept, standard error and standard deviation explained by the third main effect (either hour or sun altitude). Std. dev. depth refers to the amount of standard deviation explained by the depth smoother, and the last column shows the Akaike Information Criterion (AIC) score.

Model	Main effects	coef.est.3	coef.se.3	std. dev.3	std. dev. depth	AIC
1	fYear + s(Depth_std,k=3) + s(Hour_std, k=3)	-0.19	0.01	2.48	23.59	91818.50
2	fYear + s(Depth_std,k=3) + s(sunalt_std, k=5)	-0.15	0.08	1.01	23.83	91910.52
3	fYear + s(Depth_std,k=3)				23.9	92126.02

3.2 Environmental effects

The environmental data compiled referring to current velocity, salinity, mixed ocean layer depth and bottom temperature was analyzed in search of patterns that could be related to Northern shrimp density. For current velocity, there were no patterns detected in relation to shrimp density (Annex Figure 7.1). This could be due to most samples sites were in areas with low current velocities, creating a lack of data for medium and higher values of current velocity, with the uncertainty that this implies. This data imbalance was also observed across the other data treatments (Annex Figure 7.2), suggesting there is no relationship between current velocity and shrimp density in our data.

There was a clear pattern in the preferred salinity range, where Northern shrimp in the Barents Sea occurred in higher

densities around 35 ppt (Figure 3.1), while there were lower densities above 35.25 ppt and under 34.75 ppt. The other data treatments that involved lagged means (T2-T4) showed consistent patterns (Annex Figure 7.3, A-C). However, the data treatment consisting of the 12-month lagged standard deviation (T5), showed a different pattern (Annex Figure 7.3, D), suggesting higher shrimp densities where the yearly standard deviation of salinity is smaller, as the first interval from 0 to 0.25 SD contains the majority of the samples (48.8%), and also the largest mean shrimp density (close to 2000 kg/NM²), without accounting for intervals with less than 1% share of the data, that provide very uncertain means.

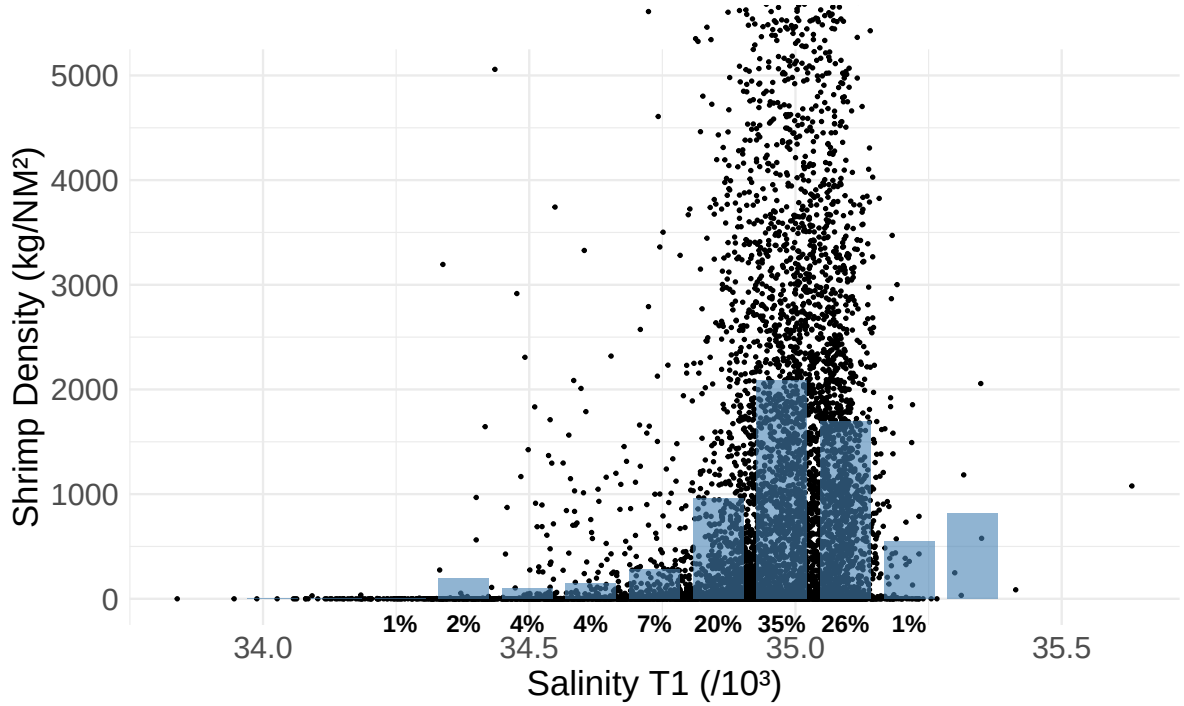

Figure 3.1: Mean monthly salinity in sampling month (data treatment 1) against shrimp density. Dots show each observed pair of current velocity and shrimp density. Blue columns represent the mean shrimp density at each interval of the environmental variable. Percentages display the amount of data concentrated at a given interval.

The mixed ocean layer depth (MLD) had a bell shape relation with shrimp density for data treatment 1, mean monthly salinity in the sampling month (Figure 3.2). Similar to the other environmental variables, the data was very imbalanced, and most sampling was carried out in stations with MLD shallower than 40 meters. The other data treatments showed variations from the pattern observed in Figure 3.2. In the case of data treatment 2, we could see a maximum in shrimp density around 24 m of MLD (Annex Figure 7.4). However, in the 6-month lagged mean data, there was not a clear maximum in shrimp density, and instead density remained relatively constant between 0 and 50 m of MLD. Also, as the lagged means involved a longer time frame (T3 and T4), mean MLD also increased (Annex Figure 7.4), suggesting cyclical patterns over the year, with higher MLD values in the winter and lower in the summer.

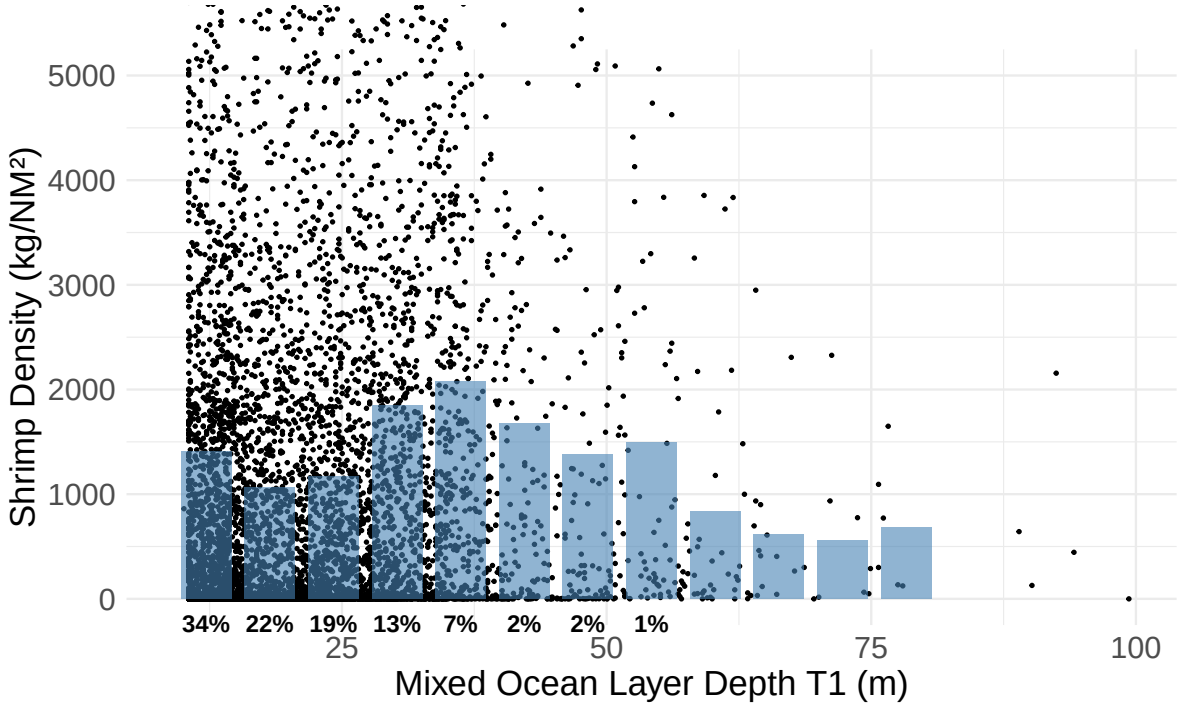

Figure 3.2: Mean monthly mixed ocean layer depth in sampling month (data treatment 1) against shrimp density. Blue columns represent the mean shrimp density at each interval of the environmental variable. Percentages display the amount of data concentrated at a given interval.

Shrimp densities were low at bottom temperatures below 0°C , while larger shrimp densities occurred at temperatures around 2°C (Figure 3.3. Shrimp densities decreased gradually with increasing temperature until being almost absent over 6°C . Other data treatments involving lagged means (Annex Figure 7.5) showed a very similar pattern to the one observed in Figure 3.3. However, in the case of the 12-month lagged standard deviation we could see a slightly different pattern, that displayed higher shrimp densities for standard deviation in bottom temperature closer to 0, with a slightly decreasing trend in shrimp density as standard deviation increased, before the trend became erratic due to lack of data.

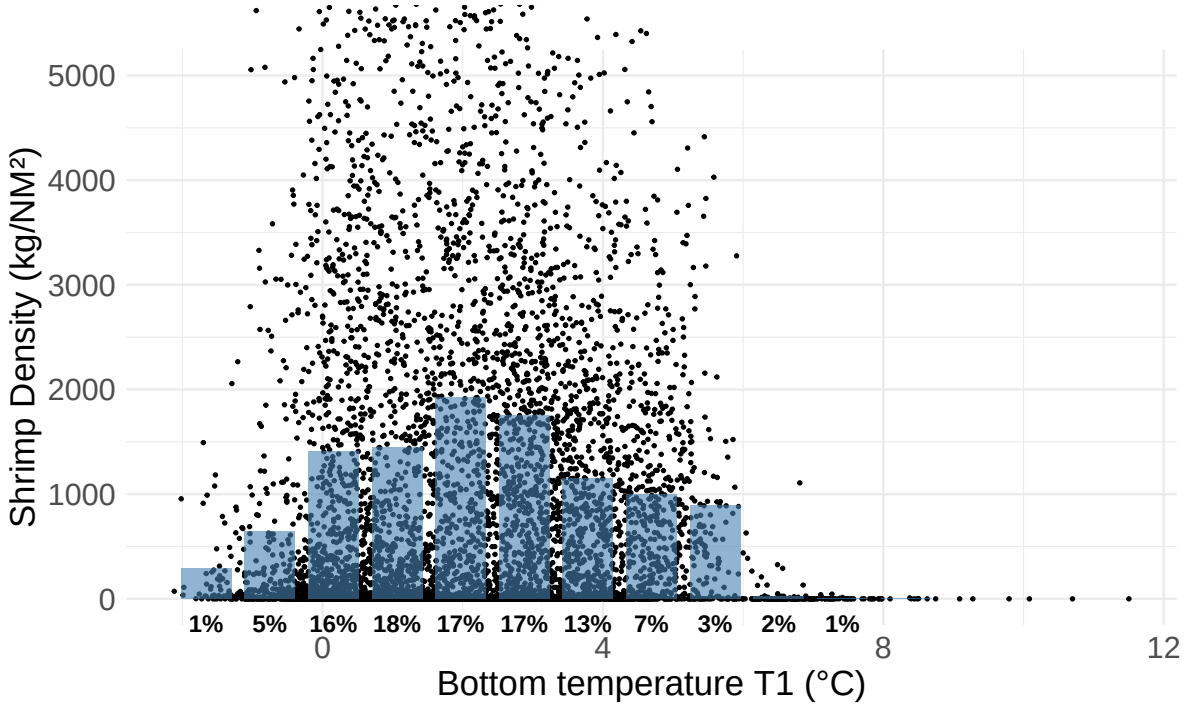

Figure 3.3: Mean monthly bottom temperature in sampling month (data treatment 1) against shrimp density. Blue columns represent the mean shrimp density at each interval of the environmental variable. Percentages display the amount of data concentrated at a given interval.

After fitting a spatiotemporal distribution model to each of the environmental variables and treatments, the AIC criterion was used to compare their performance to a baseline model that did not include any environmental factors. Only models including temperature performed better than the baseline model, indicated by lower AIC values (Figure 3.4). Remarkably, the model that performed best was the one with the 12-month lagged mean temperature (-58 units lower than the baseline model). The conditional effects of these variables in their respective models were plotted to visualize the modelled relationship between the environmental factors and the estimated shrimp densities (Figure 3.5).

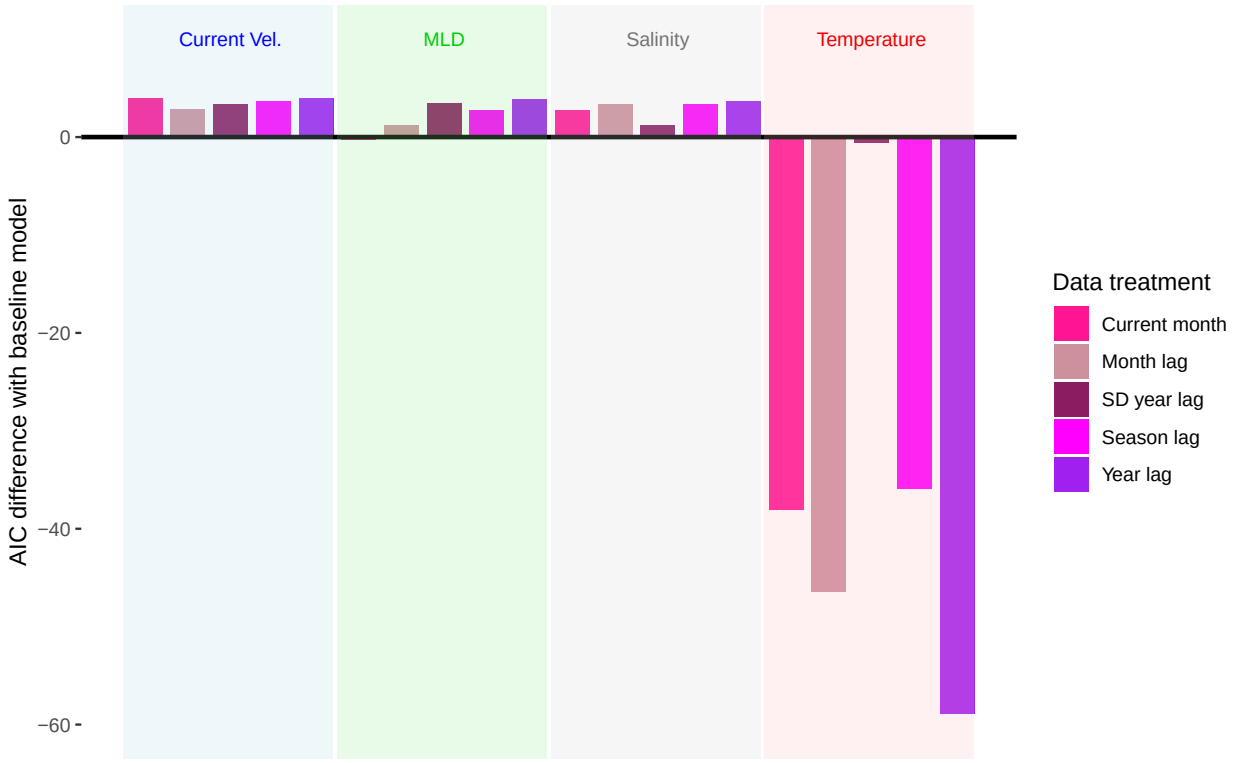

Figure 3.4: AIC score difference between baseline model and models including environmental variables.

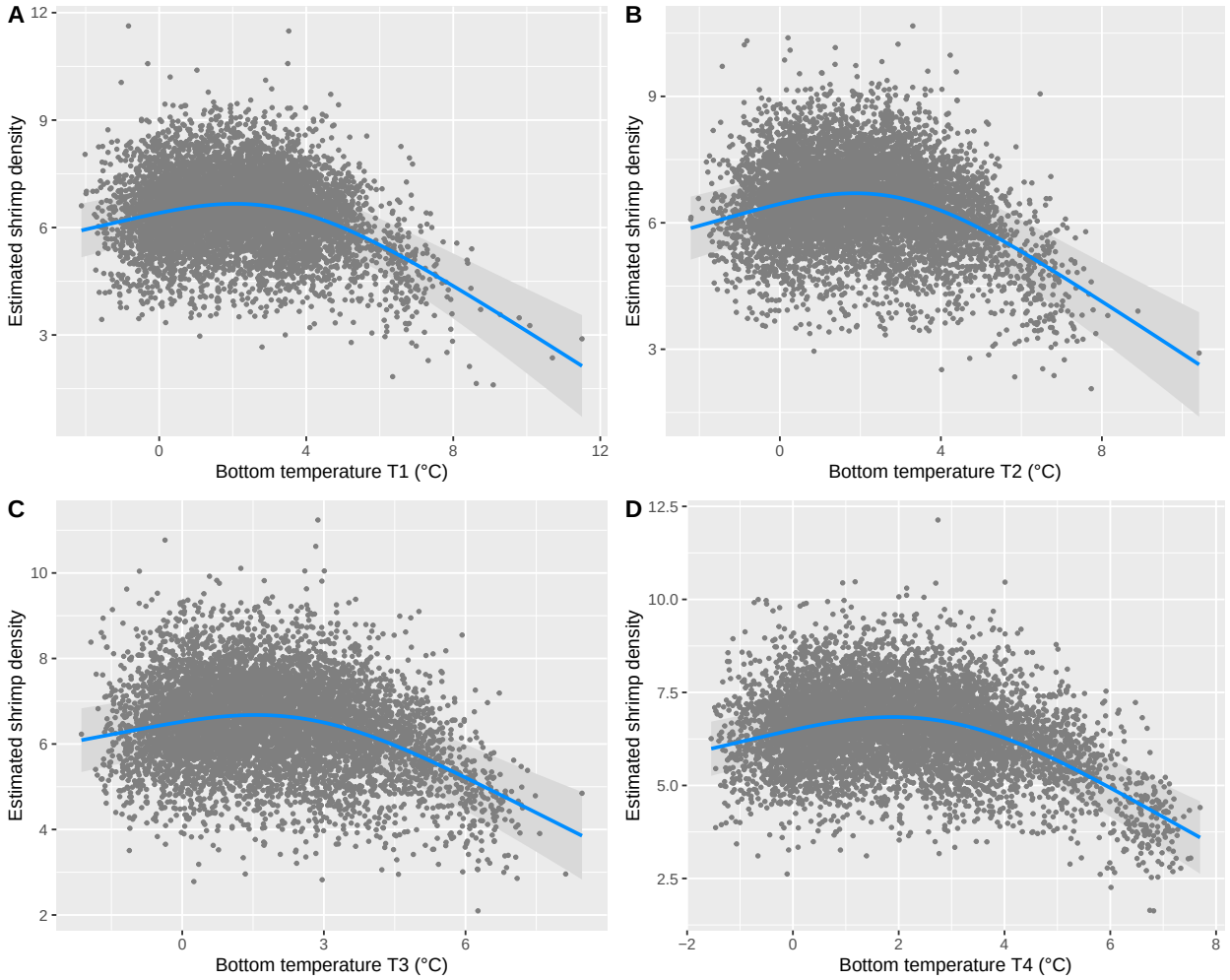

Figure 3.5: Bottom temperature conditional effects for data treatments 1-4 (A-D). Gray dots represent the observed data, and the blue lines indicate the predicted shrimp density, which the model calculates keeping all other variables constant.

While the AIC criterion points towards a clear improvement in model performance with the addition of bottom temperature, the conditional effects plots show big clouds of data which fail to cleanly follow the pattern estimated by the model (Figure 3.5). However, in the case of other variables which have been proven to be related to shrimp density, such as standardized depth, the conditional effect plot is distinctly representative of the relationship, as the data follows more clearly the line fitted by the model (Figure 3.6).

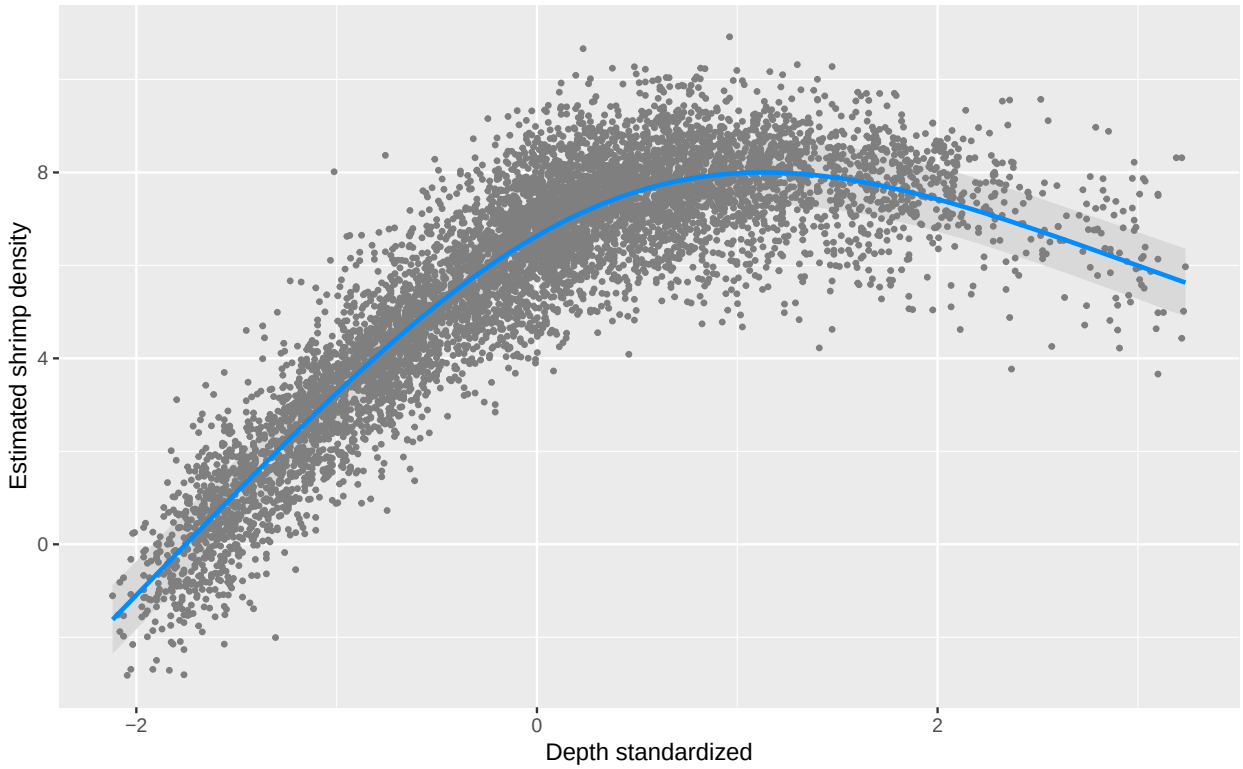

Figure 3.6: Conditional effect of depth standardized, for baseline model.

To confirm whether the addition of bottom temperature actually increased the predictive potential of the baseline model, a random sampling cross validation with 10 folds was run, comparing the baseline and the best model according to AIC selection, the one including the 12-month lagged mean of bottom temperature. The sum of log-likelihoods were compared between both models and the difference calculated, to determine which model performed best (Table 3). Since the baseline model had a higher likelihood than the environmental model, adding environmental variables did not improve predictive performance.

Table 3: Cross validation results between baseline model and alternative model with 12-month lagged mean temperature.

Model	Sum loglik	Difference	Likelihood
Null	-94418.7	0.0	Higher
Temperature (T4)	-94424.9	-6.2	Lower

3.3 Winter data relevance

Winter data was found to be representative of expected shrimp catches and consistent within the time series as well as with summer data. However, some inconsistencies, such as discrepancies between shrimp catch counts and weights, together with extreme outliers, were found in the winter data series, probably stemming from human error during data

collection. Lack of use of this dataset for analysis of shrimp over the years has kept the errors unnoticed for a long time, making it nearly impossible to trace their cause back now or correct them. Hence, the best option was to exclude unrealistic values in the winter data (Boxplot B in Figure 3.7), by comparing with outliers in the summer data (Boxplot A in Figure 3.7), which is better maintained, and hence more reliable.

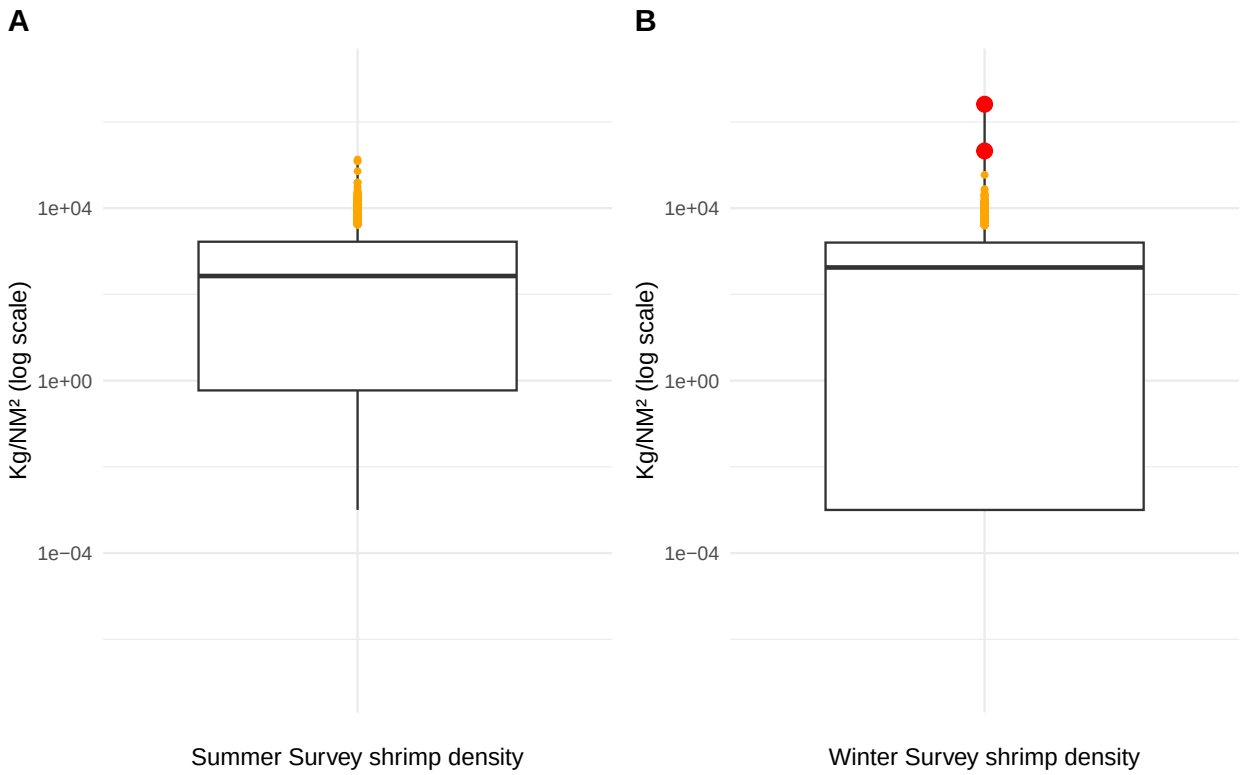

Figure 3.7: Winter and Summer Surveys shrimp density boxplots. Outliers over 1.5 interquartile ranges from the third quartile are colored. Density values over 200000 Kg/NM² are colored red.

An exponential difference between summer and winter outliers was found in some cases (Figure 3.7). This issue was solved by excluding the most extreme outliers, those with shrimp density values higher than 200 tonnes/NM² (corresponding to catch rates of 1.3 tonnes/NM). This threshold was chosen due to strong evidence that such extreme values resulted from data collection errors. However, it was set relatively high due to the highly variable nature of shrimp fishing, which can sometimes lead to very large catches.

A clear downward trend in zero catch occurrences was observed in the Winter Survey over the years (Figure 3.8), likely reflecting improvements in trawl gear efficiency and sampling techniques. However, the unusually high percentage of zero catches in 2004 deviated from this trend. Further investigation revealed that this anomaly was due to a change in shrimp sampling protocols between the 2004 and 2005 cruises: prior to 2005, all shrimp were recorded under the general category “Pandalid shrimp,” while from 2005 onward, they were identified specifically as *Pandalus borealis* (F. Zimmermann, personal communication). This change introduced inconsistencies in the data, and as a result, data from the 2004 Winter Survey were excluded from the analysis.

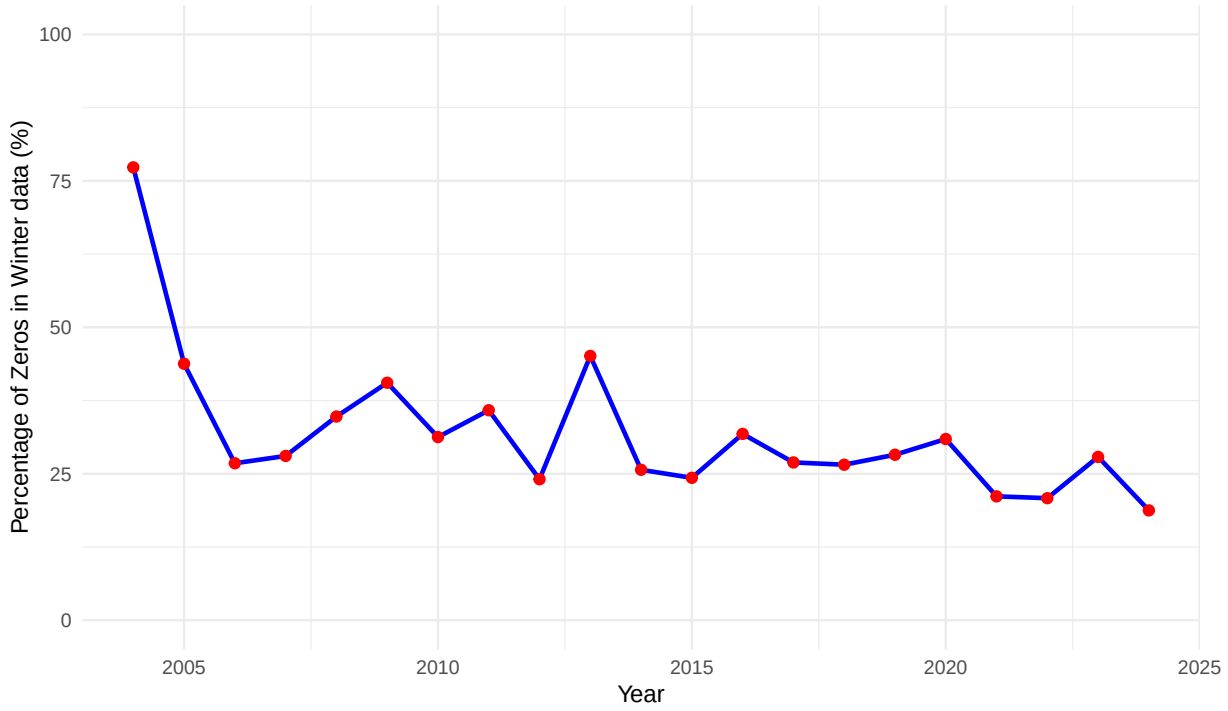

Figure 3.8: Percentage of zero catch events per year in the Winter Survey data.

As shown in Figures 2.1 and 2.2, the Winter Survey does not cover the entire study area, unlike the more comprehensive Summer Survey. This is due to sea ice, which restricts access to large portions of the northern Barents Sea during winter, making sampling impossible in those regions. To minimize bias when comparing the two survey time series, analyses were focused on an area consistently sampled in both seasons, the southwestern region (Stratum 2 in Figure 2.3) of the established shrimp strata system.

Using only data from Stratum 2, separate spatiotemporal distribution models were developed for summer and winter to estimate biomass indices (Figure 3.9). The results showed that biomass estimates from both surveys followed similar trends, with seasonal ups and downs roughly aligned. Given that winter sampling occurs earlier in the year, the data suggests that summer biomass patterns largely reflect those observed in winter.

Figure 3.9: Summer and Winter Survey indices for Stratum 2, with plus/minus one standard deviation (shaded regions).

3.4 Extended index model structure selection

Four alternative model configurations were tested by incrementally adding seasonal effects to the baseline model (Model 2 in table 2) in a parsimonious way. Of the seven total models evaluated, the two which included an interaction effect between year and season did not converge successfully (Table 4). Including season as a fixed effect with yearly time steps caused overdispersion in the spatial component, but this issue was resolved either by shortening the time steps or by modeling season as a spatially varying coefficient. Among the models that converged and met all acceptance criteria, the best performing one (Model 1 in table 4) had the lowest AIC and included season as a spatially varying coefficient (but not as a fixed effect), with whole year time steps.

Table 4: Model configurations to model the effect of seasonality. SVC(Season) refers to the addition of a spatially varying coefficient for the Season factor variable. Models are sorted by descending AIC. *Spatial random effect overdispersion parameter unusually large.

Model	Main effects	Time step	Convergence	AIC
1	Year + Depth + SunAlt + SVC(Season)	Year	TRUE	187474.7
2	Year + Depth + SunAlt + Season + SVC(Season)	Year	TRUE	187476
3	Year + Depth + SunAlt	Season	TRUE	187716.7
4	Year + Depth + SunAlt + Season	Season	TRUE	187718
5	Year + Depth + SunAlt + Season	Year	TRUE*	188076
6	Year + Depth + SunAlt + Year:Season	Year	FALSE	
7	Year + Depth + SunAlt + Season + Year:Season	Year	FALSE	

3.5 Extended index model diagnostics

Diagnostics of the extended index model showed overall a good performance, suggesting that the best fitting model and its resulting index can be accepted for assessment purposes. Residuals of the selected model were first visualized using Q-Q plots (Annex Figures 7.6 and 7.7). Both QQ plots show slight deviations from the QQ line in the tails; however, this is not uncommon in spatiotemporal distribution models and does not imply severe model assumptions violations (F. Zimmermann personal communication). Furthermore, the spatial distribution of residuals in the study area was plotted (Annex Figure 7.8). No residuals were particularly large or small in certain areas over multiple years, so the extended index model was accepted.

3.6 Extended index model predictions

Biomass predictions, which include all fixed and random effects, were mapped in the study area for every year in the time series (Annex Figure 7.9.Shrimp biomass was higher in central parts of the study area, while marginal zones consistently showed very low shrimp densities (Figure 3.10). Annual variation in shrimp biomass was also detected, with particularly low densities during 2004, 2016 and 2021 and peaks during years 2010, 2018 and 2023 (Figures 3.10 and 3.15). We could also observe slight shifts in biomass between the Hopen Deep and the “Loophole Area” over the years.

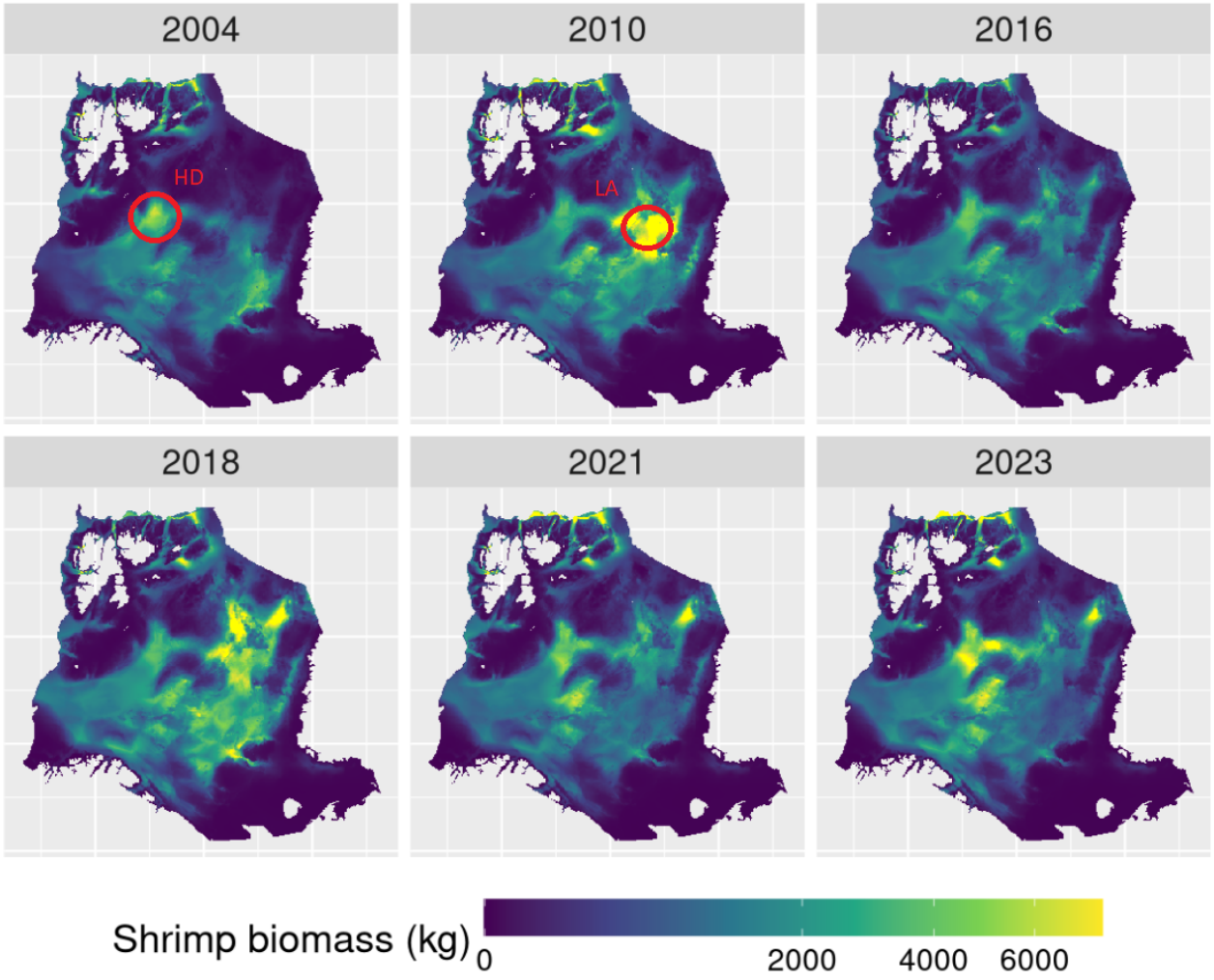

Figure 3.10: Northern shrimp biomass predictions obtained using the extended index model, showing the combined outcome of fixed and random effects predicted over the study area for years 2004, 2010, 2016, 2018, 2021 and 2023. HD refers to Hopen Deep and LA to Loophole Area.

The depths in the study area contributed to explain much of the spatial variation of shrimp densities (Annex Figure 7.10), with higher predictions in deeper areas, such as the Hopen Deep and along the Bear Island trench, that connects it to the deeper Atlantic Ocean (Figure 3.11).

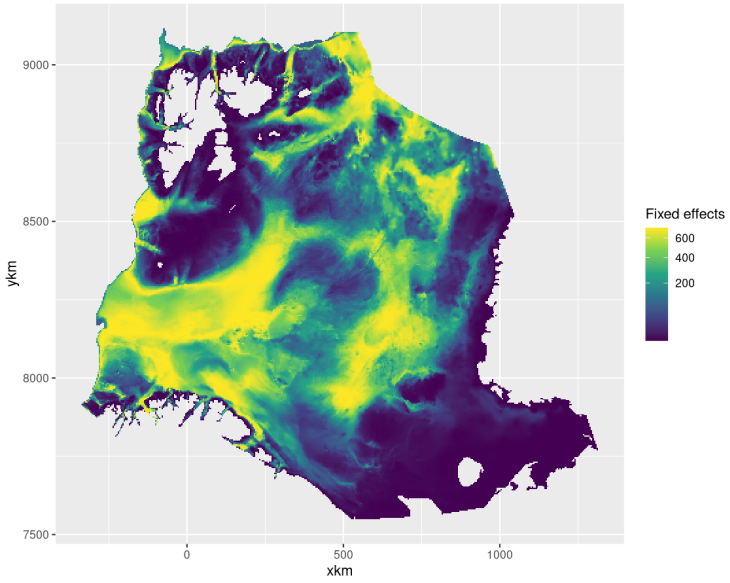

Figure 3.11: Predicted fixed effects for the extended index model for 2024. Estimates are on the log-scale, and correspond to density when back-transformed.

The season effect is not included within the fixed effects, and instead received its own spatially varying coefficient, which allows the model to change the value of the season effect across the study area (Figure 3.12). Surrounding areas west and south of Svalbard, and also some other spots towards the central Barents Sea, showed high values of spatial variation for the season component, which represent larger seasonal shrimp densities during summer, since predictions were calculated for this season.

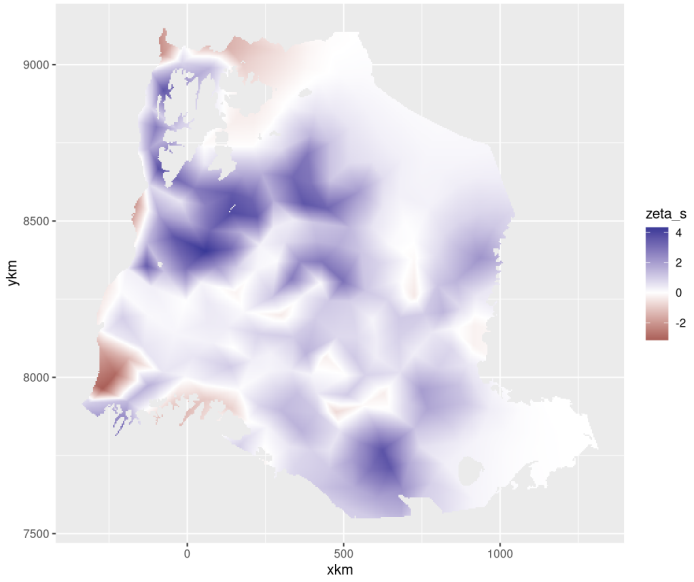

Figure 3.12: Predicted spatially varying coefficient (zeta s), modelling the season effect in the extended index model. Estimates are on the log-scale, and correspond to density when back-transformed.

Areas where shrimp biomass deviated significantly from what was predicted by fixed effects were identified across the survey region, by means of the spatial random field. Higher-than-expected biomass was observed primarily around the Svalbard archipelago and in large parts of the central Barents Sea. In contrast, lower-than-expected biomass occurred along the southwestern Barents Sea near the Norwegian coast, the southeastern Russian EEZ, and the northernmost areas bordering the Arctic Ocean. In much of the study area, however, biomass estimates aligned well with fixed effects, resulting in spatial random effects near zero or relatively small (Figure3.13).

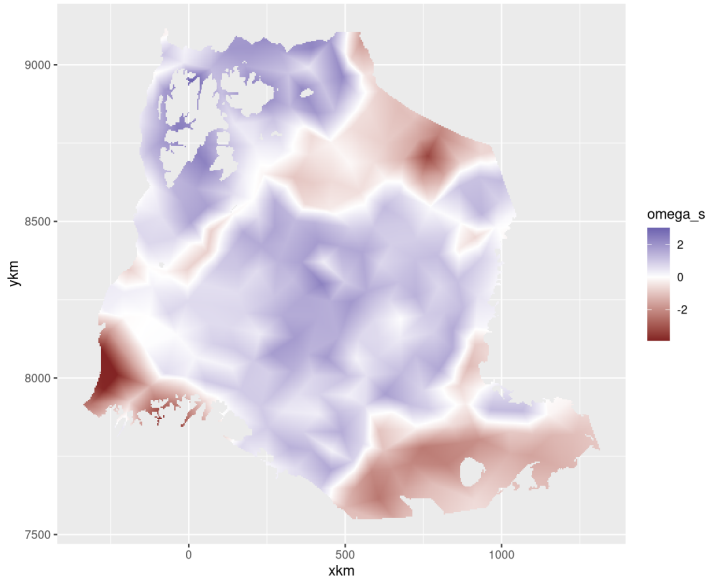

Figure 3.13: Predicted spatial random effects (omega s) for the extended index model. Estimates are on the log-scale, and correspond to density when back-transformed.

The spatiotemporal random effects revealed substantial temporal variation in shrimp biomass distribution (Annex Figure 7.11), with a moderate standard deviation of 1.28, indicating meaningful year-to-year fluctuations. Despite this variability, transitions between years were smooth, as reflected by a high first-order autoregressive correlation of 0.93. Some areas exhibited consistent patterns over time, such as persistently low estimates in the southeastern tip of the study area, suggesting biomass was systematically overestimated there by the fixed and spatial effects (Figure 3.14).

In contrast, other regions showed temporal shifts in the spatiotemporal component. For example, the northernmost Barents Sea initially displayed strong negative deviations, which gradually shifted to neutral or even positive values by 2018, indicating higher-than-expected shrimp biomass. Similarly, the Hopen Deep area south of Svalbard exhibited fluctuations between positive and negative effects over the years, even in periods of generally high shrimp abundance like 2010 and 2018 (Figure 3.10).

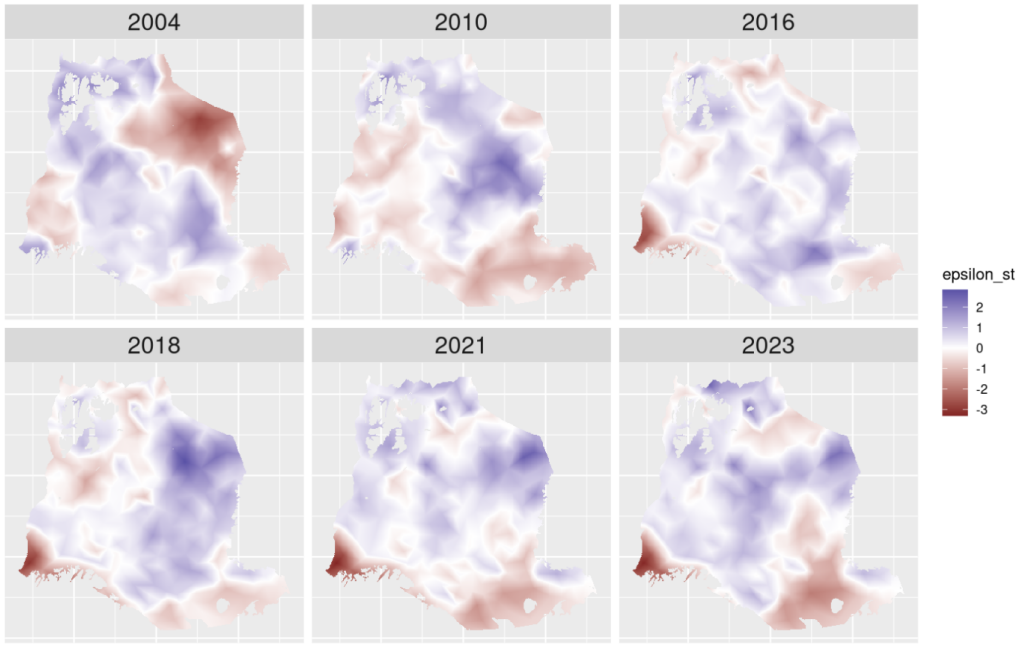

Figure 3.14: Predicted spatiotemporal random effects (epsilon st) for the extended index model, for years 2004, 2010, 2016, 2018, 2021 and 2023. The complete time series can be accessed in the Annex. Estimates are on the log-scale, and correspond to density when back-transformed.

The prediction maps were summarized into annual biomass indices, which clearly revealed recurring cycles of high and low shrimp biomass. These patterns were consistent across models: the benchmark summer index closely matched both the summer and winter indices from the extended index model. This alignment supports the inclusion of winter data as a valuable enhancement, confirming its relevance and contribution to improving model performance (Figure 3.15).

3.7 Implications for assessment

The extended assessment model, incorporating the new indices from the extended index model (Figure 3.15) produced results consistent with the benchmark assessment model. Estimates for reference points such as *Bmsy* and *Fmsy* remained nearly identical across both models, with wide and overlapping confidence intervals (Figure 3.16). The new indices also passed all one-step-ahead (OSA) residual diagnostic checks, demonstrating their suitability and reinforcing the value of including winter data in the assessment (Annex Figure 7.12).

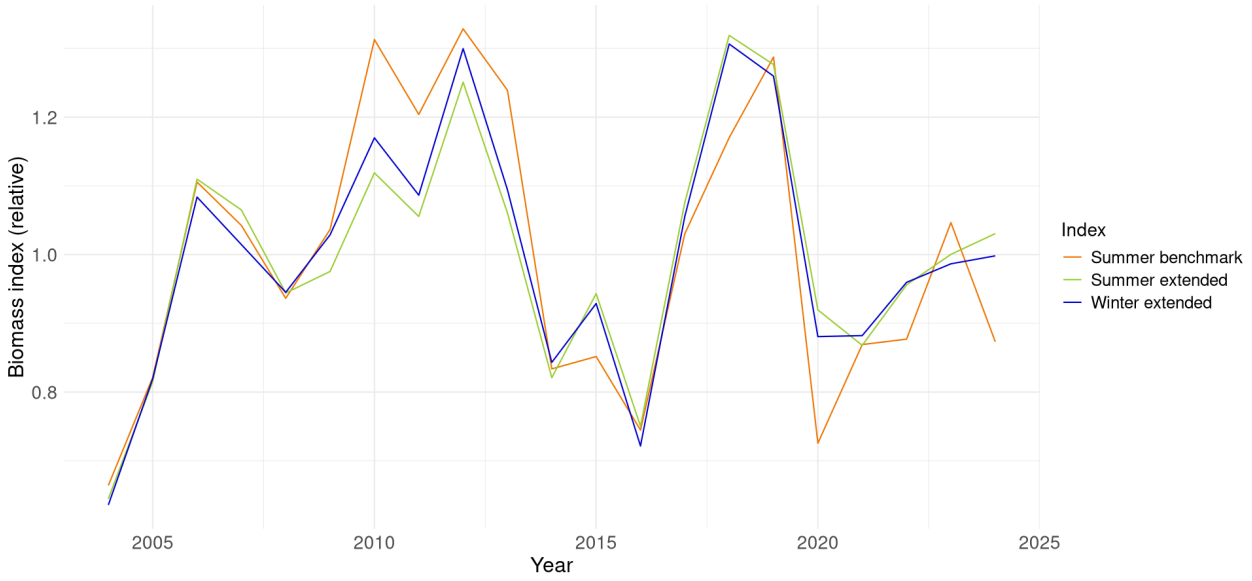

Figure 3.15: Indices of stock biomass from the benchmark index model (Summer index) and extended index model (Summer and Winter indices). Lines show the mean estimates. All indices were standardized to their respective mean.

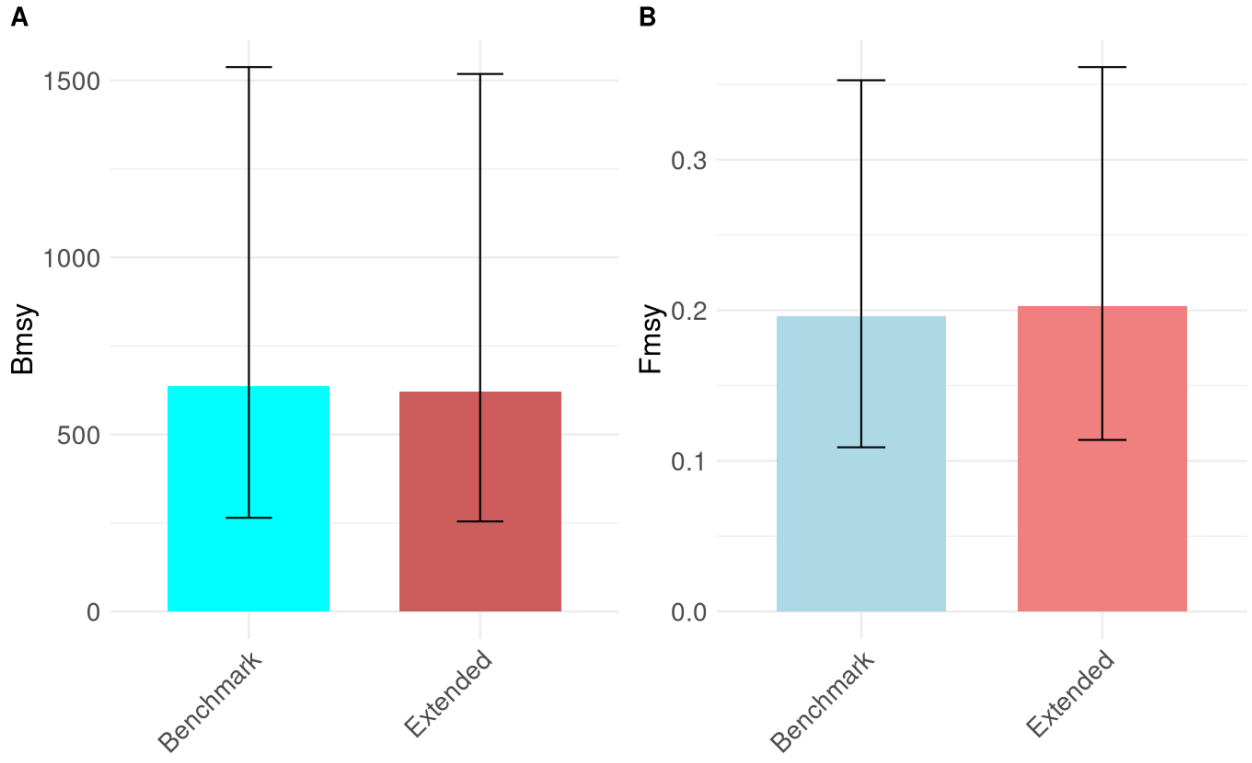

Figure 3.16: Reference points Bmsy (A) and Fmsy (B) for the benchmark and extended assessment models, with confidence intervals.

A minor diagnostic issue related to the CPUE and Historic Surveys indices was observed, but this issue was not introduced by the new model, as it was already present in the benchmark assessment model. This issue involves autocorrelation in the OSA residuals for CPUE data (Annex Figures 7.12 and 7.14), which arises from inherent inconsistencies between CPUE and survey trends. Since the model weighs survey indices more heavily due to lower observation error, the CPUE data consistently shows residual patterns, as often several years in a row fall above or below the estimated biomass (Figure 3.17). This results in autocorrelated OSA residuals and minor violations in biomass process residuals (Annex Figures 7.13 and 7.15). Nonetheless, these are minor violations, present in both the benchmark and extended assessment models.

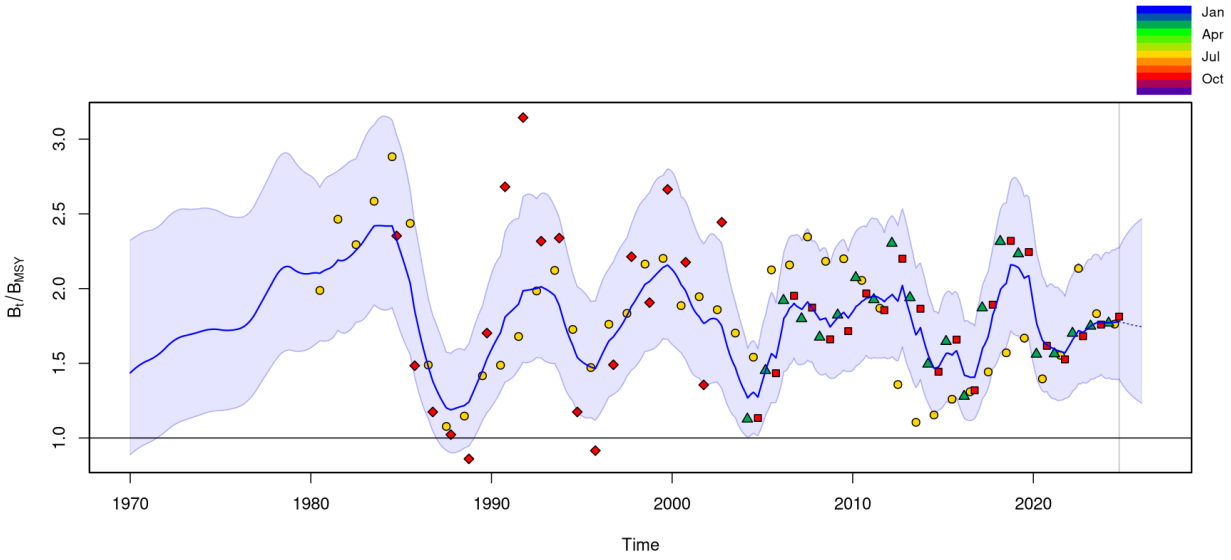

Figure 3.17: Relative biomass estimated by the extended assessment model, with 95% uncertainty ribbons and index data. Circles represent the CPUE index, diamonds are for the Historic Surveys index, Triangles refer to the winter index, and squares to the summer index. Colors refer to the month when the data was collected (see legend).

Retrospective analysis evaluated the predictive performance of the models by estimating relative biomass and fishing mortality from gradually peeled data, and comparing these values against those from the full data series (Figures 3.18 and 3.19). Total prediction error and Mohn's rho, a estimation bias diagnostic, indicated that the extended assessment model had a better predictive performance compared to the benchmark assessment model.

Referring to the biomass retrospective estimations, the extended assessment model showed a lower total prediction error compared to the benchmark assessment model, as the final year estimations aligned better with the baseline estimates. Even though Mohn's Rho values are within limits that would not initially indicate estimation bias (Hurtado-Ferro et al., 2015), caution is warranted in interpreting Mohn's Rho alone, since it can compensate strong biases in the data if they occur in opposite directions (Goto et al., 2022). This is the case especially in the benchmark assessment model retrospective analysis (Figure 3.18, where the Retro_5 peel markedly overestimated biomass and its rate of decline, while consistently underestimating biomass in the latter peels. This asymmetry skews the average retrospective pattern and can mask underlying bias. However, this issue is less pronounced in the extended asessment model, as the final

year estimates fall closer to the baseline, and do not consistently underestimate biomass (Figure 3.19).

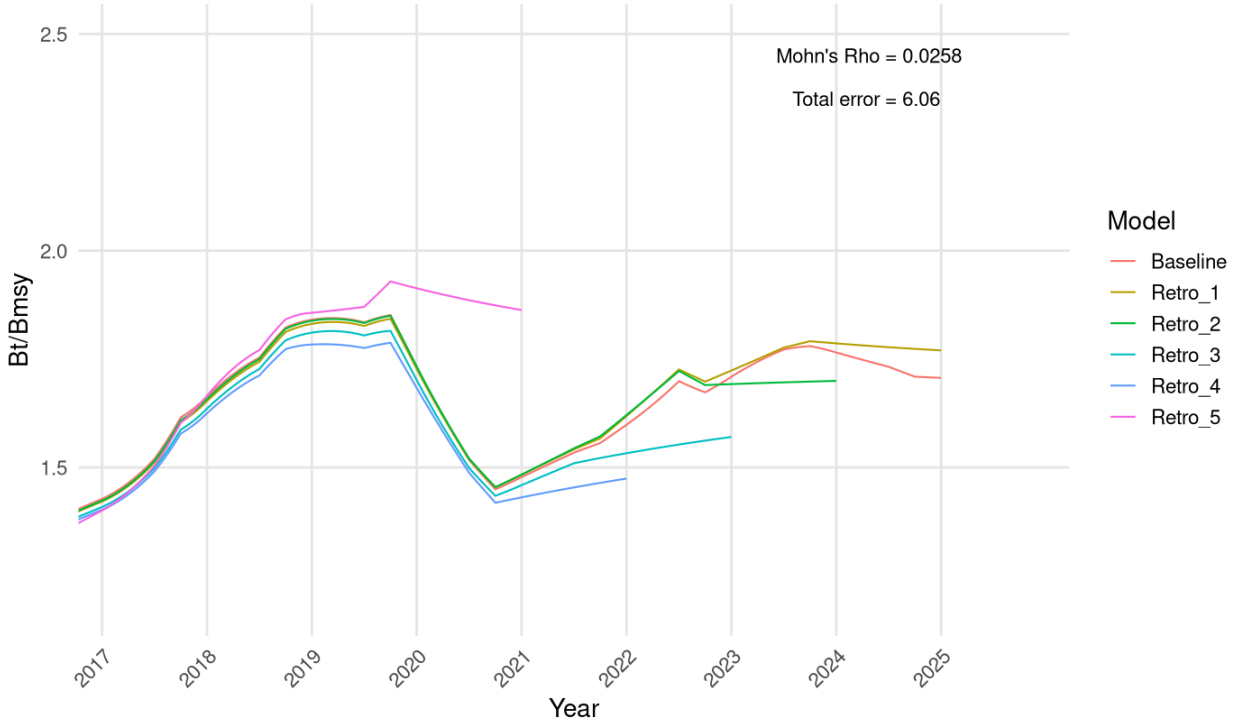

Figure 3.18: Retrospective analysis for biomass, using the benchmark assessment model, with Mohn's Rho and total prediction error for each retrospective run compared to the baseline. The baseline model represents the complete benchmark assessment model, trained with all data available until summer 2024. Each retrospective model is trained with one year less of data, and the last yearly data segment of each line is a forecast.

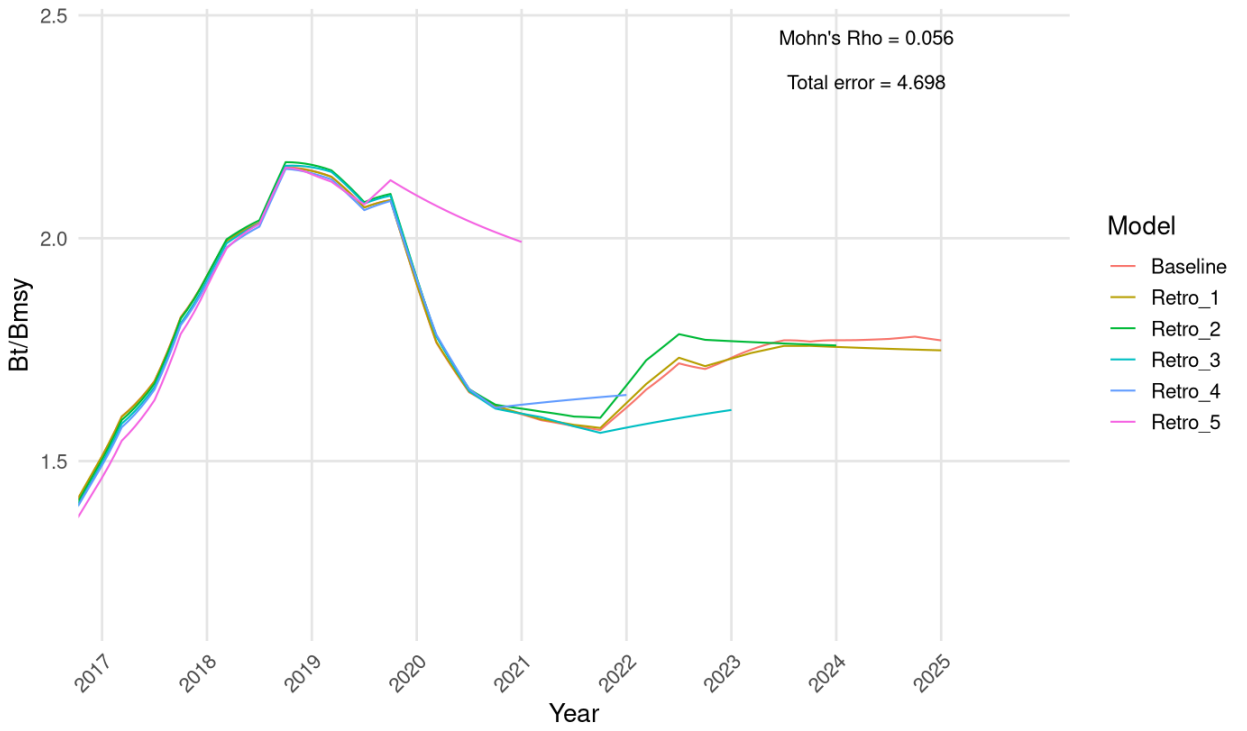

Figure 3.19: Retrospective analysis for biomass, using the extended assessment model, with Mohn's Rho and total prediction error for each retrospective run compared to the baseline. The baseline model represents the complete extended assessment model, trained with all data available until summer 2024. Each retrospective model is trained with one year less of data, and the last yearly data segment of each line is a forecast.

Fishing mortality retrospective analysis followed very similar patterns as those observed in biomass. The benchmark assessment model was less accurate in its predictions, as most of its retrospective runs diverged from the baseline (Figure 3.20), while the extended assessment model showed more accurate predictions of fishing mortality, that stayed closer to the baseline (Figure 3.21).

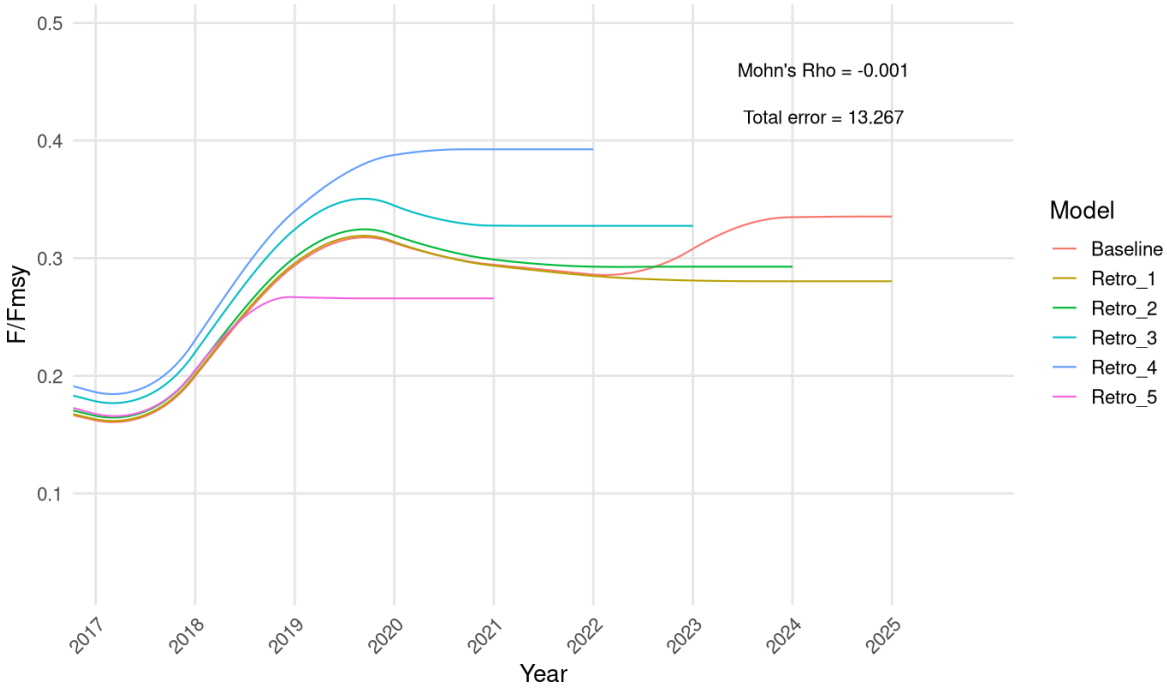

Figure 3.20: Retrospective analysis for fishing mortality, using the benchmark assessment model.

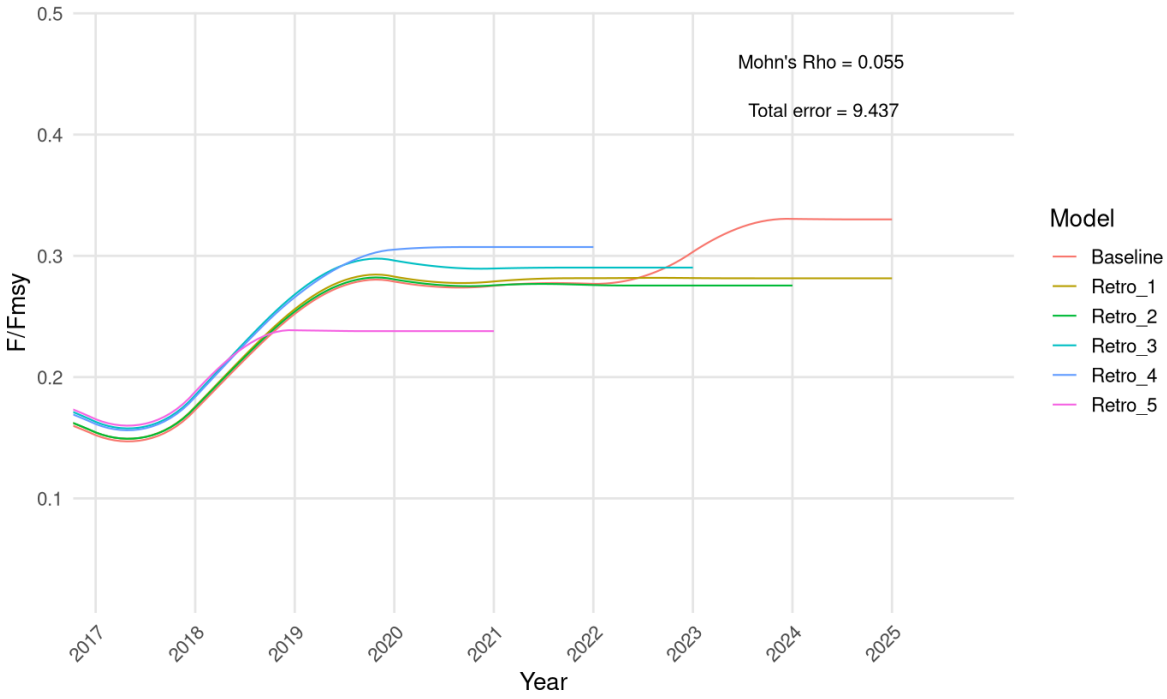

Figure 3.21: Retrospective analysis for fishing mortality, using the extended assessment model.

4 Discussion

The main findings of this study were evaluated in light of current literature, contextualising the results and their broader implications. We examined the performance and limitations of the spatiotemporal distribution model, the influence of environmental variables, the added value of winter survey data, and the implications for stock assessment. These components were critically assessed to determine how effectively the updated modeling approach captures Northern shrimp dynamics and informs sustainable management in the face of ecological variability and evolving fishing practices.

4.1 Spatiotemporal distribution model

Several model improvements were considered, to increase the accuracy of the benchmark index model. The addition of a barrier mesh to account for the limited connectivity in this area did not provide any model improvements. Instead, it created severe instability in the model, making random effects standard deviations soar, reason why it was finally discarded. Further research is recommended as to elucidate the causes of this instability, as well as a revision of the barrier mesh function in the "sdmTMBextra" package.

The decision to replace "hour" with "sun altitude" as a main effect in the model was based primarily on biological reasoning: sun altitude has a much stronger and more direct relationship with shrimp density. While hour was previously used in the benchmark index model because it explained some variability in the data, its effect on shrimp biomass is actually mediated by sun altitude. Sun altitude influences the vertical migration of shrimp (Brierley, 2014), which in turn affects catch rates throughout the day. In this context, hour functions as a proxy for sun altitude, that only holds under consistent seasonal conditions, when the relationship between time of day and sunlight remains stable. However, this assumption breaks down with the inclusion of winter data, especially in the Arctic, where daylight hours differ significantly from those in summer. Moreover, the higher AIC observed in the model using "hour" suggests it may be capturing not just the biological signal, but also excess noise and in-sample patterns, leading to overfitting, which is a common issue with large, noisy datasets. For these reasons, the model using sun altitude, which more accurately reflects the biological mechanisms involved, was selected.

4.2 Environmental effects

In contrast to expectations that environmental variables would be good predictors of shrimp biomass density based on the biology of shrimp, no significant increment in the benchmark index model performance was obtained after the integration of current velocity, salinity, MLD or temperature. Initial exploratory analyses using descriptive statistics, followed by model comparisons and AIC based selection suggested that temperature might be an important predictor of shrimp density in the study area. However, this was not supported by k-fold cross validation (k = 10), which showed that including temperature actually reduced the likelihood of the model compared to the baseline model.

The other environmental variables current velocity, salinity and MLD also failed to show any relationship with shrimp density. One explanation for these results might be the limited contrast in the data that only covers relatively homo-

geneous parts of the Barents Sea that represent mostly potential shrimp habitat (Hvingel & Zimmermann, 2023). The analysis did therefore not include many observations at the edges or outside the the environmental window that northern shrimp inhabits. In the case of salinity, for instance, its limited variation across the dataset did not include any areas of low salinity. This made it difficult to assess a relationship with shrimp density, although shrimp can not tolerate salinities outside a specific range (Hall, 2017). Nonetheless, salinity may still be useful in other modelling frameworks, particularly for predicting shrimp presence rather than abundance. Descriptive plots revealed that most shrimp biomass occurred within a narrow salinity range, between 34.75 ppt and 35.25 ppt, in line with current literature (Garcia, 2007; Krawczyk et al., 2024).

Importantly, the lack of significant relationships between environmental variables and Northern shrimp density in this study does not imply that such relationships do not exist in nature. Besides the limited contrast in the data, deriving the environmental data from monthly means represents a further limitation, as this may smooth out short term variations. For instance, brief but intense events like heatwaves lasting less than a month would be averaged out in the data, but would still have significant impacts in shrimp populations (Brander, 2010; Cheung et al., 2021).

Additionally, shrimp density is a relatively coarse measure of stock dynamics and their environmental interactions. Density is a product of abundance and individual weight, while environmental effects are likely to act more on life-history processes such as larval development, growth or maturity (T. Rasmussen & Tande, 1995; Wieland & Siegstad, 2012). More specific biological indicators, such as individual fitness, reproductive output, or larval survival, may offer better insights into environmental drivers of stock dynamics. While this type of data is more costly and less commonly collected, survey protocols are starting to incorporate metrics related to reproductive potential and size structure of the shrimp population. Future studies should therefore focus on potential links between environment, life history and stock dynamics.

4.3 Winter data relevance

The trends in the winter data aligned well with those from the Summer Survey, confirming that shrimp distribution and densities are relatively inert due to limited mobility. Northern shrimp typically remain within the same area throughout their lives (Corre et al., 2020). The correspondence between biomass indices from Summer and Winter Surveys was high, facilitating the integration of the two datasets into a joint model despite challenges such as outliers, inconsistencies, and issues from long-term maintenance problems in the Winter Survey data.

That AIC selected the extended index model with a spatially varying coefficient by season indicates that the seasonal effect on shrimp density changes across different parts of the study area. In other words, there is considerable spatial variability present on a finer time scale in the Barents Sea despite longer-term consistency in distribution and density. This implies that seasonality can impact local shrimp populations in different ways. Potential reasons for this might be the heterogeneous spatiotemporal distribution of the shrimp fishery and predators such as cod, impacting the shrimp stock differently at a local scale.

Shrimp biomass prediction maps over time reveal how shrimp biomass abundance and distribution have evolved over

the years. The areas with consistently high biomass, such as the Hopen Deep and the Loophole area, also coincide with the areas where most of the fishing effort concentrates. In contrast, large regions with medium or low biomass remain relatively unfished, potentially representing refuges that support the long-term productivity of the stock. The observed variability, not only in the seasonality effect but also on the spatial and spatiotemporal random fields, raises important questions on whether a single stock assessment for the whole Barents Sea shrimp is appropriate. Spatial stock structure should be therefore explored to consider a stock assessment of a meta-stock or multiple separate stocks based on environmental and biological criteria, as has been proposed in other studies (Cardinale et al., 2023; Hansen et al., 2021; Jorde et al., 2015).

4.4 Implications for assessment

An extended assessment model was developed by incorporating a newly created winter index and an updated summer index, both based on the extended index model. The extended assessment model integrated well the winter index. However, issues with fits of the CPUE and Historical Survey indices persisted, identical to those previously described for the benchmark assessment model (ICES, 2022). These discrepancies likely stem from the differing trends in the CPUE index compared to the BESS and Winter Survey indices (Hvingel & Zimmermann, 2023).

One key factor behind these discrepancies is how fishing effort is accounted for in the CPUE. The Northern shrimp fishery has undergone significant technological advancements over time, such as but not limited to increases in engine power and vessel capacity. This technological creep can bias CPUE data (Marchal et al., 2007). In contrast, fishery independent surveys aim to produce accurate and standardized biomass estimates, making them more reliable for assessment purposes.

Moreover, CPUE data only reflects fishing activity in specific areas where Norwegian industrial fleets operate, which are primarily Hopen Deep, the Loophole area, and occasionally Svalbard. Today, these fleets represent less than half of the total fishing activity. Over the past 40 years, the area where the fishing fleet is active has shrunk substantially, contracting to specific areas of high shrimp densities (Zimmermann et al., 2024). Given these limitations, survey data were prioritized in the assessment model, with reduced reliance on CPUE.

When comparing the extended assessment model with the benchmark assessment model, both produced similar estimates for stock status and reference points. However, both models exhibited high levels of uncertainty, especially for the reference points, which is not unusual when estimating absolute values in stock assessments. Surplus production models generally perform better when used to assess relative trends (Kokkalis et al., 2024; Pedersen & Berg, 2017).

To evaluate whether the extended model improved performance, a retrospective analysis was conducted peeling input data back in time to simulate forecasting scenarios. Afterwards, these retrospective estimations were compared with the observed data from the complete time series. The results showed that the extended model outperformed the benchmark model, with lower prediction errors for both biomass and fishing mortality. This highlights the value of incorporating winter data to enhance accuracy, especially when BESS data for the assessment year is incomplete or unavailable.

5 Conclusions

This study combined additional survey data, environmental information, and advanced modeling techniques to improve the stock assessment of Barents Sea shrimp. While some elements, like exploring the use of alternative mesh or distribution family configurations in the biomass index model did not contribute meaningfully, others yielded important improvements. The results provide therefore an important basis for the further development of the stock assessment, contributing to a more robust catch advice in the future.

By grounding our modeling approach in biological and ecological understanding, we adapted both the biomass index and stock assessment models to include Winter Survey data for the first time in Barents Sea shrimp assessments. Although environmental variables ultimately did not improve model performance and were excluded, the comprehensive evaluation improved on prior analyses that were much more limited in scope and confirmed the limitations of using biomass as a coarse metric. Future research should explore biological indicators with more direct, mechanistic link to environmental drivers, such as those reflecting specific responses to environmental conditions at different life stages. This includes specifically the need to investigate the impacts of food availability and predation as direct sources of growth and mortality. Finer weekly or daily environmental data could also be relevant for unraveling the relationships between Northern shrimp and environmental conditions in future research. The results also revealed substantial spatial and spatiotemporal variability in shrimp densities reflected in significant effects of spatial random fields. These random effects are likely linked to both biotic and abiotic processes that are currently not explicitly accounted for in the index model and should be subject to further research.

Finally, even though the Barents Sea shrimp fishery is currently considered sustainably exploited, the growing pressure of increasing fishing activity combined with other anthropogenic impacts such as climate change, pose serious risks for a vulnerable arctic marine ecosystem such as the Barents Sea. Northern shrimp can be considered a keystone species given its large biomass and important role as food source for many higher trophic species such as cod and haddock. This should prompt managers and policy makers to start actively managing this valuable resource, with a focus on long-term ecological, social and economic sustainability.

6 Bibliography

Anderson, S. C. (2024). *sdmTMBextra: Extra functions for working with 'sdmTMB' models*.

Anderson, S. C., Ward, E. J., English, P. A., Barnett, L. A. K., & Thorson, J. T. (2025). *sdmTMB: An r package for fast, flexible, and user-friendly generalized linear mixed effects models with spatial and spatiotemporal random fields*. https://doi.org/10.1101/2022.03.24.485545

Ariza, P., & Ouellet, P. (2009). Diet components of northern shrimp pandalus borealis first stage larvae in the northwest gulf of st. lawrence. *Journal of Crustacean Biology*, *29*, 532–543. https://doi.org/10.1651/08-3113.1

Aschan, M. (2000). Spatial variability in length frequency distribution and growth of shrimp (pandalus borealis krøyer 1838) in the barents sea. *Journal of Northwest Atlantic Fisheries Science*, *27*, 93–105. http://journal.nafo.int

Aschan, M., Bakenev, S., Berenboim, B., & Sunnanå, K. (2004). *Management of the shrimp fishery (pandalus borealis) in the barents sea and spitsbergen area*. Institute of Marine Research, Polar Research Institute of Marine Fisheries; Oceanography(PINRO).

Aschan, M., & Ingvaldsen, R. (2009). Recruitment of shrimp (pandalus borealis) in the barents sea related to spawning stock and environment. *Deep-Sea Research Part II: Topical Studies in Oceanography*, *56*, 2012–2022. https://doi.org/10.1016/j.dsr2.2008.11.012

Barr, L. (1970). Diel vertical migration of pandalus borealis in kachemak bay, alaska. *Journal Fisheries Research Board of Canada*, *27*.

Beguin, J., Martino, S., Rue, H., & Cumming, S. G. (2012). Hierarchical analysis of spatially autocorrelated ecological data using integrated nested laplace approximation. *Methods in Ecology and Evolution*, *3*, 921–929. https://doi.org/10.1111/j.2041-210X.2012.00211.x

Bergström, B. (1992). Growth, growth modelling and age determination of pandalus borealis. *MARINE ECOLOGY PROGRESS SERIES Mar. Ecol. Prog. Ser*, *83*, 167–183.

Bergström, B. (2000). The biology of pandalus. In *Advances in Marine Biology* (Vol. 38).

Björnsson, B., Reynisson, P., Solmundsson, J., & Valdimarsson, H. (2011). Seasonal changes in migratory and predatory activity of two species of gadoid preying on inshore northern shrimp pandalus borealis. *Journal of Fish Biology*, *78*, 1110–1131. https://doi.org/10.1111/j.1095-8649.2011.02923.x

Bodur, Y. V., Renaud, P. E., Goraguer, L., Amargant-Arumí, M., Assmy, P., Dąbrowska, A. M., Marquardt, M., Renner, A. H. H., Tatarek, A., & Reigstad, M. (2023). Seasonal patterns of vertical flux in the northwestern barents sea under atlantic water influence and sea-ice decline. *Progress in Oceanography*, *219*. https://doi.org/10.1016/j.pocean.2023.103132

Brander, K. (2010). Impacts of climate change on fisheries. *Journal of Marine Systems*, *79*, 389–402. https://doi.org/10.1016/j.jmarsys.2008.12.015

Brander, K. (2013). Climate and current anthropogenic impacts on fisheries. *Climatic Change*, *119*, 9–21. https://doi.org/10.1007/s10584-012-0541-2

Brierley, A. S. (2014). Diel vertical migration. In *Current Biology* (Vol. 24, pp. 1074–1076). Cell Press. https://doi.org/10.1016/j.cub.2014.08.054

Cardinale, M., Zimmermann, F., Søvik, G., Griffiths, C. A., Nord, M. B., & Winker, H. (2023). Spatially explicit stock assessment uncovers sequential depletion of northern shrimp stock components in the north sea. *ICES Journal of Marine Science*, *80*, 1868–1880. https://doi.org/10.1093/icesjms/fsad111

Cheung, W. W. L., Frölicher, T. L., Lam, V. W. Y., Oyinlola, M. A., Reygondeau, G., Sumaila, U. R., Tai, T. C., Teh, L. C. L., & Wabnitz, C. C. C. (2021). Marine high temperature extremes amplify the impacts of climate change on fish and fisheries. *Science Advances*, *7*, 15. https://doi.org/10.1126/sciadv.abh0895

CMEMS. (2024). *GLORYS12V1*. Copernicus Marine Environment Monitoring Service; https://doi.org/10.48670/moi-

00021.

Corre, N. L., Pepin, P., Burmeister, A. D., Walkusz, W., Skanes, K., Wang, Z., Brickman, D., & Snelgrove, P. V. R. (2020). Larval connectivity of northern shrimp (pandalus borealis) in the northwest atlantic. *Canadian Journal of Fisheries and Aquatic Sciences*, *77*, 1332–1347. https://doi.org/10.1139/cjfas-2019-0454

Cushing, D. H. (1990). Plankton production and year-class strength in fish populations: An update of the match/mismatch hypothesis. *Advances in Marine Biology*, *26*, 249–293.

Galappaththi, E. K., Susarla, V. B., Loutet, S. J. T., Ichien, S. T., Hyman, A. A., & Ford, J. D. (2022). Climate change adaptation in fisheries. *Fish and Fisheries*, *23*, 4–21. https://doi.org/10.1111/faf.12595

Garcia, E. G. (2007). The northern shrimp (pandalus borealis) offshore fishery in the northeast atlantic. In *Advances in Marine Biology* (Vol. 52, pp. 147–266). https://doi.org/10.1016/S0065-2881(06)52002-4

Goethel, D. R., Berger, A. M., & Cadrin, S. X. (2023). Spatial awareness: Good practices and pragmatic recommendations for developing spatially structured stock assessments. *Fisheries Research*, *264*. https://doi.org/10.1016/j.fishres.2023.106703

Goto, D., Devine, J. A., Umar, I., Fischer, S. H., Oliveira, J. A. A. D., Howell, D., Jardim, E., Mosqueira, I., & Ono, K. (2022). Running head: Managing harvest with biased assessments shaping sustainable harvest boundaries for marine populations despite estimation bias 2 3 present address open research statement. *Ecosphere*, *13*(2), e3923. https://doi.org/10.6084/m9.figshare.13281266

Hall, E. F. (2017). *The vulnerability of different populations of the commercially-important shrimp pandalus borealis to environmental stress* [Thesis, University of Plymouth]. https://pearl.plymouth.ac.uk/bms-theses/140

Hansen, A., Westgaard, J.-I., Søvik, G., Hanebrekke, T., Nilssen, E. M., Jorde, P. E., Albretsen, J., & Johansen, T. (2021). Genetic differentiation between inshore and offshore populations of northern shrimp (pandalus borealis). *ICES Journal of Marine Science*, *78*, 3135–3146. https://doi.org/10.1093/icesjms/fsab181

Hilborn, R., Amoroso, R. O., Anderson, C. M., Baum, J. K., Branch, T. A., Costello, C., Moor, C. L. D., Faraj, A., Hively, D., Jensen, O. P., et al. (2020). Effective fisheries management instrumental in improving fish stock status. *Proceedings of the National Academy of Sciences*, *117*(4), 2218–2224.

Horsted, S. A. (1956). The deep sea prawn (pandalus borealis KR.) in greenland waters. *Medd. Dan. Fisk. Havunders., N. S.*, *1*(11), 1–118.

Hudon, C., Parsons, D. G., & Crawford, R. (1992). Diel pelagic foraging by a pandalid shrimp (pandalus montagui) off resolution island (eastern hudson strait). *Canadian Journal of Fisheries and Aquatic Sciences*, *49*.

Hurtado-Ferro, F., Szuwalski, C. S., Valero, J. L., Anderson, S. C., Cunningham, C. J., Johnson, K. F., Licandeo, R., McGilliard, C. R., Monnahan, C. C., Muradian, M. L., Ono, K., Vert-Pre, K. A., Whitten, A. R., & Punt, A. E. (2015). Looking in the rear-view mirror: Bias and retrospective patterns in integrated, age-structured stock assessment models. *ICES Journal of Marine Science*, *72*, 99–110. https://doi.org/10.1093/icesjms/fsu198

Hvingel, C., & Zimmermann, F. (2023). Barents sea shrimp-stock assessment report 2023. In *IMR/PINRO Joint Report Series*. Institute of Marine Research, PINRO.

ICES. (2022). Benchmark workshop on pandalus stocks (WKPRAWN). *ICES Scientific Reports*, *4*, 249. https://doi.org/10.17895/ices.pub.19714204

Isaac, N. J. B., Jarzyna, M. A., Keil, P., Dambly, L. I., Boersch-Supan, P. H., Browning, E., Freeman, S. N., Golding, N., Guillera-Arroita, G., Henrys, P. A., Jarvis, S., Lahoz-Monfort, J., Pagel, J., Pescott, O. L., Schmucki, R., Simmonds, E. G., & O'Hara, R. B. (2020). Data integration for large-scale models of species distributions. *Trends in Ecology and Evolution*, *35*, 56–67. https://doi.org/10.1016/j.tree.2019.08.006

Ivanov, B. G., & Stolyarenko, D. A. (1995). Relationship between water currents and orientation of shrimp, and the effect on trawl catchability, with special reference to pandalus borealis. *ICES Mar. Sci. Symp.*, *199*, 357–363.

https://doi.org/10.17895/ices.pub.19271468

Johnson, J., Young, C. D., Bahri, T., Soto, D., Virapat, C., & eds. (2019). *Proceedings of FishAdapt: The global conference on climate change adaptation for fisheries and aquaculture* (61; p. 240). FAO.

Jónsdóttir, I. G., Magnússon, Á., & Skúladóttir, U. (2013). Influence of increased cod abundance and temperature on recruitment of northern shrimp (pandalus borealis). *Marine Biology*, *160*, 1203–1211. https://doi.org/10.1007/s00227-013-2172-1

Jorde, P. E., Søvik, G., Westgaard, J. I., Albretsen, J., André, C., Hvingel, C., Johansen, T., Sandvik, A. D., Kingsley, M., & Jørstad, K. E. (2015). Genetically distinct populations of northern shrimp, pandalus borealis, in the north atlantic: Adaptation to different temperatures as an isolation factor. *Molecular Ecology*, *24*, 1742–1757. https://doi.org/10.1111/mec.13158

Kokkalis, A., Berg, C. W., Kapur, M. S., Winker, H., Jacobsen, N. S., Taylor, M. H., Ichinokawa, M., Miyagawa, M., Medeiros-Leal, W., Nielsen, J. R., & Mildenberger, T. K. (2024). Good practices for surplus production models. *Fisheries Research*, *275*, 107010.

Krawczyk, D. W., Vonnahme, T., Burmeister, A. D., Maier, S. R., Blicher, M. E., Meire, L., & Nygaard, R. (2024). Arctic puzzle: Pioneering a northern shrimp (pandalus borealis) habitat model in disko bay, west greenland. *Science of the Total Environment*, *929*. https://doi.org/10.1016/j.scitotenv.2024.172431

Lundesgaard, Ø., Sundfjord, A., Lind, S., Nilsen, F., & Renner, A. H. H. (2022). Import of atlantic water and sea ice controls the ocean environment in the northern barents sea. *Ocean Science*, *18*, 1389–1418. https://doi.org/10.5194/os-18-1389-2022

Marchal, P., Andersen, B., Caillart, B., Eigaard, O., Guyader, O., Hovgaard, H., Iriondo, A., Fur, F. L., Sacchi, J., & Santurtún, M. (2007). Impact of technological creep on fishing effort and fishing mortality, for a selection of european fleets. *ICES Journal of Marine Science*, *64*(1), 192–209.

Melaa, K. W., Zimmermann, F., Søvik, G., & Thangstad, T. H. (2022). *Historic landings of northern shrimp (pandalus borealis) in norway-data per county for 1908-2021*. Institute of Marine Research.

Mendenhall, E., Hendrix, C., Nyman, E., Roberts, P. M., Hoopes, J. R., Watson, J. R., Lam, V. W. Y., & Sumaila, U. R. (2020). Climate change increases the risk of fisheries conflict. *Marine Policy*, *117*. https://doi.org/10.1016/j.marpol.2020.103954

NGU. (2013). *Bunnsedimenter (kornstørrelse)*. Geological Survey of Norway (NGU); https://www.mareano.no.

Oanta, G. A. (2018). International organizations and deep-sea fisheries: Current status and future prospects. *Marine Policy*, *87*, 51–59. https://doi.org/10.1016/j.marpol.2017.09.009

Ouellet, P., Savard, L., & Larouche, P. (2007). Spring oceanographic conditions and northern shrimp pandalus borealis recruitment success in the north-western gulf of st. lawrence. *Marine Ecology Progress Series*, *339*, 229–241.

Palacios-Abrantes, J., Frölicher, T. L., Reygondeau, G., Sumaila, U. R., Tagliabue, A., Wabnitz, C. C. C., & Cheung, W. W. L. (2022). Timing and magnitude of climate-driven range shifts in transboundary fish stocks challenge their management. *Global Change Biology*, *28*, 2312–2326. https://doi.org/10.1111/gcb.16058

Pebesma, E. (2018). Simple features for r: Standardized support for spatial vector data. *The R Journal*, *10*.

Pedersen, M. W., & Berg, C. W. (2017). A stochastic surplus production model in continuous time. *Fish and Fisheries*, *18*, 226–243. https://doi.org/10.1111/faf.12174

Perry, A. L., Low, P. J., Ellis, J. R., & Reynolds, J. D. (2005). Climate change and distribution shifts in marine fishes. *Science*, *308*. https://www.science.org

Pinsky, M. L., Reygondeau, G., Caddell, R., Palacios-Abrantes, J., Spijkers, J., & Cheung, W. W. L. (2018). Preparing ocean governance for species on the move. *Science*, *360*(6394), 1189–1191.

Pörtner, H. O., & Peck, M. A. (2010). Climate change effects on fishes and fisheries: Towards a cause-and-effect

understanding. *Journal of Fish Biology*, *77*, 1745–1779. https://doi.org/10.1111/j.1095-8649.2010.02783.x

Punt, A. E. (2019). Spatial stock assessment methods: A viewpoint on current issues and assumptions. *Fisheries Research*, *213*, 132–143.

Rasmussen, B. (1953). On the geographical variation in growth and sexual development of the deep sea prawn (pandalus borealis kr.). *Reports on Norwegian Fishery and Marine Investigations*.

Rasmussen, T., & Tande, K. (1995). Temperature-dependent development, growth and mortality in larvae of the deep-water prawn pandalus borealis reared in the laboratory. *Marine Ecology Progress Series*, *118*, 149–157.

Rubec, P. J., Kiltie, R., Leone, E., Flamm, R. O., McEachron, L., & Santi, C. (2016). Using delta-generalized additive models to predict spatial distributions and population abundance of juvenile pink shrimp in tampa bay, florida. *Marine and Coastal Fisheries*, *8*, 232–243. https://doi.org/10.1080/19425120.2015.1084408

Shumway, S. E., Perkins, H. C., Schick, D. F., & Stickney, A. P. (1985). Synopsis of biological data on the pink shrimp, pandalus borealis krøyer, 1838. In *FAO Fisheries Synopsis* (Vol. 144, p. 57). National Marine Fisheries Service, National Oceanic; Atmospheric Administration, US Department of Commerce.

Smith, J. A., & Johnson, D. D. (2024). Evaluating drivers and predictability of catch composition in a highly mixed trawl fishery using stacked and joint species distribution models. *Fisheries Research*, *279*. https://doi.org/10.1016/j.fishres.2024.107151

Stiansen, J. E., Korneev, O., Titov, O., Arneberg, P., Filin, A., Hansen, J. R., Høines, Å., & Marasaev, S. (2009). *Joint norwegian-russian environmental status 2008. Report on the barents sea ecosystem. Part II – complete report* (3; p. 375). IMR/PINRO Joint Report Series.

Stokke, O. S. (2010). Barents sea fisheries – the IUU struggle. *Arctic Review on Law and Politics*, *1*, 207–224. https://doi.org/10.2307/48710119

Thieurmel, B., & Elmarhraoui, A. (2022). *Suncalc: Compute sun position, sunlight phases, moon position and lunar phase*. https://CRAN.R-project.org/package=suncalc

Turner, B., Hewitt, S. A., & Thrush, L. B. (2023). Effects of pollution on fish health and fisheries management: A comprehensive review. *Journal of Fisheries Science*, *5*(1).

Wieland, K., & Siegstad, H. (2012). Environmental factors affecting recruitment of northern shrimp pandalus borealis in west greenland waters. *Marine Ecology Progress Series*, *469*, 297–306. https://doi.org/10.3354/meps09794

Wieland, K., Storr-Paulsen, M., & Sünksen, K. (2007). Response in stock size and recruitment of northern shrimp (pandalus borealis) to changes in predator biomass and distribution in west greenland waters. *Journal of Northwest Atlantic Fishery Science*, *39*, 21–33. https://doi.org/10.2960/J.v39.m579

Wood, S. N. (2011). Fast stable restricted maximum likelihood and marginal likelihood estimation of semiparametric generalized linear models. *Journal of the Royal Statistical Society B*, *73*, 3–36. https://academic.oup.com/jrsssb/article/73/1/3/7034726

Zimmermann, F., Ellerine, H., Danielsen, H., Marcussen, J. B., Trochta, J. T., Vickery, G., Olsen, S. A., Berg, E., Stesko, A., & Bakanev, S. (2024). Assessment report for northern shrimp (pandalus borealis) in the barents sea (ICES subareas 1 and 2). In *IMR/PINRO Joint Report Series*. Institute of Marine Research, Polar Research Institute of Marine Fisheries; Oceanography(PINRO).

Zimmermann, F., Søvik, G., & Thangstad, T. H. (2019). Kunnskapsstatus rekefelt langs norskekysten-bestilling fra fiskeridirektoratet. *No. 2019–15; Rapport Fra Havforskningen*, 13.

7 Annex

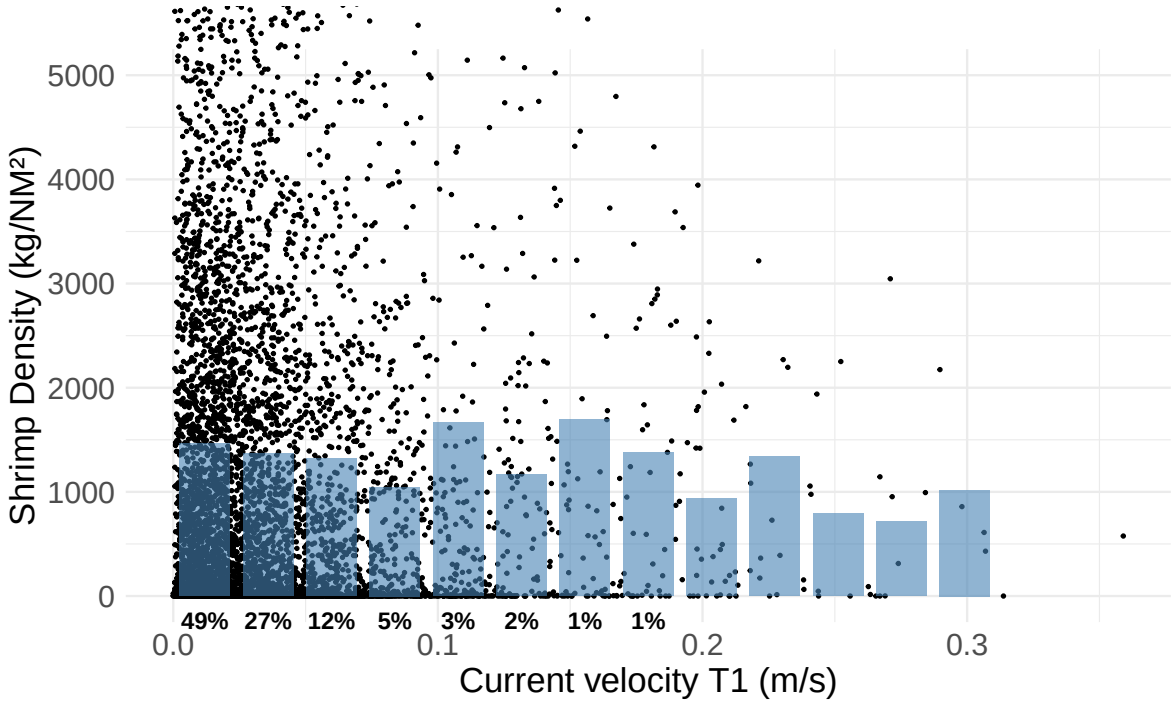

Figure 7.1: Mean monthly current velocity in sampling month (data treatment 1) against shrimp density. Dots show each observed pair of current velocity and shrimp density. Blue columns represent the mean shrimp density at each interval of the environmental variable. Percentages display the amount of data concentrated at a given interval.

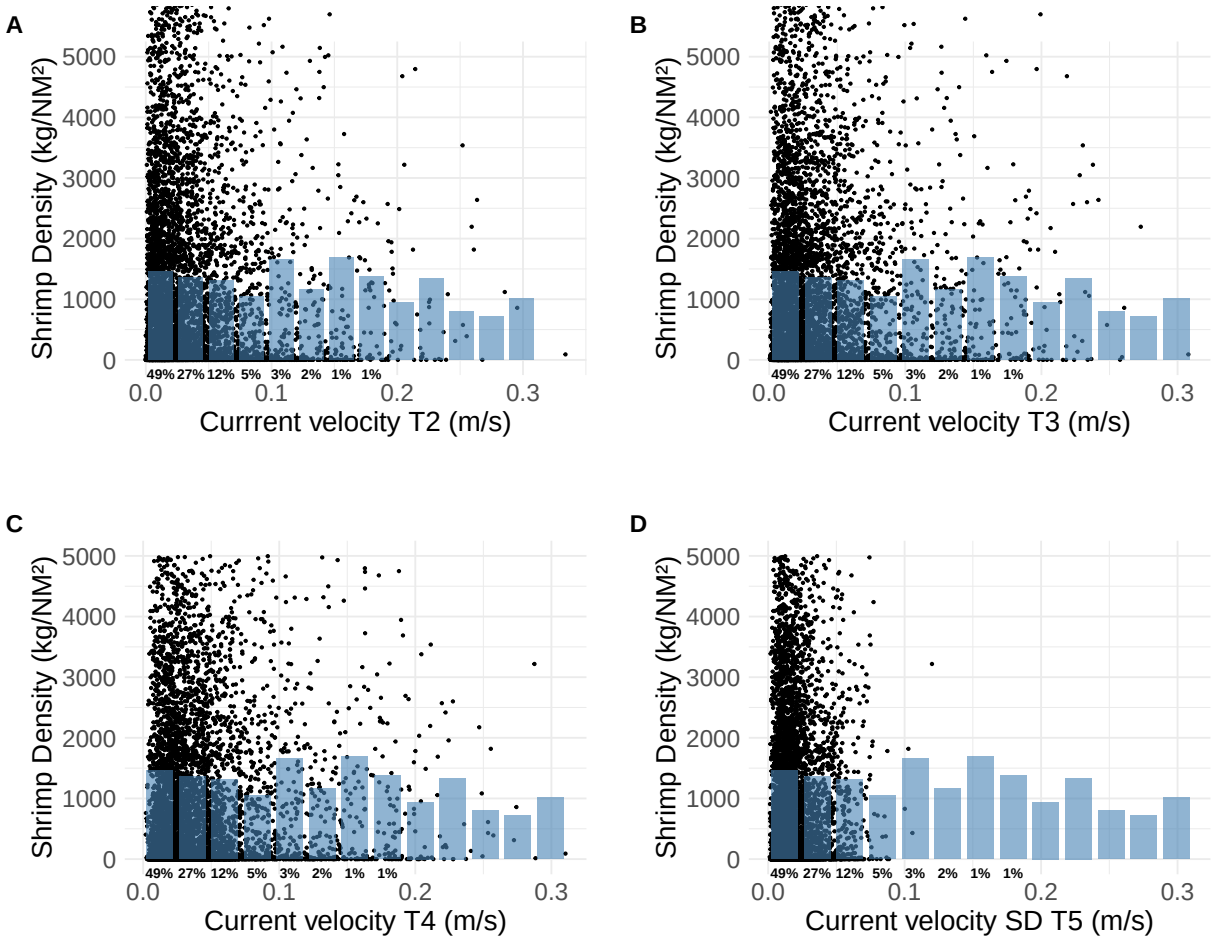

Figure 7.2: Current velocity against shrimp density for data treatments 2 through 5 (A-D): A (1-month lagged mean), B (6-month lagged mean), C (12-month lagged mean) and D (12-month lagged standard deviation). Dots show each observed pair of current velocity and shrimp density, blue columns represent the mean shrimp density at each interval of the environmental variable, and percentages display the amount of data concentrated at a given interval.

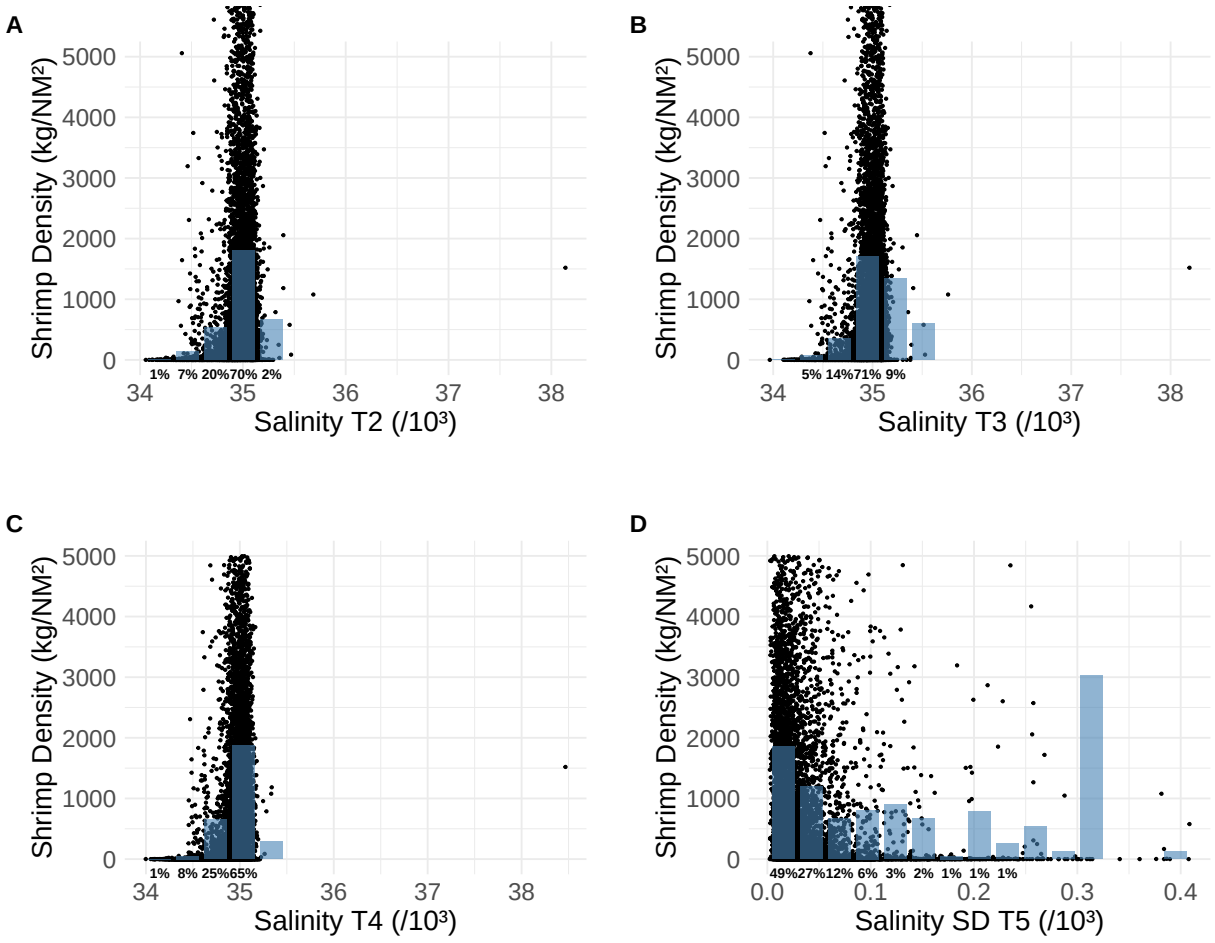

Figure 7.3: Salinity against shrimp density for data treatments 2 through 5 (A-D): A (1-month lagged mean), B (6-month lagged mean), C (12-month lagged mean) and D (12-month lagged standard deviation). Dots show each observed pair of current velocity and shrimp density, blue columns represent the mean shrimp density at each interval of the environmental variable, and percentages display the amount of data concentrated at a given interval.

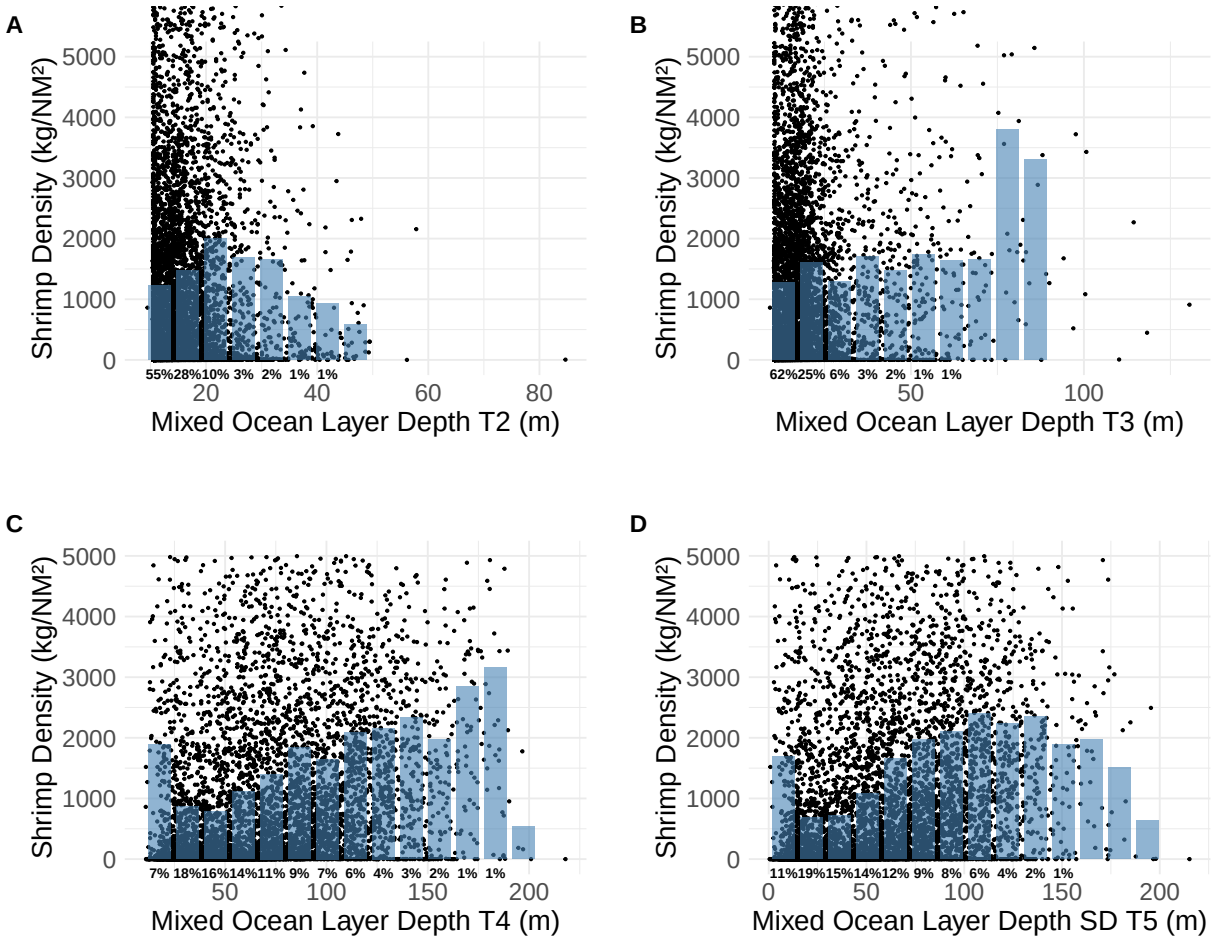

Figure 7.4: Mixed ocean layer depth against shrimp density for data treatments 2 through 5 (A-D): A (1-month lagged mean), B (6-month lagged mean), C (12-month lagged mean) and D (12-month lagged standard deviation).

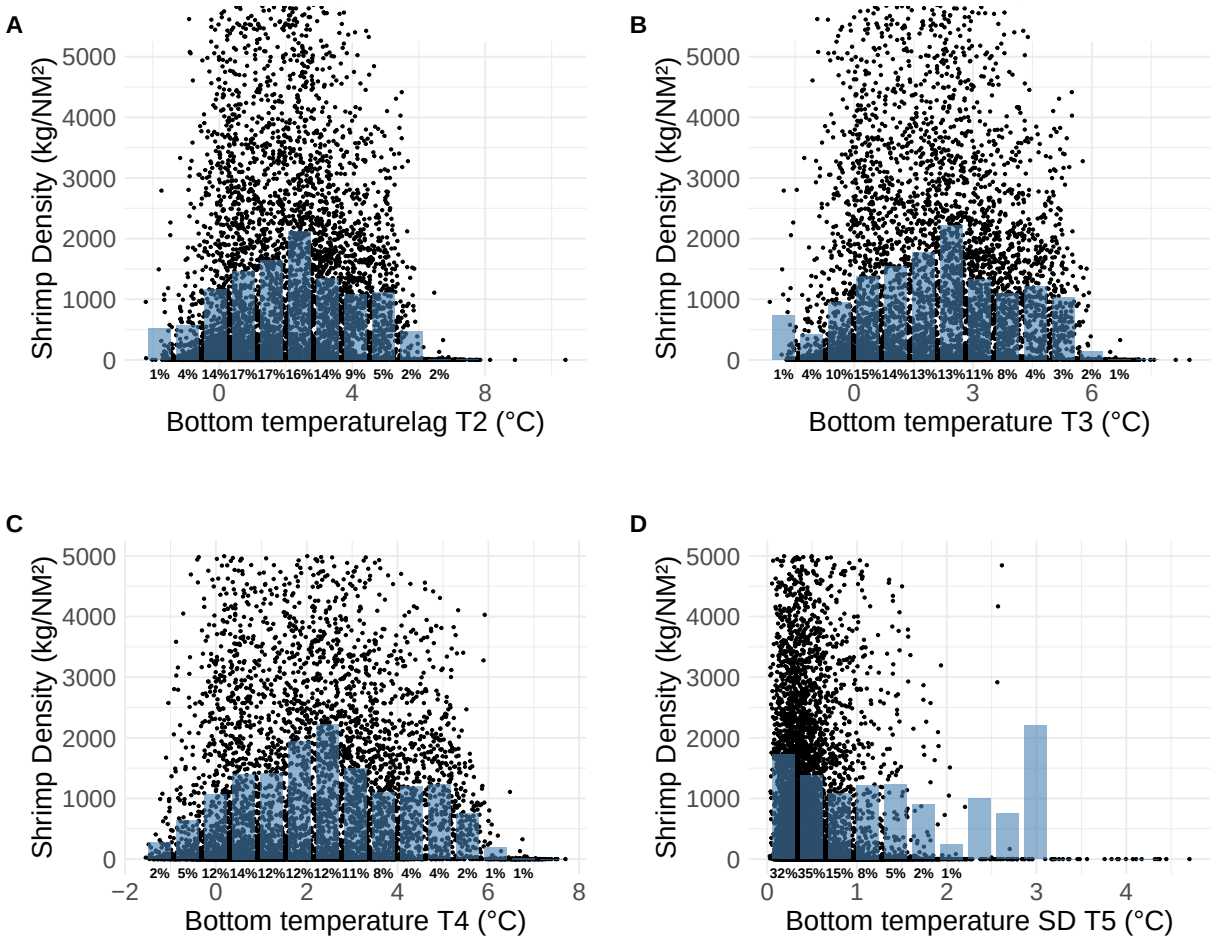

Figure 7.5: Bottom temperature against shrimp density for data treatments 2 through 5 (A-D): A (1-month lagged mean), B (6-month lagged mean), C (12-month lagged mean) and D (12-month lagged standard deviation).

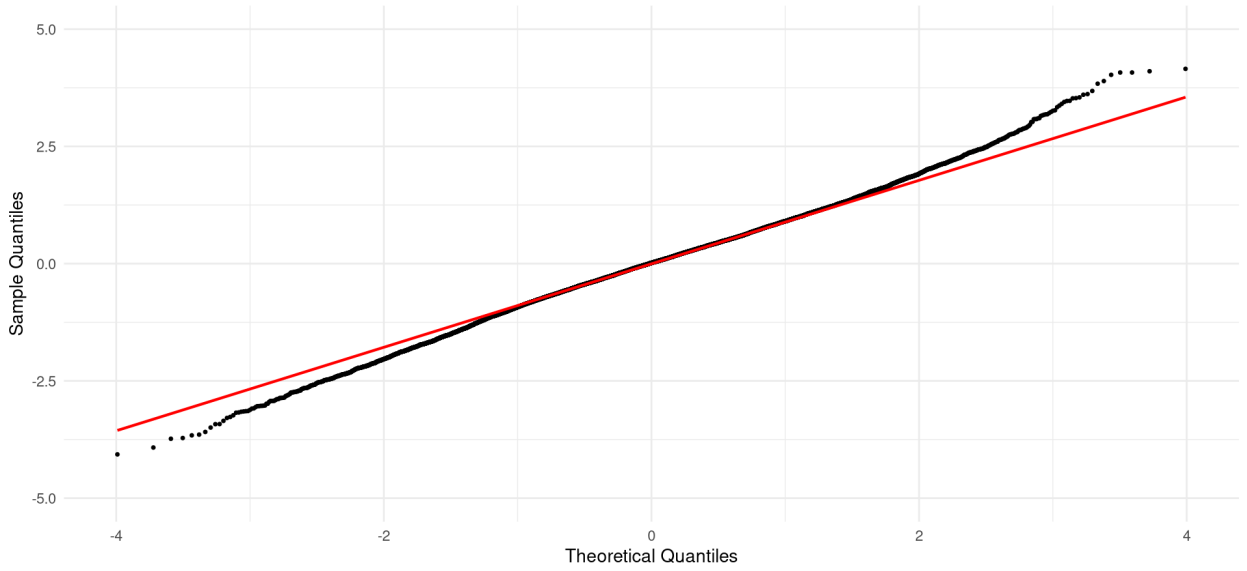

Figure 7.6: Q-Q plot showing mle-mvn calculated residuals from the extended index model.

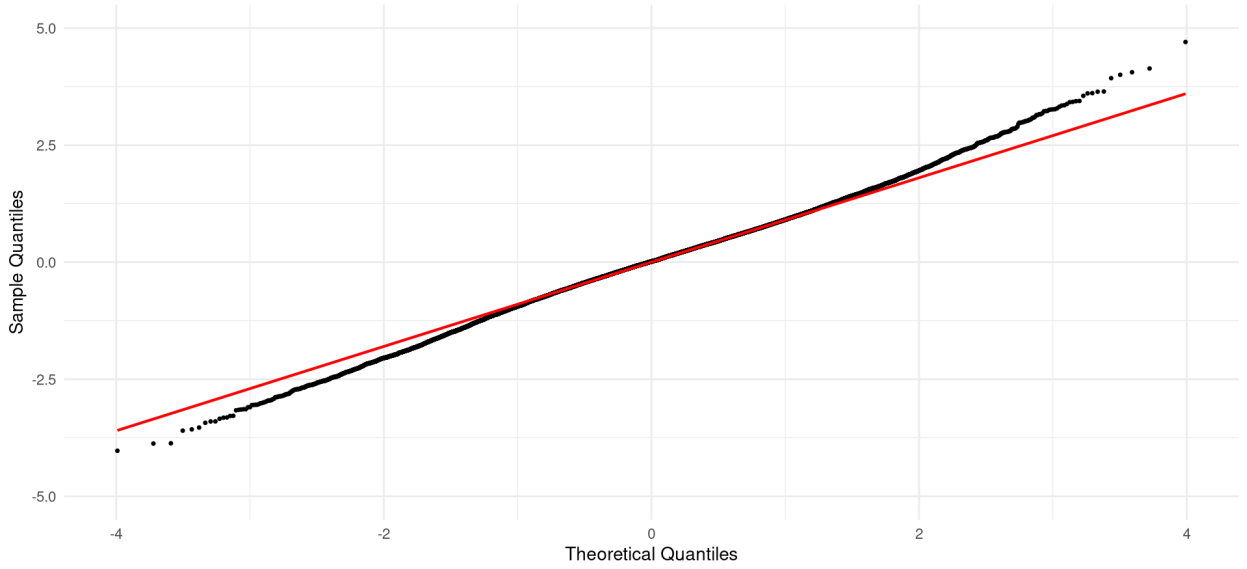

Figure 7.7: Q-Q plot showing mcmc calculated residuals from the extended index model.

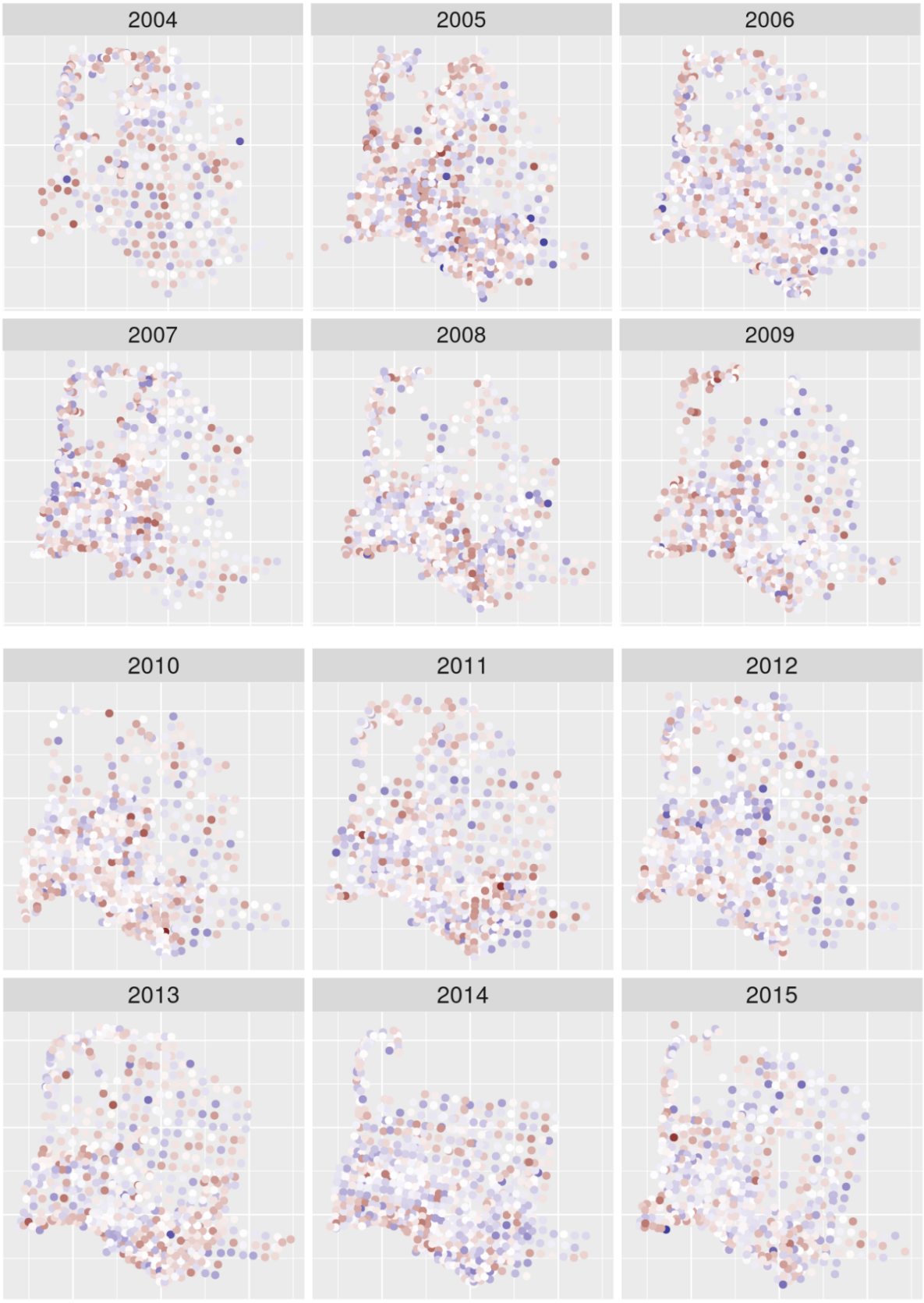
2004
2005
2006
2007
2008
2009
2010
2011
2012
2013
2014
2015

Figure 7.8: Model residuals distribution from the extended index model in the study area between 2004 and 2024.

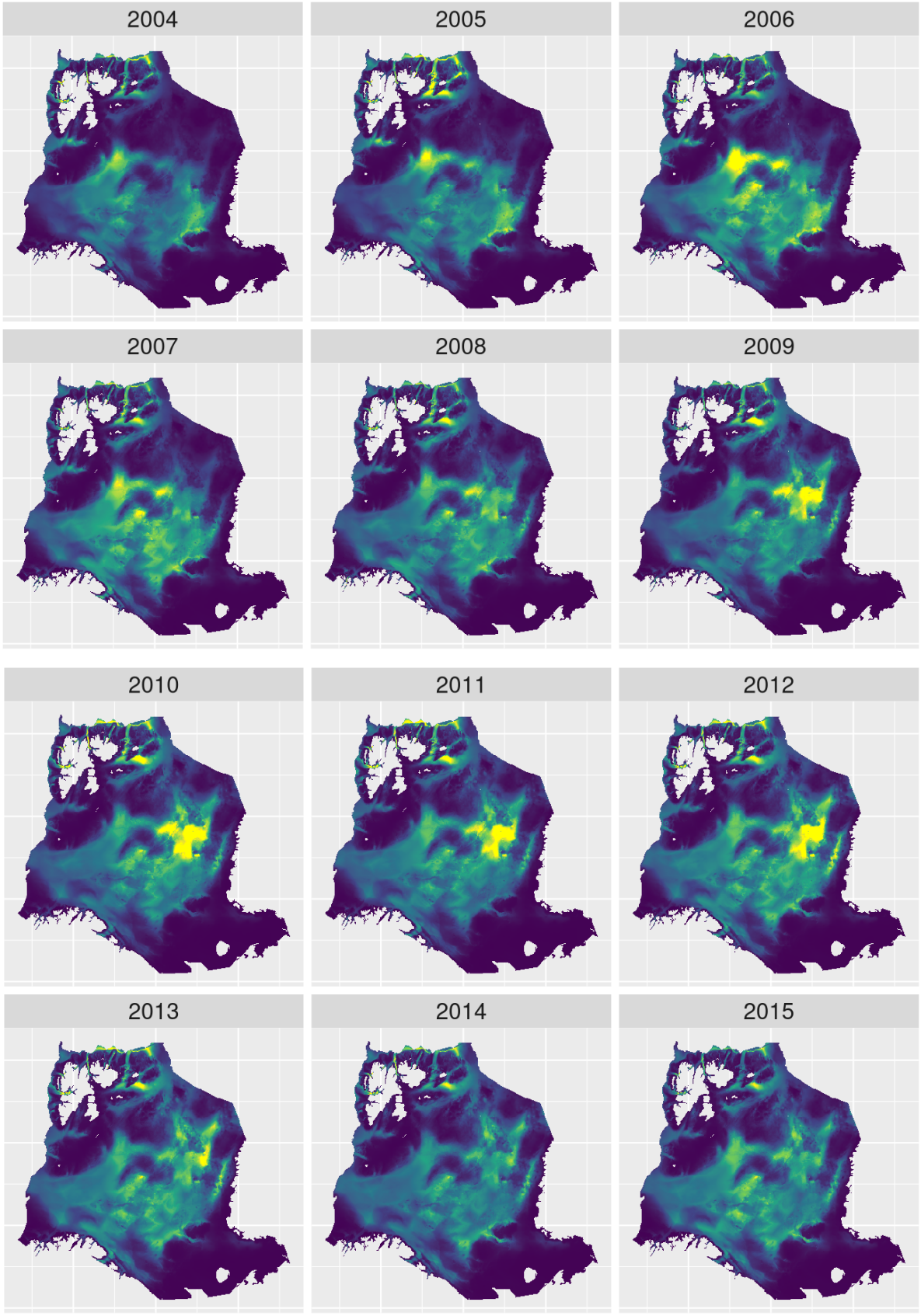
2004
2005
2006
2007
2008
2009
2010
2011
2012
2013
2014
2015

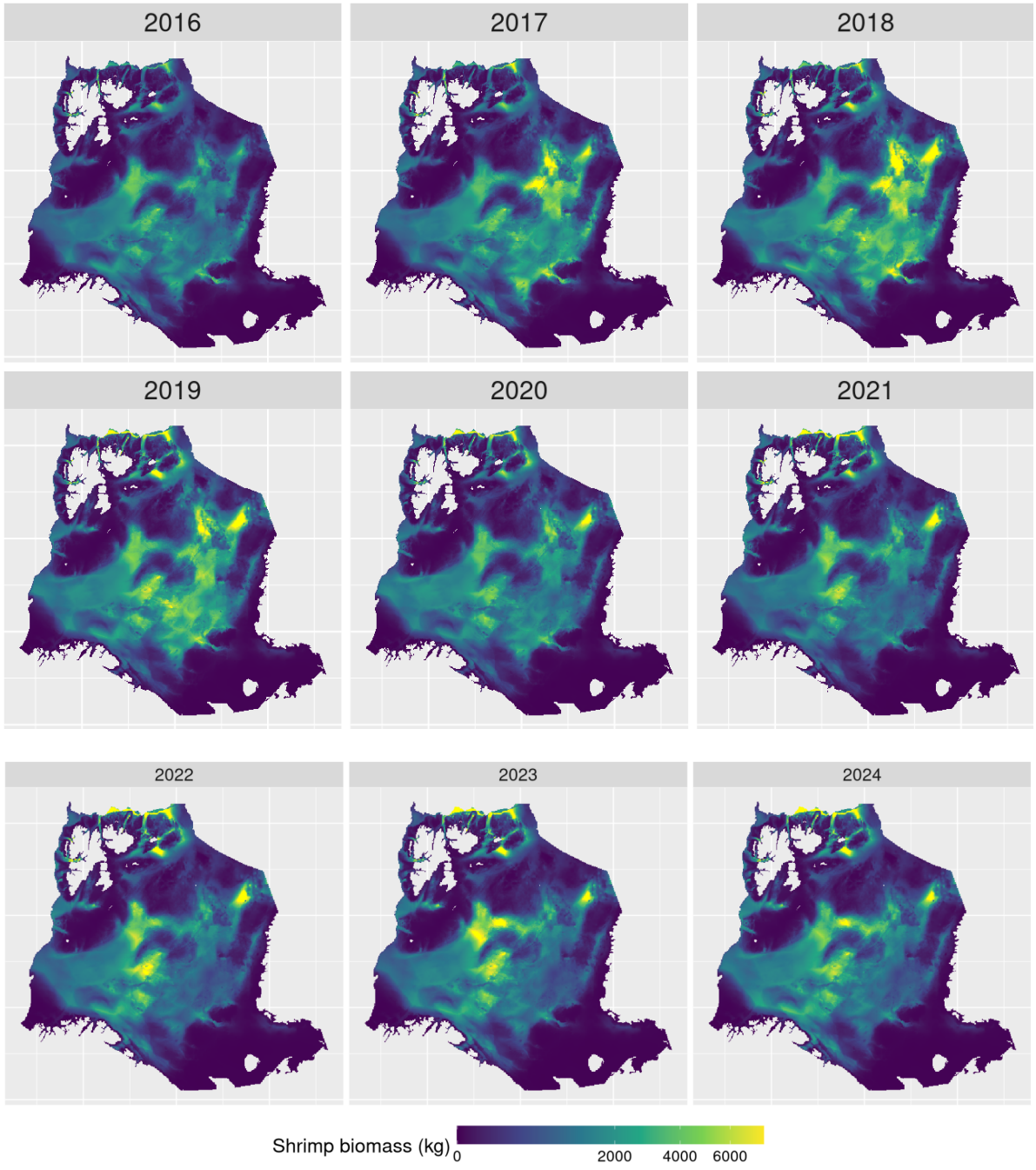

Figure 7.9: Northern shrimp biomass predictions obtained using the extended index model, showing the combined outcome of fixed and random effects predicted over the study area between 2004 and 2024.

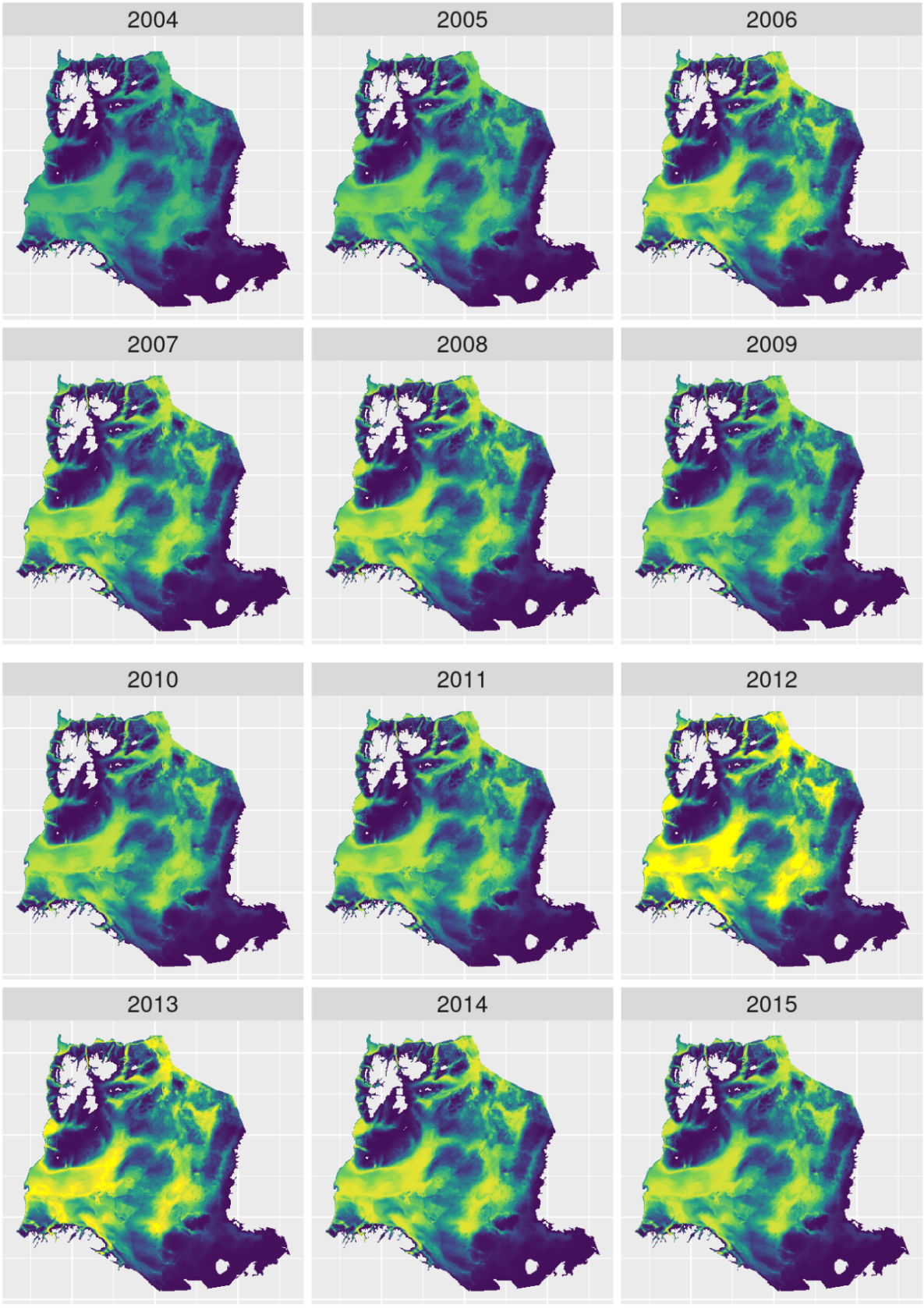
2004
2005
2006
2007
2008
2009
2010
2011
2012
2013
2014
2015

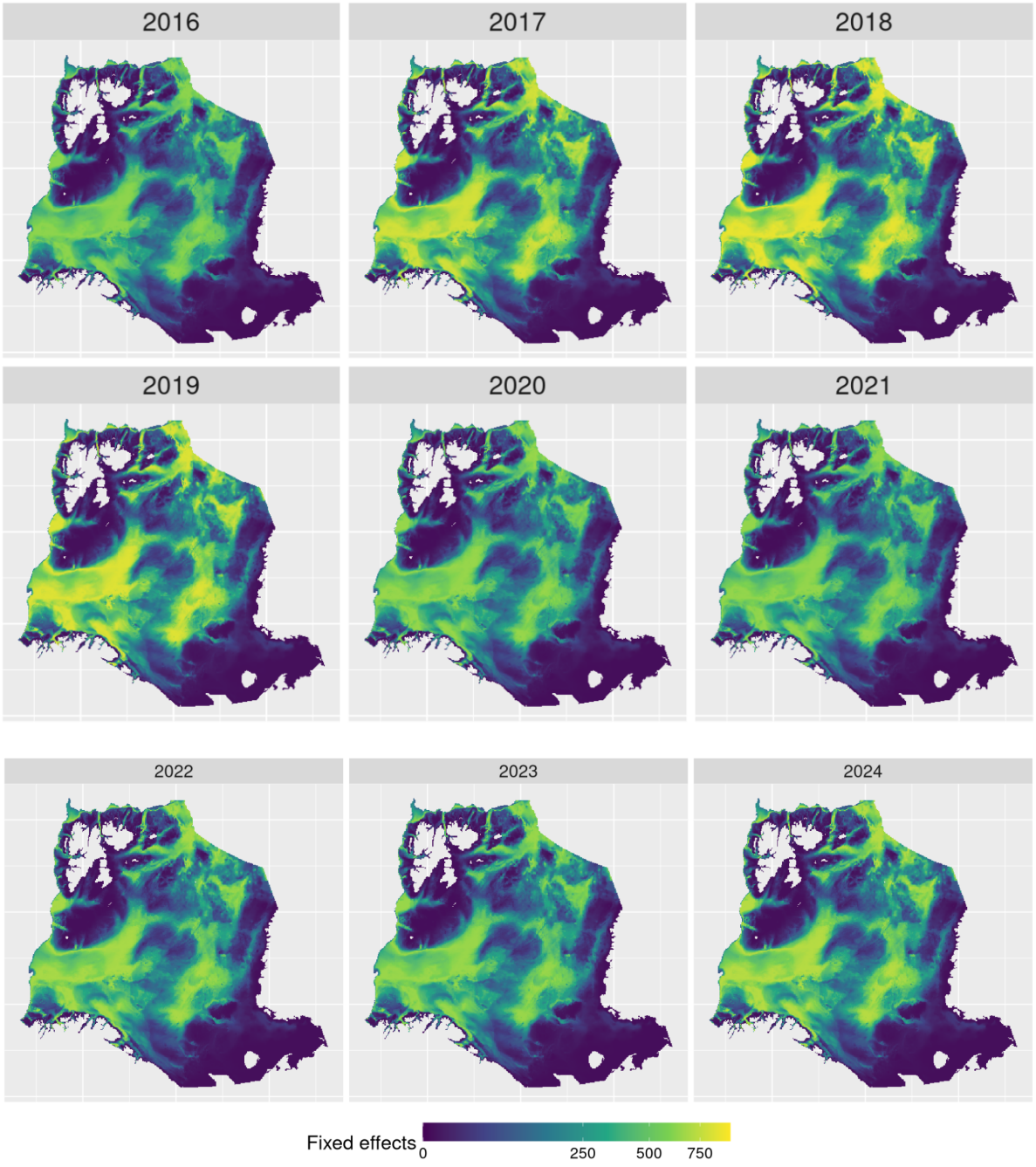

Figure 7.10: Predicted fixed effects from the extended index model over the study area between 2004 and 2024. Estimates are on the log-scale, and correspond to density when back-transformed..

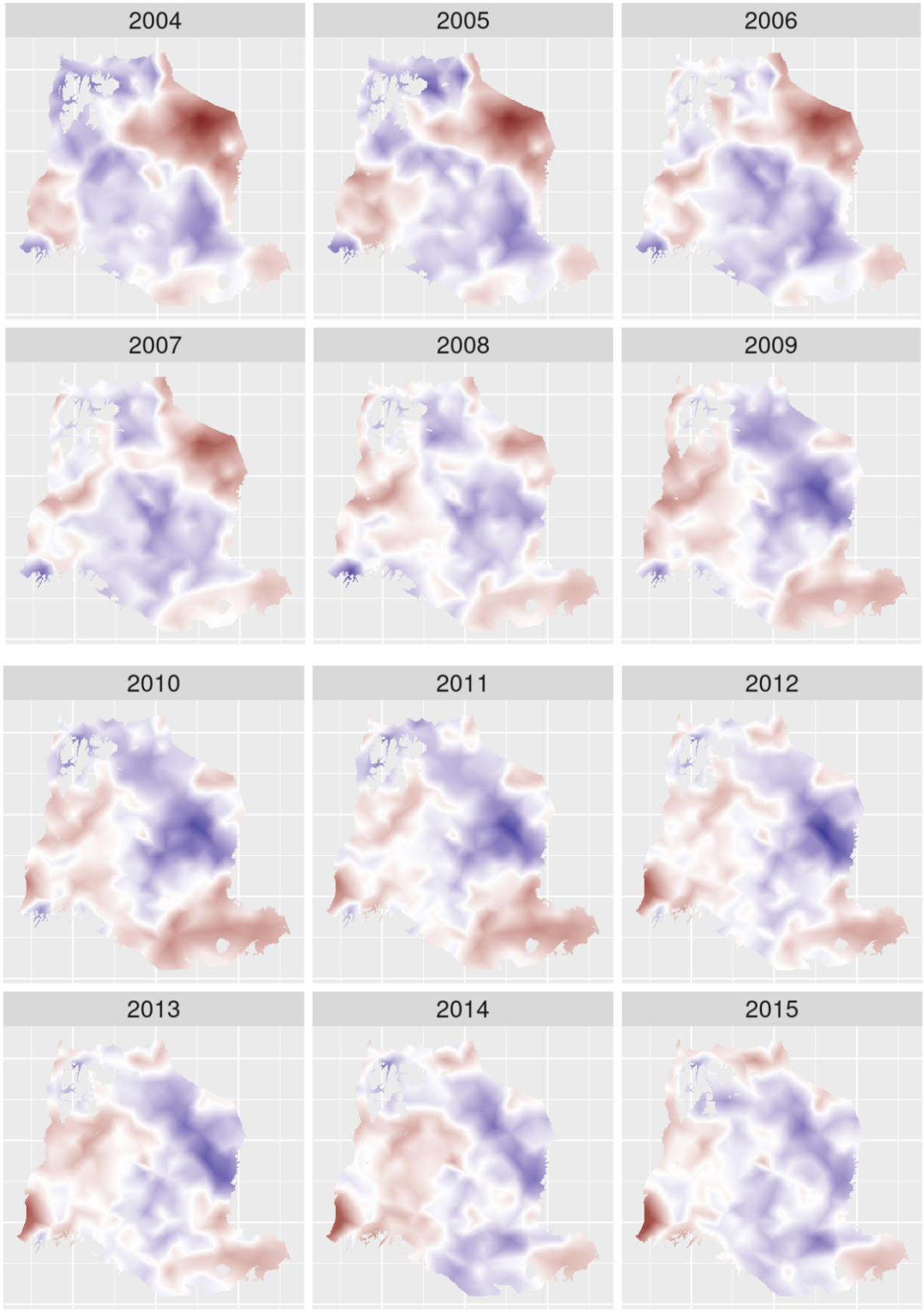
2004
2005
2006
2007
2008
2009
2010
2011
2012
2013
2014
2015

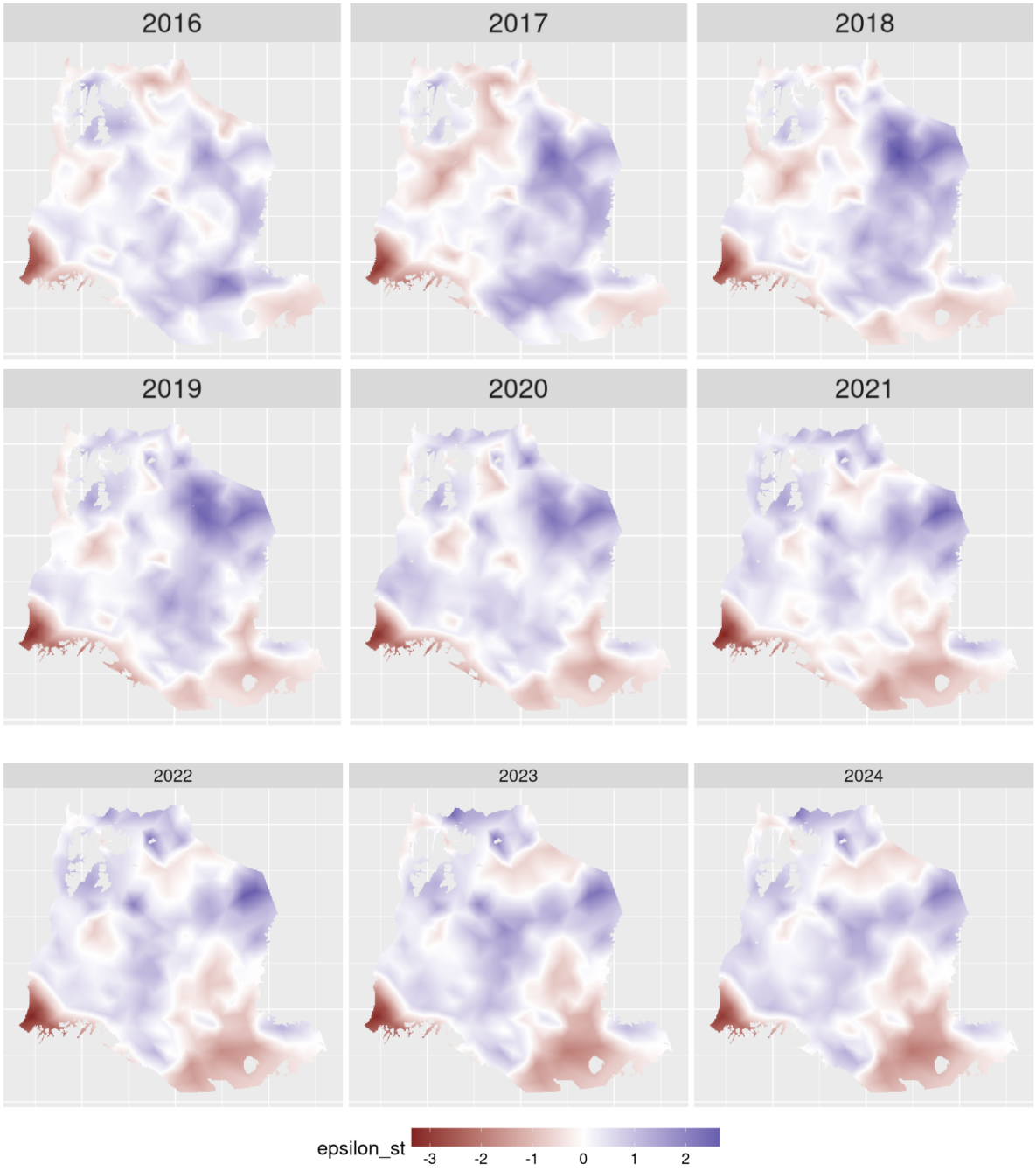

Figure 7.11: Predicted spatiotemporal random effects (omega s) from the extended index model over the study area between 2004 and 2024. Estimates are on the log-scale, and correspond to density when back-transformed.

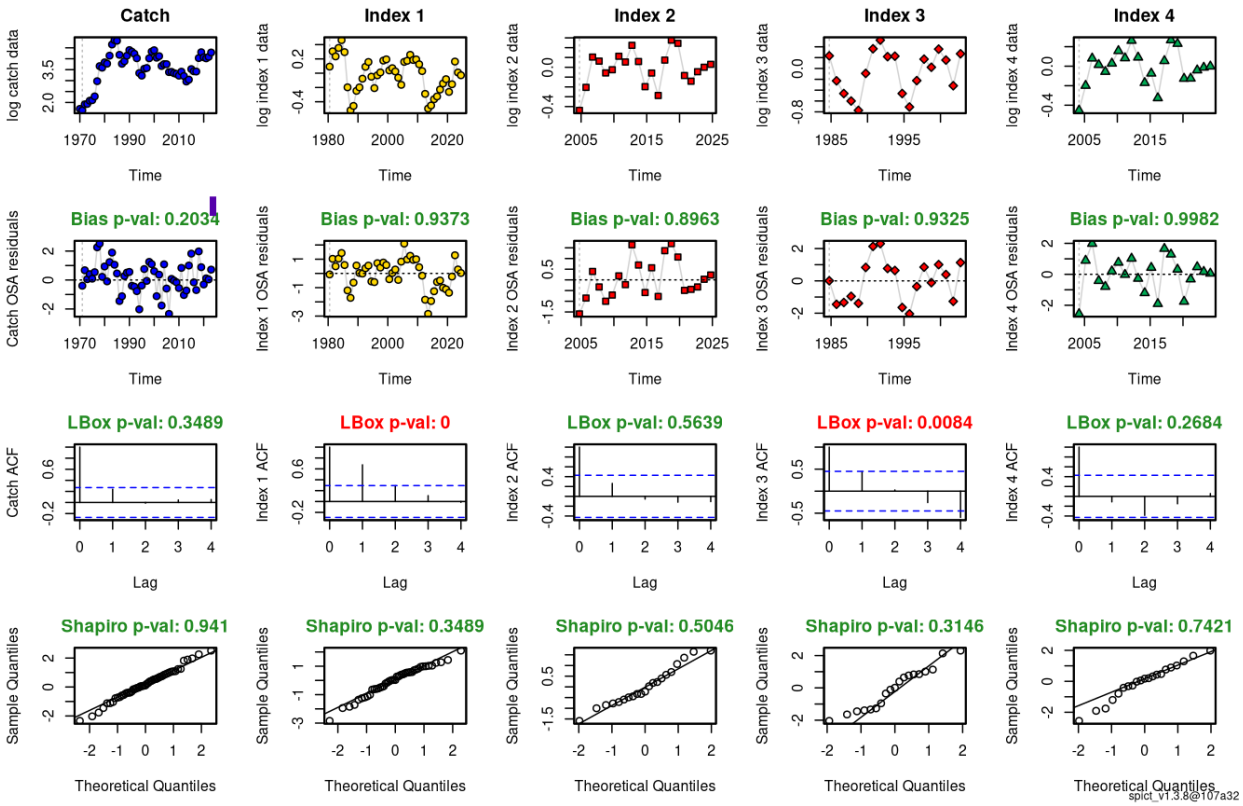

Figure 7.12: Extended assessment model OSA residuals.

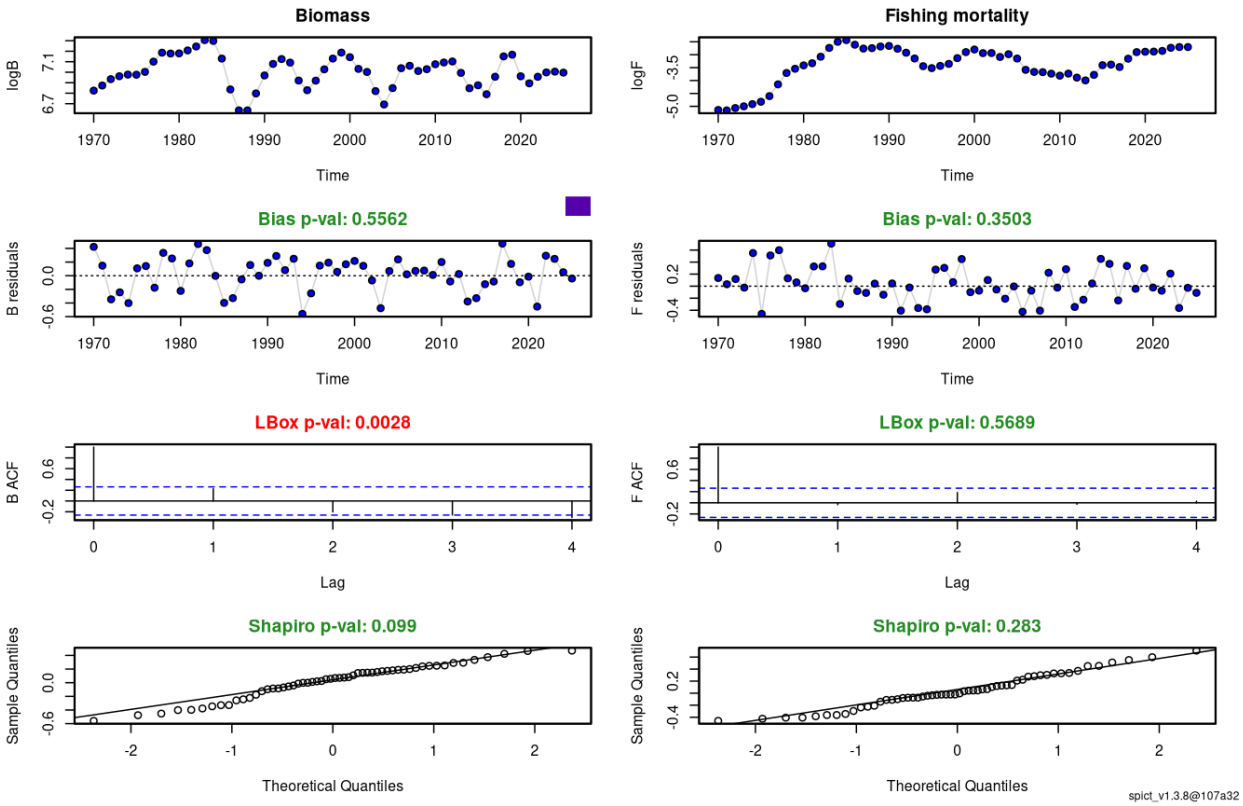

Figure 7.13: Extended assessment model process residuals.

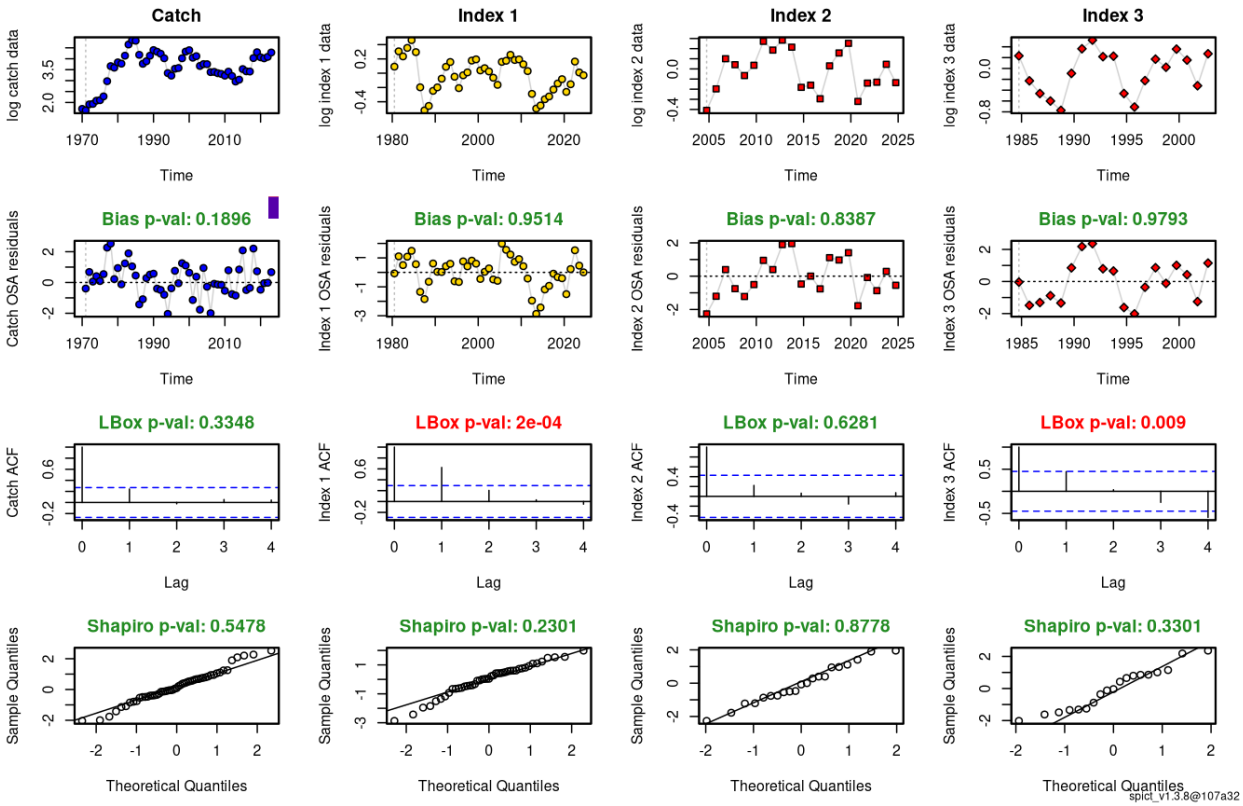

Figure 7.14: Benchmark assessment model OSA residuals.

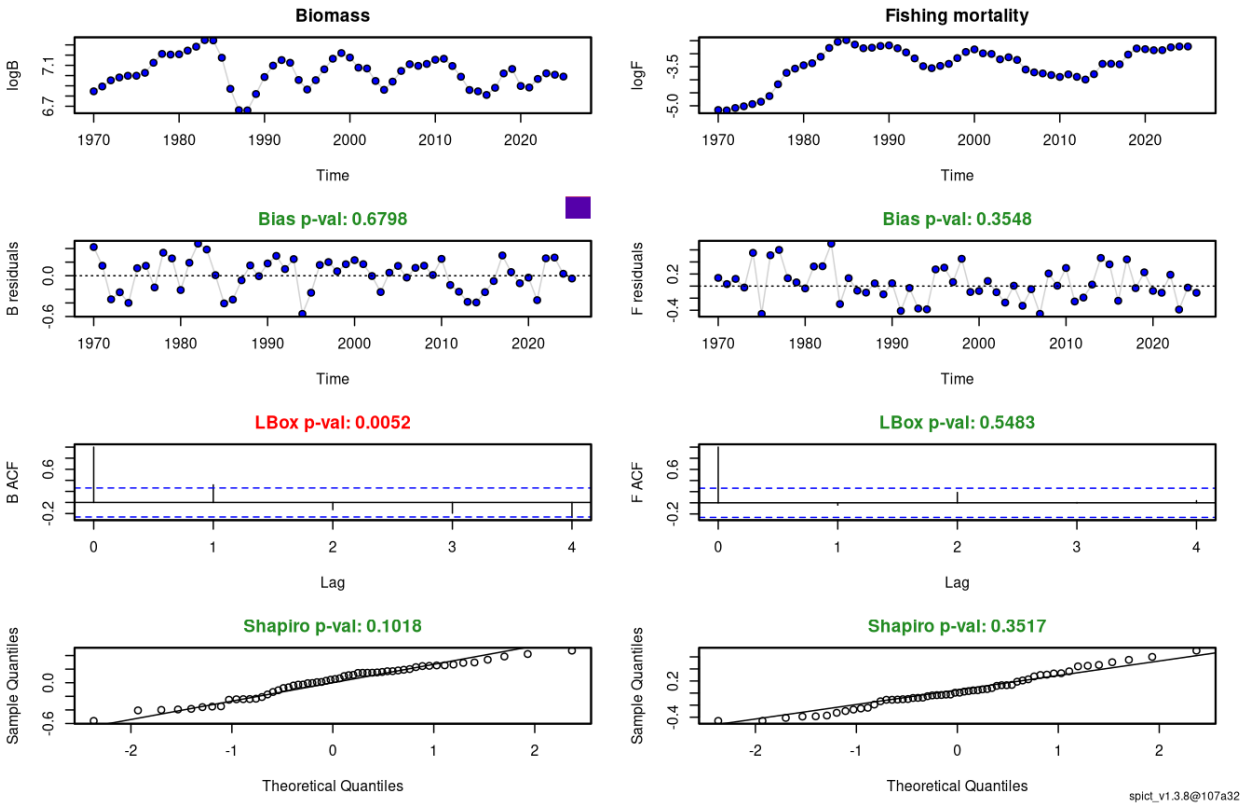

Figure 7.15: Benchmark assessment model process residuals.